# REGIONAL GEOLOGY, SEISMICITY, AND GENERAL GROUND MOTION CONSIDERATIONS FOR THE MOKELUMNE AND STANISLAUS HYDROELECTRIC SYSTEMS

## Alpine, Amador, Calaveras, and Tuolumne Counties, California

**FERC Projects 137, 1061, and 2130**

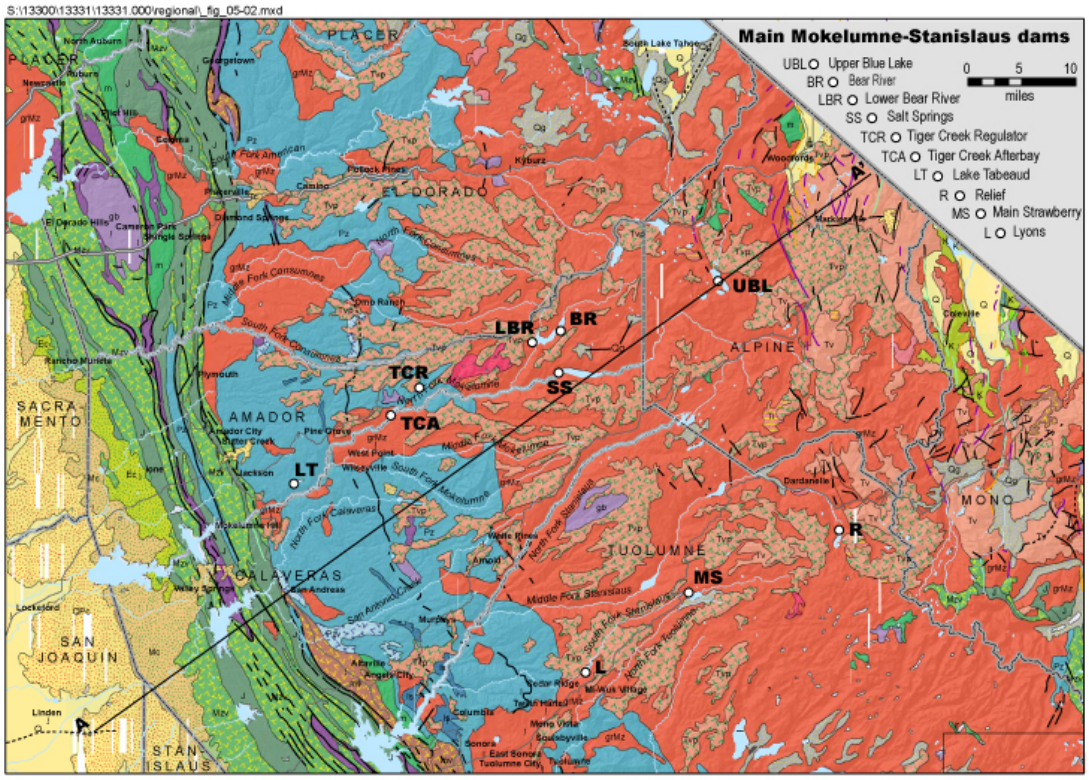



by
William D. Page, Yi-Ben Tsai and Marcia McLaren,
PG&E Geosciences Department
Todd Crampton and Courtney Johnson, Geomatrix Consultants
and
Thomas L. Sawyer, Piedmont GeoSciences, Inc.

for
Hydro Generation Department
Pacific Gas and Electric Company


**October 2007**

# REGIONAL GEOLOGY, SEISMICITY, AND GENERAL GROUND MOTION CONSIDERATIONS FOR THE MOKELUMNE AND STANISLAUS HYDROELECTRIC SYSTEMS

## Alpine, Amador, Calaveras, and Tuolumne Counties, California

**FERC Projects 137, 1061, and 2130**

by

William D. Page, Yi-Ben Tsai and and Marcia McLaren,
PG&E Geosciences Department
Todd Crampton and Courtney Johnson, Geomatrix Consultants
and
Thomas L. Sawyer, Piedmont GeoSciences, Inc.

for

Hydro Generation Department
Pacific Gas and Electric Company

**October 2007**

**REGIONAL GEOLOGY, SEISMICITY, AND GENERAL GROUND MOTION CONSIDERATIONS FOR THE MOKELUMNE AND STANISLAUS HYDROELECTRIC SYSTEMS**

**Alpine, Amador, Calaveras, and Tuolumne Counties, California**

## TABLE OF CONTENTS

**7.0 TABLES**



**8.0 FIGURES**

# REGIONAL GEOLOGY, SEISMICITY, AND GENERAL GROUND MOTION CONSIDERATIONS FOR THEMOKELUMNE AND STANISLAUS HYDROELECTRIC SYSTEMS

## 1.0 INTRODUCTION

### 1.1 DESCRIPTION AND HISTORY

The Mokelumne and Stanislaus hydroelectric systems are in the central Sierra Nevada, in Alpine, Amador, Calaveras and Tuolumne counties (Figure 1-1). The main PG&E dams in Mokelumne system (FERC Project 137)) are Upper Blue Lake, Upper Bear, Bear River, Salt Springs, Tiger Creek diversion, Tiger Creek Afterbay, and Lake Tabeaud dams; the small dams include Lower Blue Lake, Twin lakes, Meadow Lake, Tiger Creek Forebay, Electra Diversion and Electra Afterbay. The main dams in the Stanislaus system (FERC Projects 2130 and 1061) are Relief, Main Strawberry, and Lyons dams; the system has one small dam, Stanislaus Forebay and the Philadelphia Diversion.

Construction of the Mokelumne Part 12 dams began with Upper Blue in 1881, Lower Blue in 1885, Twin Lakes 1898, Upper Bear in 1900, Lake Tabeaud in 1901 and Meadow Lake in 1903. The construction of Electra Diversion in 1931 and Electra Afterbay in 1948 followed. Construction of the Stanislaus dams began with Stanislaus Forebay in 1908 and Relief in 1909, followed by Strawberry in 1916 and Lyons in 1930,

The Mokelumne and the Stanislaus hydroelectric systems have an operating capacity that totals 314.5 megawatts. The individual power plants operating capacities are as follows:

Spring Gap (1921): 7 MW

Tiger Creek (1931): 58 MW

Salt Springs unit 1 (1931): 11 MW

Electra (1948): 98 MW

West Point (1948): 14.5 MW

Salt Springs unit 2 (1952): 33 MW

Stanislaus (1963): 91 MW

Phoenix (1898): 2 MW

**Mokelumne Hydroelectric System -** The Mokelumne system is in the Mokelumne River watershed, which heads along the Sierra Nevada crest between Carson Pass and Ebbitts Pass. The PG&E Mokelumne Hydroelectric system starts just west of the range crest in the upper reaches of Meadow Creek where several small dams and reservoirs that hold water for release during the summer and fall. These include Upper Blue Lake, Lower Blue Lake, Twin Lakes and Meadow Lake dams. Meadow Creek feeds the Mokelumne River and below the confluence it is dammed by the Salt Springs Dam. The Salt Springs Powerhouse No. 1 is fed by a penstock

from Salt Springs Reservoir and Powerhouse No. 2 is fed by a penstock from Lower Bear River Dam and Reservoir. Upstream of Lower Bear is the Bear River Dam and Reservoir, a storage reservoir for the system. From Salt Springs powerhouse the Tiger Creek canal and tunnel system feeds water to the Tiger Creek Regulator Dam and Reservoir that in turn feeds the Tiger Creek Forebay above the Tiger Creek Powerhouse. Below the powerhouse the Tiger Creek Afterbay supplies water through a tunnel to the West Point Powerhouse. From there the Electra Diversion Dam supplies water through a tunnel to Lake Tabeaud, the Forebay for the Electra Powerhouse. The Electra Afterbay is the last dam of the PG&E system.

**Stanislaus Hydroelectric System** - The PG&E Stanislaus hydroelectric system is on the Middle and South Fork of the Stanislaus River that drains west from the range crest between Ebbitts Pass and Sonora Pass in Yosemite National Park. The highest dam in the system is Relief Dam on Summit Creek in the upper reaches of the Middle Fork and above the Clark Fork confluence. Relief Reservoir regulates water to the dams down stream. Donnell and Beardsley dams and associated powerhouses are on the Middle Fork and are owned and operated by the Tri-Dam Project. These facilities are above the PG&E Spring Gap Powerhouse. The Spring Gap Powerhouse is fed by a canal and penstock from the Philadelphia Diversion on the South Fork Stanislaus River below Main Strawberry Dam and its reservoir, Pinecrest Lake. Below the Spring Gap Powerhouse water is transported through a tunnel to the Stanislaus Forebay and Powerhouse. The Stanislaus Afterbay is on the Stanislaus River below the junction of the Middle Fork and North Fork. Water in the South fork that is not diverted into the Spring Gap Powerhouse continues to Lyons Reservoir. Water below Lyons Dam is diverted at the Lyons cushion dam into the Tuolumne Ditch and tunnel to the PG&E Phoenix powerhouse.

## 1.2 PURPOSE AND SCOPE OF WORK

The purpose of this report is to compile and summarize the existing geologic and seismic information for the Mokelumne and Stanislaus hydroelectric systems. This report supports the Standard Technical Information Document (STID) for the main dams in these systems. This report supplies general background information on the regional geology, seismicity, and ground motions that pertains to all the dams in these systems. This report uses the results of the previous analyses of both the floating or "background" earthquake for the Sierra Nevada and of potential ground motions recently developed under the auspices of the Pacific Earthquake Engineering Research Center (PEER). Earlier analyses of the background earthquake and other ground motion issues are discussed in the regional report for the southern Sierra Nevada (Piedmont GeoSciences and PG&E Geosciences Department, 2004). Other regional reports for the adjacent regions summarize the geology and seismicity for PG&E's Yuba and Bear River hydroelectric systems (PG&E Geosciences Department and Piedmont GeoSciences, 2003) and the Merced, San Joaquin, and Kings hydroelectric Systems (Piedmont GeoSciences and PG&E Geosciences Department, 2004).

The information in this and the individual STIDs is part of the data provided by PG&E to the FERC 5-year independent reviewers to help in their inspection of the dam and in discussions of potential failures of the dam (Potential Failure Mode Analysis, or PFMA).

The scope of the present study includes the following:

1. Reviewing data in PG&E's files
2. Compiling and reviewing recently published data
3. Analysis of the data
4. Preparation of this report

## 1.3 ACKNOWLEDGEMENTS

This report was prepared at the request of Andrew Yu, Senior Civil Engineer, who is responsible for the FERC-5-year safety reviews of PG&E's dams. William D. Page, Senior Engineering Geologist, PG&E Geosciences Department, prepared tectonics section and compiled the report. Todd Crampton and Courtney Johnson, Geomatrix Consultants compiled the regional geology section. Thomas L. Sawyer, Principal Geologist, Piedmont GeoSciences, described and assessed the potential seismic sources for the dams. Marcia McLaren, Senior Seismologist, and Megan Stanton, Seismologist, PG&E Geosciences Department, analyzed the seismicity and prepared that section of this report. Ti-Ben Tsai, Senior Seismologist, PG&E Geosciences Department, prepared the ground section.

# 2.0 REGIONAL TECTONICS

## 2.1 SIERRAN MICROPLATE

The Sierran Microplate (Figure 2-1) encompasses two geomorphic provinces: the Central Valley in the west and the Sierra Nevada in the east. It is is 680 km long and 80 to 190 km wide, and is a relatively rigid tectonic block that lies within the 1000-km-wide zone of distributed deformation between the Pacific plate and stable North America (Argus and Gordon, 1991, 2001; Dixon and others, 2000; Page and others in preparation). This contemporaneous motion is in response to the differential movement between the Pacific and North American lithospheric plates. The microplate lies within a 1500 km-wide boundary between the Pacific plate and North America plate. The main boundary fault is the San Andreas fault system. However, the plate boundary motion bifurcates eastward from the San Andreas fault system in southern California and about a quarter of the plate motion is transferred to the Eastern California shear zone and northward to Oregon through the Walker Lane belt. The Eastern California shear zone and Walker Lane belt collectively form an active transtensional zone (right-slip and normal) that transfers 12 ± 2 mm/yr that is approximately 25 percent of the contemporary Pacific-North American plate motion between the Sierran microplate and the Basin and Range (e.g., Weldon and Humphreys, 1986; Savage and others, 1990; Dokka and Travis, 1990; Sauber and others, 1994; Bennett and others, 1999, 2003; Thatcher and others, 1999; Dixon and others, 2000). Space-based geodesy confirms that the entire Sierra Nevada is moving as part of a 'rigid' block about 12 to 14 millimeters per year (mm/year) northwest with respect to stable North America (Argus and Gordon, 1991, 2001; Dixon and others, 2000).

Motion of the Sierran microplate with respect to surrounding provinces is accommodated primarily by active deformation along its margins that are marked by moderate seismic activity (Figure 2-2). The geologic structures that separate the microplate from the surrounding tectonic provinces are (a) the Sierra Nevada Frontal fault system that forms the western side of the Walker Lane belt on the east, (b) the Coast Range-Sierran Block boundary zone between the Central Valley and the Coast Ranges on the west, (c) the Garlock fault and the associated Wheeler Ridge and White Wolf faults at the south end of the Central Valley on the south, and (d) inferred contraction structures between the Central Valley and the Klamath Mountains on the north. The physiography records uplift and westerly tilting of the Sierra Nevada, and basin sediments document subsidence of the Central Valley during the Miocene and then again within the past approximately 4.5 to 4 million years (Unruh, 1991). Part of the present topography consists of inherited landforms that formed before 4.5 million years ago (e.g., Wakabayashi and Sawyer, 2001).

Although the Sierran microplate moves as an independent block, it is not perfectly rigid. Seismicity within the microplate, though at a los level, indicates that distributed brittle deformation is occurring within the block. Historical earthquakes within the Sierran microplate include the 1975 (M 5.7) Oroville earthquake and the 1946 (M 6.0) Walker Pass earthquake. Only eleven other earthquakes larger than magnitude 5 have been recorded within the microplate, and magnitude 4 earthquakes are relatively rare. With the exception of the linear 1980s Durrwood Meadows swarm (Jones and Dollar, 1986) in the southern Sierra Nevada that

lies about 10 kilometers east of the Kern Canyon fault, the predominant seismicity patterns in the microplate are diffuse trends and scattered clusters of earthquakes.

The northern and central parts of the microplate lie north of the San Joaquin River. Bedrock as exposed in the range is predominantly metamorphic terranes in the western foothills with granitic intrusions dominant near the range crest. Remnants of Cenozoic volcanic lahars and eruption deposits that blanketed the bedrock north of the Tuolumne River and extend into the Central Valley. These are the Valley Springs and Mehrten formations between the Tuolumne and Feather rivers and the Tuscan Formation between the North Fork Feather River and Lassen Peak. North of there the north end of the sierra is covered with Quaternary volcanic deposits from the southern Cascade volcanoes. The basement rocks beneath the Central Valley are buried by Cretaceous marine sedimentary rocks that dip westward; these overlain by the Cenozoic volcanic rocks mentioned above and Quaternary alluvial depsoits.

The southern part of the microplate extends for 120 km from Fresno and the San Joaquin River on the north to Bakersfield and the Tehachapi Mountains on the south. The bedrock that underlies the southern Sierra Nevada is mostly Mesozoic granitic intrusive rocks but. metamorphic terrane "roof pendants" occur within the batholiths. South of the San Joaquin River the metamorphic terrane follows the east margin of the Central Valley to Porterville, where they project beneath the alluvial deposits that burry the basement rocks in the valley. Small Pliocene and Quaternary volcanic flows, cones, and vents are scattered across the southern range crest. As in the northern and central parts of the microplate the basement rocks beneath the Central Valley are buried by Cretaceous marine sedimentary rocks that dip westward.

## 2.2 LATE CENOZOIC TECTONICS

The Quaternary faults of the Sierra Nevada Frontal fault system form the boundary between the eastern margin of the Sierran microplate and the western side of the Walker Lane. These typically exhibit evidence of Quaternary east-down normal and/or dextral faulting. Between Owens Valley and Lake Tahoe, the fault system displays a left-stepping *en echelon* pattern with individual faults oriented oblique to the trend of the range (Bateman and Wahrhaftig, 1966; Wakabayashi and Sawyer, 2001; Unruh and others, 2003). The orientation and left-stepping geometry of these faults is evidence that they have formed in a transcurrent regime and primarily accommodate Sierra Nevada-North American motion (Unruh and others, 2003)(Figure 2-1). The largest seismic event to occur in the Walker Lane east of the central and southern Sierra Nevada is the M 7.5-7.7 Owens Valley earthquake that occurred in 1872 that ruptured the Owens Valley fault zone (Gilbert, 1884; Beanland and Clark, 1994)(Figure 2-1). The surface rupture extended 121 $\pm$12 kilometers, extending from the southern shore of Owens Lake to north of Big Pine (Jennings, 1994; Peterson and others, 1996), with ground deformation caused from shaking documented as far north as Bishop (Vittori and others, 1993; Beanland and Clark, 1994) and as far west as Yosemite Valley (Muir, 1971). Displacement was oblique slip, having $6.0 \pm 2.0$ meters of right-lateral and $1.0 \pm 0.5$ meters of down-east normal slip (Beanland and Clark, 1994). Other seismic events along the frontal fault system are discussed in the section 4 of this report.

The Sierra Nevada-Coast Range boundary zone bounds the west side of the Sierran microplate. Convergence between the two plates is causing the subsidence of the Central Valley and uplift of the Coast Ranges. The eastern margin of the Coast Ranges and western side of the subsiding Central Valley is marked by a zone of active anticlines that are the surface expression of the thrust and reverse fault system that extend from southwest of Bakersfield to at least Red Bluff (Wong and Ely, 1983; Wong and others, 1988; Wakabayashi and Smith, 1994). The faults in the system have moderate activity with slip rates of 1 to 3 mm/yr. The 1892 Vacaville-Winters earthquake ($M_w$ 6.8) and 1983 Coalinga ($M_w$ 6.5) earthquakes are associated with different fault segments in the zone.

The most recent pulse of uplift started between 4.5 and 4 million years ago, marking the onset of the current tectonic regime (Unruh, 1991). During the current tectonic uplift, limited faulting within the block has occurred. In the northern Sierra Nevada the uplifted block contains Quaternary faults, such as short, reactivated sections within the ancient Mesozoic Foothills fault system; these are generally less than 20 kilometers long and have slip rates generally less than 0.01 mm/year (e.g., Schwartz and others 1977; Page and Sawyer 2001). Another ancient fault zone that has been only recently recognized as being reactivated in the current tectonic regime is the Kern Canyon fault (Nadin and Saleeby, 2001; Nadin, 2007).

The Owens Valley and the structural basins and valleys east of the Sierra Nevada crest were formed by late Cenozoic tectonic deformation associated with a period of uplift of the Sierra Nevada that began after 10 to 12 million years ago, marking the onset of east-west directed extension related to Basin and Range style faulting (e.g., Lueddecke and others, 1998; Stockli and others, 2000). The current ongoing period of uplift of the Sierra Nevada began approximately 3 to 5 million years ago (Unruh, 1991; Wakabayashi and Sawyer, 2001). The uplift was accompanied by westward tilting of the range and related stream incision and downwarping of the Central Valley. Between 3 to 5 million years ago, the oldest lacustrine sediments were deposited in what is now the White-Inyo Mountains and Coso Range, east of the Sierra Nevada. These sediments were deposited in a half graben created by early movements along the Walker Lane Belt and displacement on the Sierra Nevada Frontal fault system (Bachman, 1978; Bacon and others, 1979; Lueddecke and others, 1998; Berman, 1999). After approximately 3 million years ago, the formation of the White-Inyo frontal faults and consequent formation of the Owens Valley graben are marked by the end of lacustrine deposition and the beginning of coarse clastic deposition and volcanic activity (Lueddecke and others, 1998). Graben formation east of the Sierra Nevada front during the Pliocene is largely related to reactivation of older extensional structures and truncation of Miocene tilted fault blocks by the Owens Valley and White Mountain fault zones driven by transtension associated with the Walker Lane belt and Eastern California shear zone (e.g., Lueddecke and others, 1998; Stockli and others, 2000).

Deformation within the Sierra Nevada microplate south of Lassen Peak and north of Mariposa is distributed across the full width of the range (Sawyer and others, 1993; Jennings, 1994; Page and Sawyer, 2001). The faults with higher rates of deformation, up to 0.1 mm/yr (vertical) are localized directly west of the crest, where *en echelon* east-down frontal faults "bleed" cross the crest (Sawyer and others, 1993; Wakabayashi and Sawyer, 2000; 2001; Unruh and others,

2003). Within the range, internal deformation commonly occurs along reactivated, optimally oriented sections of the ancient Sierra Nevada Foothills fault system (e.g., the late Cenozoic Giant Gap fault), an early Mesozoic subduction zone (Clark, 1960; Schweickert and Cowan, 1975). Late Cenozoic deformation rates are very low, ranging from 0.001 to 0.01 mm/yr (e.g., Alt and others, 1977; Woodward-Clyde Consultants, 1978; Biggar and others, 1978; Sawyer and others, 1993; PG&E, 1992, 1994a, 1994b; Wakabayashi and Sawyer, 2001; and Page and Sawyer, 2001).

Late Cenozoic faults in the southern Sierra Nevada are few, likely due in part to the lack of late Cenozoic deposits that are used to the north to identify late Cenozoic faults (e.g., Page and Sawyer, 2001). Quaternary faults at the southern end of the southern Sierra Nevada include the Kern Canyon and Breckenridge faults and a group of small faults north of Bakersfield that show activity from oil production. A possible Quaternary fault is the northwest-striking prominent lineament along the base of Blue Mountain, 25 miles east of Delano, identified in an earlier reconnaissance study by PG&E (W.D. Page, personal communication, 2004).

The causes of the uplift are currently being debated and the model that explains most of the features in the southern Sierra Nevada is called ”foundering,” with the Sierra being uplifted after the loss of its eclogitic root by detachment and descent into the mantle (Jones and others 2004). The cause of uplift in the central and northern Sierra remains uncertain.

# 3.0 REGIONAL GEOLOGY

PG&E's Mokelumne and Stanislaus hydroelectric system are in the watershed of the North Fork Mokelumne River and the South Fork Stanislaus river systems in the north-central Sierra Nevada. From their headwaters near the Sierran crest, where local elevations reach about 9,000 feet, the rivers flow westward about 150 miles to their confluences with the San Joaquin River in and south of the delta in the Central Valley. The watershed encompasses parts of Alpine, Amador, Calaveras, and Tuolumne counties.

The geology of the north-central Sierra Nevada is complex, reflecting a long and diverse geologic history (Figures 3-1 and 3-2). The foothills in this region are composed of Paleozoic and Mesozoic metamorphic rocks that represent the vestiges of island arc terranes that were accreted to the North American continent along ancient subduction zones. The higher parts of the Sierra Nevada are predominantly composed of Mesozoic granitic rocks that have intruded the older Mesozoic and Paleozoic rocks during the late Jurassic to Late Cretaceous Nevadan orogeny. Tertiary volcanic flows and volcaniclastic rocks overlie the granitic and metamorphic rocks throughout the central and northern parts of the range, forming broad, concordant divides between the major west flowing rivers. These rocks are composed of the Valley Springs and Mehrten formations. Extensive weathering has altered the various rocks where erosion has been restricted, such as on the flat topped divides and interfluves.

## 3.1 GEOMORPHOLOGY OF THE CENTRAL SIERRA NEVADA

The Sierra Nevada consists of two distinct physiographic regions that are divided at the San Joaquin River. The northern region is typically a gently west-sloping range that culminates in a narrow zone of high peaks; the southern part is a high plateau with higher peaks and a moderate west slope; both parts have a steep eastern slope or escarpment.

The Mokelumne-Stanislaus region is typical of the northern region. The western slope of the north-central Sierra Nevada forms a gently westward sloping surface that is the tilted partly preserved, relict landscapes from the Cretaceous and middle Tertiary and the depositional surface on the Mehrten Formation that buries the older erosion surfaces (Figure 3-3). Remnants of the Tertiary landscapes and volcanic deposits remain as the broad relatively flat divides between the major rivers. The eastern escarpment reflects the normal faulting on the Sierra Nevada Frontal fault system.

Carved into this landscape are the deep canyons of all the major west flowing rivers in response to the tectonic tilting in the late Cenozoic. The topography in the higher parts of the central Sierra Nevada is rugged, with steep-walled canyons up to several thousand feet deep carved by glaciers where large areas of predominantly granitic bedrock are exposed on canyon walls, along the ridge tops, and in the glacially-scoured bottoms of canyons. Soil cover in the higher parts of the range is generally thin, and vegetative cover ranges from very sparse to moderate. Slope instability in this area typically is rockfall and snow avalanches, and less common debris flows.

The deep canyons near the range crest shallow toward the west and become wide valleys in the

foothills at the eastern margin of the Central Valley.

Canyons in the foothills of the range are up to about 2,000 feet deep with steep slopes that are generally more densely vegetated and Rock outcrops are less common. Soil and colluvium is thicker than in the higher parts. in the lower parts of the range, and deep weathering of the metamorphic, granitic, and volcaniclastic bedrock is common, especially along less eroded interfluves and adjacent upper canyon walls. Below the glacial limit the combination of steep slopes, deeper bedrock weathering, and locally thick deposits of colluvium, result in more numerous occurrences of slope failures, including debris flows, mud flows, and landslides. Rockfall also occurs on steeper canyon slopes. The deep weathering of the basement rocks from these ancient erosion surfaces has been preserved and is important because it affects the engineering characteristics of the foundation rocks of the dams in the Mokelumne-Stanislaus region

## 3.2 ACCRETED TERRANES IN THE SIERRA NEVADA FOOTHILLS

The oldest rocks in the region are the Paleozoic and Mesozoic accreted terranes exposed in the foothills of the central and northern Sierra Nevada (Figure 3-1). These rocks, which are collectively referred to as the western metamorphic belt (e.g., Bateman and Wahrhaftig, 1966), form relatively continuous, northwest-trending bands of different rock units that are separated by the Melones fault zone. Local, isolated masses of Sierran granitic rocks occur within the western metamorphic belt throughout the region (Jennings, 1977; Wagner and others, 1981). The rocks of the western metamorphic belt are pervasively foliated and closely fractured, and typically are strong and resistant to erosion.

The Paleozoic terranes include metasedimentary and metavolcanic rocks of the Calaveras Complex west of the Melones fault zone and the Shoo Fly Complex east of the Melones fault zone. These terranes were initially deposited in an island arc setting near what was then the western margin of the North American continent (Harden, 1998). The Paleozoic terranes were accreted to the North American continent during various phases of subduction beginning in the early Devonian and culminating with the early Triassic Sonoma orogeny (Harden, 1998). These rocks become progressively younger to the west, with the Calaveras Complex being the younger of the two terranes. The Shoo Fly Complex are the oldest rocks in the central and northern Sierra Nevada and generally consists of quartzite and schist, with minor limestone and dolomite. The Calaveras Complex generally consists of chert, argillite, and slate, with minor amounts of limestone, dolomite, and volcanic rocks. The western boundary of the Calaveras Complex is the Melones fault zone (Jennings, 1977; Wagner and others, 1981).

The Mesozoic terranes to the west of the Melones fault zone represent a younger series of island arc deposits that were subducted beneath the North American continent during the Mesozoic. This period of subduction produced an arc of active Andean-type volcanoes located in the approximate position of the present-day Sierra Nevada (Harden, 1998). The accreted Mesozoic terranes are collectively referred to as the Foothills Metamorphic Belt (Norris and Webb, 1990), or the Foothills terrane (Harden, 1998), the term that we use in this report. The Foothills terrane in the central Sierra Nevada consists of numerous northwest-trending narrow zones and slivers

of metasedimentary and metavolcanic rocks. These rocks are subdivided (e.g., Wagner and others, 1981) into four fault-bounded belts/terranes. From east to west these are the Mother Lode belt that consists predominantly of slate and metavolcanic rocks, the mélange belt that consists of chaotically intermixed metasedimentary and metavolcanic rocks, the ophiolite terrane that consists of metasedimentary, metavolcanic and ultramafic rocks that are bounded by faults in the Bear Mountains fault zone, and the Western belt that consists of metavolcanic rock and slate.

The Tiger Creek Regulator, Tiger Creek Afterbay, and Lake Tabeaud dams in the Mokelumne River drainage are sited on rocks of the western metamorphic belt. The engineering properties of the rocks in the region vary greatly, depending on rock type, degree and depth of weathering, and fracture density. In general, the metamorphic rocks are strong and hard where slightly weathered and fresh; however, where moderately to severely weathered, they may have engineering properties similar to those of a soil. Slopes underlain by massive (unfractured) to widely fractured rock also tend to be more stable than slopes underlain by closely fractured rock. In the lower parts of the range, the depth of weathering may be on the order of several tens of feet, commonly remnants of the Cretaceous and Tertiary weathering profiles, whereas in the higher parts of the range the weathering depth is much less due to removal of the weathered zone by glaciers.

## 3.3 GRANITIC ROCKS OF THE SIERRA NEVADA BATHOLITH

The Nevadan orogeny marked the culmination of Mesozoic subduction along the western margin of North America and was accompanied by widespread emplacement of granitic plutons that collectively form the Sierra Nevada batholith. These rocks are as old as about 200 million years (mid-Late Jurassic), but mainly are about 125 to 82 million years old (Early to Late Cretaceous) (Bateman and Wahrhaftig, 1966). The plutons generally consist of granite, quartz monzonite, granodiorite, quartz diorite, and gabbro, and are distributed throughout the range (Bateman and Wahrhaftig, 1966). In the Mokelumne-Stanislaus region, granitic rocks are exposed locally in the foothills and throughout the higher parts of the range. Where unweathered these rocks generally are very hard, massive to closely fractured, and resistant to erosion. Steeply-dipping, northwest- and northeast-trending joints are prominent throughout the Sierra Nevada, as are exfoliation, or sheeting joints, that generally parallel or subparallel the local topographic surfaces. At higher elevations, Pleistocene glaciers have removed the weathering profile by erosion. At lower elevations, the granite has a weathering profile that in places is up to several tens of feet thick except where rivers and the larger streams have eroded through the deep weathering and expose fresh rock in the lower canyons.

Upper Blue Lake, Lower Blue Lake, Meadow Lake, Bear River, Lower Bear River, and Salt Springs dams in the Mokelumne drainage and Relief, Main Strawberry and Lyons dams in the Stanislaus drainage are founded on granitic rocks of the Sierra Nevada batholith. The engineering properties of the rocks in the region vary greatly, depending on rock type, degree and depth of weathering, and fracture density. In general, the granitic rocks are strong and hard where slightly weathered and fresh; however, where moderately to severely weathered, they may have engineering properties similar to those of a soil. Slopes underlain by massive

(unfractured) to widely fractured rock also tend to be more stable than slopes underlain by closely fractured rock. In the lower parts of the range, the depth of weathering may be on the order of several tens of feet, commonly remnants of the Cretaceous and Tertiary weathering profiles, whereas in the higher parts of the range the weathering depth is much less due to removal of the weathered zone by glaciers.

## 3.4 TERTIARY STRATIGRAPHY

During the Late Cretaceous to middle Eocene, the Sierra Nevada underwent a period of uplift that was followed by widespread erosional denundation (e.g., Wakabayashi and Sawyer, 2001). This period of erosion exposed much of the Nevadan plutonic rocks and is recorded by two overlying Eocene deposits, the Ione Formation and "auriferous gravels" that were deposited by low-gradient westerly flowing drainages. These deposits occur in places throughout the region: the auriferous gravels as narrow channels beneath the overlying younger Cenozoic deposits and the Ione Formation forming a discontinuous band along the western margin of the foothills between the Mokelumne and Consumes Rivers (Figure 3-1). The Ione Formation typically rests on a deeply weathered surface with as much as 1000 feet of local relief cut into the underlying granitic basement (Bateman and Wahrhaftig, 1966).

Between the Oligocene and the early Pliocene, intermittent periods of volcanic activity resulted in thick accumulations of ash, volcanic flows, and mudflows on the eroded and weathered surface in the northern and central Sierra Nevada. Rhyolitic tuffs, flows, and volcaniclastic sediments of the 20 to 30 Ma Valley Springs Formation stratigraphically overlie the Ione Formation and "auriferous gravels". The Valley Springs Formation occurs as local remnants throughout the western metamorphic belt, and as a discontinuous band along the western margin of the foothills. Extensive andesitic mudflows and conglomerates overlying the Valley Springs Formation that range in age from 5 to 20 Ma have been termed the Mehrten Formation (e.g., Wagner and others, 1981). The Mehrten Formation occurs locally throughout the higher parts of the central and northern Sierra Nevada, and along the western margin of the foothills (Figure 3-1). The Mehrten rocks consists of agglomerate, conglomerate, tuffaceous siltstones and sandstones, and lahars (volcanic mudflow) deposits (Wagner and others, 1981), all of which are derived from andesitic volcanic sources that existed along and east of the present range crest (Bateman and Wahrhaftig, 1966). These regionally extensive deposits once blanketed the northern and central Sierra Nevada, covering all but a few scattered basement highs (Wakabayashi and Sawyer, 2001). Estimated thicknesses of the Mehrten Formation range from about 3,000 near the range crest to about 500 feet in the foothills (Slemmons, 1966). Today, dissected remnants of the Mehrten Formation cap the broad divides between the major, west-flowing rivers in the region. The distinctive Table Mountain latite is a 9-million-yearold lava flow within the Mehrten that originated in the upper Stanislaus drainage near the Dardanelles and flowed both east and west (Slemmons, 1966). It caps the long ridge north and west of Sonora called Table Mountain, a classic example of inverted topography and a great stratigraphic marker to measure post latite tectonic deformation and faulting (Figure 3-4).

The late Cenozoic Mehrten Formation and other volcanic rocks in the region generally are indurated, moderately to strongly consolidated, and moderately resistant to erosion. These rocks

are not close to the PG&E dams but slope failures can affect access.

## 3.5 QUATERNARY STRATIGRAPHY

Quaternary deposits are sparse in the north-central Sierra Nevada (Figure 3-1), except for extensive colluvium that covers the slopes below the glacier limits. The oldest Quaternary deposits in the region are basalts that occur as small, isolated bodies southwest of Lake Tahoe. These basalts likely are related to Late Cenozoic extensional tectonics in the region, as opposed to the arc-type volcanism that predominated in the middle to late Tertiary (e.g., Wakabayashi and Sawyer, 2001). Remnants of glacial moraines occur locally in the higher parts of the region, and are generally more extensive along the crest of the range. Within the headwaters of the Mokelumne and Stanislaus rivers, thin glacial deposits are common but significant remnants are scattered and isolated.

Quaternary alluvial deposits limited with the most extensive occurring as alluvial fill in fault-bounded basins along the east side of the range. On the west side alluvium is restricted to thin, narrow deposits along stream and river channels. Small, alluvial-filled valleys also occur locally in the higher, glaciated parts of the range. Although not shown on the regional-scale published maps of the region, colluvial deposits locally mantle the hillslopes throughout the north and central Sierra Nevada. These deposits locally overlie severely weathered bedrock (saprolite), and vary in thickness from a foot or less to several tens of feet. These deposits generally are more widespread in the foothills, as repeated Pleistocene glaciations have removed most of the colluvial and saprolitic deposits in the higher parts of the range. In the lower foothills, colluvial deposits range in age from modern to about 500,000 years (Swan and Hanson, 1977).

Quaternary surficial deposits include narrow alluvial deposits along the main steams and rivers, thin colluvium that mantles most of the slopes, particularly below the glacial limits. Landslides and debris flow deposits occur locally throughout the north-central Sierra Nevada. Glacial deposits of several ages occur throughout the higher parts of the range above approximately 3,900 feet elevation but have been extensively eroded by rivers and creeks that stripped out the deposits along the rivers as the glaciers retreated. Glacial deposits are typically more common near the range crest and are less eroded on the eastern slope of the range.

The Quaternary deposits in the region vary widely in their degree of consolidation, and generally are susceptible to erosion.

## 3.6 LATE CENOZOIC FAUTS IN THE MOKELUMNE-STANISLAUS REGION

Active faults in the Mokelumne –Stanislaus region are divided into two groups based on their activity in the late Cenozoic: those in the Sierra Nevada frontal fault system that have moderate slip rates, generally 1 to 2 mm/yr, and those within the Sierran microplate that have very low activity, generally less than 0.01 mm/yr. In this region the frontal faults are stepping left from the Walker River to Lake Tahoe and several cross the range crest before dieing out in the microplate (Figures 3-3, 3-5). These faults include the Antelope Valley-West Walker, Carson Range fault zone, and the West Tahoe and Waterhouse Peak faults.

The faults that are considered significant potential seismic sources for PG&E dams in the

Mokelumne-Stanislaus region are shown on Figure 3-5, listed in Table 3-1, and described in Appendix A. The most active faults are those in the Sierra Nevada Frontal fault system and include the Carson Range, West Tahoe, Waterhouse Peak, Antelope Valley and West Walker faults. The low activity faults within the Sierran microplate include the Gopher Gulch, Douds Landing, and Post Corral faults.

# 4.0 REGIONAL SEISMICITY

PG&E dams in the Mokelumne and Stanislaus region are in the central Sierra Nevada, an area of low to moderate seismicity in the past 150 years (Figure 4-1). The seismicity patterns of magnitude 3 and larger earthquakes show a few scattered events in the general area of the dams with most of the seismic activity concentrated along a southeast trend near the California/Nevada state line that is associated with structures in the Walker Lane.

The earthquake catalog used in this study includes historical seismicity from 1868 through 1965 and more recent instrumentally recorded data from 1966 through March 13, 2007. The historical period covers the time prior to the installation of local seismographs. Selected earthquakes for the two time periods are described in sections 4.1 and 4.2 below. Sources of earthquake data include Bolt and Miller (1975), Toppozada and others (1978; 1981; 2000), the Advanced National Seismic System (ANSS) catalog (ANSS, 2007) and Stover and Coffman (1993). The ANSS catalog combines data from regional seismic networks, including the northern and southern California U.S. Geological Survey (USGS), University of Nevada, Reno, and U. C. Berkeley (including Bolt and Miller, 1975), into one online searchable catalog.

The catalog for the Mokelumne/Stanislaus region is generally complete for magnitude 4 and greater since 1868. Magnitude 3, instrumentally recorded earthquakes began appearing in the catalog in the early 1940's, and are exclusively from the U.C. Berkeley catalogs until about 1963, when the University of Nevada, Reno, took over the U.C. Berkeley station in Reno. The pre-instrumental magnitudes (M) for events before about 1940 are local (Richter, $M_L$) magnitudes estimated from intensity data (Toppozada and others, 1978; 1981; 2000) or magnitudes based on felt area (Mfa). Post-1940 magnitudes generally are either local (Richter, $M_L$) or coda duration ($M_D$) magnitudes.

The accuracy of the epicentral locations for historical earthquakes depends on the number and distribution of the reporting localities. The epicentral uncertainty for most of the pre-1900 earthquakes is less than 50 kilometers (Toppozada and others 1981). Location uncertainties for the instrumentally recorded events in the region improved with time. U.C. Berkeley installed seismographs as early as 1963, at Oroville, Mineral, and Jamestown, which helped constrain epicentral locations to within 5-10 km. However, depth control for these events remains poor due to large distances between stations and between stations and the earthquake source. Until 1972 there were no seismographic stations within 50 kilometers of the dams. With the addition of local short-period seismographs, station coverage and velocity models were sufficient to reduce epicentral uncertainties to typically less than 5 kilometers. However, depth uncertainties near the dams are still poor (~50km), as the modern stations are 30 km from the dams on average with station coverage only along the crest and the valley of the Sierra Nevada range.

## 4.1 HISTORICAL SEISMICITY, 1868 THROUGH 1965

The historical earthquake record consists of newspaper reports, personal diaries, records from U.S. Army outposts, and other historical documents. These records generally provide a good estimate of the time of earthquake occurrence and magnitude, but the location precision depends

on the number of people observing the event and the accuracy of their observations. The record of historical earthquakes in the study area began with the settlement of gold mining camps in the Sierra Nevada foothills in the western section of the study area in 1849. Similar settlements in western Nevada, primarily related to gold and silver mining in the Virginia Range, were founded in the 1850's. It was not until the 1870's, when the population had increased along the east side of the Sierra Nevada from the Owens Valley in the south to the Modoc Plateau in the north, that newspaper coverage was complete throughout most of the study area (Toppozada and others, 1981). The seismicity record within approximately 50 kilometers of the PG&E dams in the Mokelumne/Stanislaus region contains six earthquakes that were documented between 1868 and 1966 and were assigned magnitudes of 5 or greater, described below. The earthquake locations are shown in Figure 4.

**September 17, 1868** – A M 5.6 earthquake occurred about 70 km southeast of Lake Tahoe (Toppozada and others, 2000). The magnitude was an update from the earlier estimate of 5.2 (Toppozada and others, 1981). The intensity reported was V; the felt area was 42,000 $km^2$ (Stover and Coffman, 1993).

**July 10, 1877** – This earthquake occurred at the southern end of Lake Tahoe near the Tahoe-Sierra frontal fault zone (U.S. Geological Survey, 2007). The event was originally reported by Slemmons and others (1965), as an Mfa 5.00, and later updated to an M 5.5 by Toppozada and others (2000).

**January 11, 1939** – This $M_L$ 5.5 (ANSS, 2007) earthquake occurred about 35 kilometers southeast of Lake Tahoe and 25 kilometers northwest of the September 17, 1868 event. The shock was felt over 8,000 square miles; MM intensities of VI were felt in Coleville, and V in Altaville and Tuolumne, California and Gardnerville and Hudson, Nevada (Bolt and Miller, 1975).

**December 17, 1942** – This was an $M_L$ 5.1 event that occurred near the California-Nevada border, south east of Lake Tahoe (ANSS, 2007).

**March 22, 1953** – This $M_L$ 5.0 event (Stover and Coffman, 1993) occurred 10 kilometers due south of Lake Tahoe and 20 kilometers north of Upper Blue Lake Dam, south of the Tahoe-Sierra frontal fault zone (U.S. GEOLOGICAL SURVEY and others, 2007).

**April 13, 1962** – This was a $M_L$ 5.1 earthquake (Stover and Coffman, 1993) that occurred approximately 80 kilometers northeast of Sonora.

## 4.2 INSTRUMENTAL SEISMICITY, 1966 THROUGH 2007

The Mokelumne/Stanislaus region, as shown in Figure 4-1, is generally a quiet seismic area. Only a few scattered M3's have been recorded and no significant (M≥5) events have occurred between the Sierran crest to the northeast and the San Andreas fault system across the valley to the southwest. Clusters of events are common near the San Andreas fault zone southwest of Modesto, to the northwest in the Sierra foothills near Oroville, southeast near Mammoth. The largest earthquakes occurring within 50 km of the dams are an $M_L$ 6 earthquake in 1994, two $M_L$ 5 earthquakes in 1978 and 1979, and an $M_L$ 4.7 earthquake in 2007; focal mechanisms for

the 1978 and 1994 earthquakes show right lateral strike slip motion to the north, consistent with right lateral shear within the Walker Lane belt (Figure 4-1). The events are described in more detail below.

**September 4, 1978** – At $M_L$ 5.3 (Stover and Coffman, 1993), this was the largest of 28 events from September 3rd through September 4th. The events were located approximately 80 kilometers southeast of Lake Tahoe. Damage was minimal with only cracks in drywall and hairline cracks in exterior walls reported (Stover and Coffman, 1993).

**October 07, 1979** – UC Berkeley reported this event as a $M_L$ 5.0. The earthquake occurred about 100 kilometers southeast of Lake Tahoe and approximately 10 kilometers due east of the April 13, 1962 $M_L$ 5.1 event. The maximum intensity was IV and the event was felt over an area of 15,000 $km^2$ (Stover and Coffman, 1993).

**September 12, 1994** – The $M_L$ 6.0 (dePolo and others, 1995) Double Spring Flat earthquake occurred in Nevada near the California border, 45 kilometers south of Carson City, Nevada. The earthquake epicenter was beneath the hills near Double Spring Flat between Pine Nut Mountains and the foothills of the Sierra Nevada. The earthquake hypocenter was relatively shallow, less than 8 kilometers deep (Dianne dePolo, personal communication, 1994). The earthquake focal mechanism shows right slip along a northwest-striking fault plane, which is consistent with late Quaternary structural trends in the area (PG&E, 1994). Damage was minimal since the area has a relatively low population and no injuries were reported. Ground cracking was noted in the epicentral area, but appears to be secondary in nature. (dePolo and others, 1997) Aftershocks extended over a distance of about 12 km and are distributed in the stepover area north and northwest of the Antelope Valley fault (PG&E, 1994). Several small foreshocks occurred over a 12 day period leading up to the main shock and background seismicity notably occurred in the area over the year or two before the event (dePolo and others, 1997).

**March 8, 2007** – The Bridgeport earthquake occurred 14 miles NNW of Bridgeport, CA and 22.3 miles ESE of Relief Dam. The ANSS (2007) reported an $M_L$ 4.7 for the earthquake and a hypocentral depth of 6.5 miles. The event was preceded by one $M_D$1.8 and followed by over 100 aftershocks; the largest was an $M_L$ 3.8 event three minutes after the main shock. The main shock focal mechanism shows normal motion along a north-northeast striking fault, which is consistent with the traditional Basin and Range faults in the eastern part of the Walker Lane Belt. The closest PG&E accelerometer at Salt Springs dam, about 44 miles ENE of the epicenter, did not trigger on the earthquake. This earthquake occurred about 6.2 miles south east of the 1939 M5.5 event and 12.4 miles north of the 1979 M5.2 event.

## 4.3 CONCLUSIONS FROM SEISMICITY

Based on our analysis of the seismicity in the central and southern Sierra Nevada region, we conclude the following:

1. The low level of seismicity within the Sierran microplate is consistent with the low activity faults within the range.

2. Focal mechanisms of microearthquakes within the microplate indicate normal and strike slip mechanisms in the eastern part of the microplate and reverse mechanisms the western part.
3. The Sierra Nevada frontal faults and adjacent faults in the Walker Lane have low to moderate activity, and focal mechanisms with normal and strike slip mechanisms consistent with the geology known in this area.
4. Most of the earthquakes in the swarms near Mammoth are associated with volcanic activity on the Long Valley Caldera. Some strike slip events indicate tectonic events as well in this area.
5. The depth of the seismogenic crust along the Sierra Nevada frontal fault system is 10 to 20 kilometers, similar to estimated depths to the north (PG&E Geosciences Department and Piedmont GeoSciences, 2003).

# 5.0 OVERVIEW OF GROUND MOTION ESTIMATES, PG&E DAMS

## 5.1 INTRODUCTION

PG&E reviews the estimates of potential ground motions for the dams in the PG&E hydroelectric system every 5 years as part of the FERC 5-year independent consultants inspection of the PG&E dams. We also review the ground motions following significant earthquakes (greater than magnitude 5). As discussed below the estimated ground motions have changed over time reflecting increases in knowledge and understanding of tectonics, faulting and ground shaking.

As part of PG&E's Dam Safety program, we have installed and maintain strong ground motions instruments at several dams: Salt Springs Dam on the Mokelumne River, Almanor Dam and Butt Valley dams on the North Fork Feather River, McCloud Dam on the McCloud River, and Scott Dam on the Eel River. Each site has an instrument on the dam crest and one on bedrock at an abutment. To date these instruments have recorded ground motions from four earthquakes:

September 12, 1994, ML 6.0, Double Springs Flat at Salt Springs Dam.

May 17, 2000, ML4.2 - McCreary Glade at Scott Dam

August 1, 2001, ML 5.3, Downieville at Almanor and Butt Valley Dams, and

April 18, 2007, Mw 4.8, McCreary Glade at Scott Dam,

**Active faults** – Paralleling the development of ground motion models discussed in this section was the progression in the understanding of the characteristics and mechanics of earthquake faulting. The concept of plate tectonics, introduced in its modern concept in the mid-1960s, was accepted and refined as new seismic and geologic information in the decades that followed developed from the nuclear power industry's urgent need for better tectonic models and better understanding of active faulting. In particular detailed mapping and trenching to locate and characterize active faults, and improved age-dating techniques, were used to obtain the needed key parameters to estimate potential ground motions at a particular site: the size of earthquake, its distance from the site, and the degree of activity of the causative fault.

In the 1960s and early 1970s experienced researchers used data from historic and instrumentally located earthquakes, alignments of microearthquakes, and existing information on active faults (mostly those associated with historic earthquakes and historic displacement) to estimate potential ground motions. This technique was refined with the explosion of data from the nuclear studies that discovered many 'new' faults with varying degrees of activity (expressed as displacement rate in mm/yr). With the increased knowledge the definition of active faults changed depending on the facility potentially affected and the agency responsible for the safety of these facilities, such as nuclear power plants and dams.

The State of California published one of the first maps of active faults (Jennings, 1975) and updated the map 20 years later (Jennings, 1994). This reference was extensively used as the

basic source for information on faults to estimate earthquake magnitudes. In many studies, this information was augmented by site specific studies and in PG&E's case the studies included the extensive published and unpublished investigations of faults in the Sierra Nevada that followed the 1975 Oroville earthquake. Since about 2,000 the U.S. Geological Survey, the California Geological Survey and other state agencies have compiled a comprehensive data base for active faults that has been digitized and available for use (U.S. Geological Survey, 2007). These digital data bases are now the resources of choice for obtaining information on active and potentially active faults in these areas.

One of the more important events occurred in the late 1980s when investigations for the PG&E Diablo Canyon Power Plant compiled the complete world-wide data set of fault length, width, displacement recorded in historic earthquakes. This comprehensive regression analysis that related statistically the above parameters to earthquake magnitude was published by Wells and Coppersmith in 1994 and has become the accepted practice for estimating potential earthquake magnitudes.

## 5.2 DEVELOPMENT OF GROUND MOTION ATTENUATION MODELS

Estimates of expected ground motion for a site at a given distance from an earthquake of a given magnitude are fundamental inputs to earthquake hazard assessments. These estimates are usually made using equations, called attenuation relationships or models, that express a ground motion parameter (for example, PGA and SA at a given period) as a function of magnitude and distance (and lately other variables, such as type of faulting or site classification).

Ground motion attenuation models may be determined in two different ways: empirically, using previously recorded ground motions, or theoretically, using seismological models to generate synthetic ground motions that account for source, site, and path effects. There is overlap in these approaches, however, since empirical approaches often fit the data to a functional form suggested by theory, and theoretical approaches often use empirical data to determine some parameters.

Most commonly used ground motion attenuation models are developed by empirical approaches based on statistical analyses of recorded ground motions which are updated as new strong motion data become available. Estimates of ground motion parameters for PG&E dams have followed closely with major developments of the ground motion attenuation models. The following is a brief review of three generations of ground motion attenuation models used for estimating ground motions at PG&E dams.

**Ground Motion Attenuation Models in 1980's** – Many empirical ground motion attenuation models were available in literatures based on relatively few recorded ground motion data. For example, Seed and Idriss (1982) listed 32 available empirical attenuation models for peak ground acceleration (PGA) developed before 1981. Several of these models were more relevant for shallow crustal earthquakes in Western United States, particularly California: Seed and Schnabel and Seed (1973), Campbell (1981), and Joyner and Boore (1981). The last significant set of ground motion records used in these studies was that of the 1979 Ms 6.9 Imperial Valley, California Earthquake. Figure 5-1 shows the attenuation curves of horizontal PGA on rock

(Seed and Idriss, 1982). Figure 5-2 compares the four PGA attuation curves for stiff soils from a Ms 7.5 earthquake. It is interesting to note large differences over all distances, particularly at distances less than 10 km, due to poor constraint by only a few records.

It was found at the time that of the various characteristics of earthquake ground motions, none is so much influenced by the local soil conditions as the shape of the response spectrum (Seed and others, 1976). Since this is the most significant engineering characteristics of an earthquake motion, local site conditions can exert significant influence on earthquake ground motions and therefore on potential structural damage. The spectral shape representative of any group of earthquake ground motion records is obtained by first determining the normalized acceleration response spectrum for each motion in the group. A normalized acceleration response spectrum is obtained by expressing the ordinates of a conventional spectrum as a proportion of the maximum ground acceleration on the record from which the spectrum was derived, or the zero-period ordinate value. For all normalized spectra, the zero-period ordinate is therefore unity, and "mean" or "mean + 1 standard deviation" spectral shapes can readily be determined.

Studies of this type were made for group of ground motion records obtained at four different soil conditions:

1. Rock sites
2. Stiff soil sites (less than 200 ft. deep)
3. Deep cohesionless soil sites (greater than 250 ft. deep)
4. Sites underlain by soft to medium stiff clay deposits.

Figure 5-3 shows the "mean" and "mean + 1 standard deviation" spectral shapes at 5% damping for above four different site conditions. It is readily apparent that there are large differences in spectral shapes depending on the soil conditions, particularly at periods greater than about 0.5 second. Above this period, spectral amplifications are much higher for deep cohesionless soil deposits and for soft to medium stiff clay deposits than for stiff soil conditions or rock. It is interesting to note that a total of only 104 records were used for these analyses.

For engineering purposes these empirical response spectral shapes were simplified by smoothed curves anchored at five points, as shown by 1, A, B, C, D in the top panel of Figures 5.3 and 1, P, Q, R, S in the bottom panel of Figure 5-3. Eventually, these simplified response spectral shapes were consolidated and recommended for use in building code, as shown in Figure 5-4 for three different categories of soil: rock and stiff soils; deep cohesionless soils; and soft to medium stiff clays and sands.

For estimation of earthquake ground motions at PG&E dam sites, the GM attenuation models developed by Seed and Idriss (1982) were commonly used in 1980's.

**Ground Motion Attenuation Models in 1990's -** Development of ground motion attenuation models for shallow earthquakes in active tectonic regions, such as California, entered a new stage with simultaneous publication of five models in the January/February, 1997 issue of the Seismological Research Letters. Details of these models were described in Abrahamson and Silva (1997), Boore and others, 1997), Campbell (1997), Sadigh and others (1997), Spudich and

others (1997). The following is an overview of these models according to Abrahamson and Shedlock (1997). The strong motion records available for use to develop these models were significantly expanded since 1980's and covered major events up to 1994 M 6.7 Northridge, California earthquake, as shown in Figure 5-5.

As shown in Figure 5-6 these models all used the moment magnitude to represent earthquake size and the average of two orthogonal horizontal components to represent the ground motion parameter in the models. With a large data set, effects of parameters other than magnitude, distance, and site condition were included in these models. For example, most models included a style-of-faulting factor to account for distinction between the ground motion from reverse earthquakes and strike-slip earthquakes. Due to small number of records available for normal faulting earthquakes in most data sets, the differences between strike-slip and normal faulting events were not statistically significant, so normal faulting events were usually assumed to generate the same level of ground motion as strike-slip events. Some models also include a factor for the hanging wall effects. The five models are briefly described below.

Abrahamson and Silva (1997) developed empirical response spectral acceleration attenuation models for both the horizontal and vertical components of ground motion. They explicitly include a factor to account for the systematic increase in ground motions recorded at sites over the hanging wall of dipping faults. They also explicitly allow non-linear soil response as a function of the expected peak acceleration on rock. Their approach allows a single functional form to account for attenuation at both soil and rock sites while still allowing for non-linear site response.

Boore and others (1997) summarized their previously published work on estimating SA and PGA for shallow earthquakes in western North America. Their equations were an update of their earlier model (Boore and others, 1993; 1994) and now differentiated the responses for strike-slip, reverse-slip, and unspecified faulting. They also specify more restrictive ranges of M and $R_{jb}$ for use of their updated equations than previous equations. Unlike the other models, they use a quantitative measure for the site classification based on the average shear wave velocity in the upper 30 m.

Campbell (1997) also summarized the results of several years' work developing empirical attenuation models for horizontal and vertical PGA, PGV, and SA in active tectonic regions. These latest versions were developed using a much larger data set (including the 1989 Loma Prieta, 1992 Landers, and 1992 Petrolia earthquakes) than earlier versions. Campbell's models were designed for use to estimate ground motion from earthquakes of $M > 5$ at sites within 60 km.

Sadigh and others (1996; 1997) present attenuation models for horizontal and vertical PGA and SA for shallow crustal earthquakes determined from strong motion records obtained primarily in California. Their models are applicable to earthquakes of M 4 to 8+ at distances of up to 100 km.

Spudich and others (1997) developed new predictive models for PGA and SA using a global data set of earthquake ground motions recorded in extensional tectonic regimes. They

constrained their input data to be from earthquakes occurring and recorded in extensional regimes, defined as "regions in which the lithosphere is expanding areally". In general, their values for PGA and SA are smaller than those derived by other researchers for active tectonic regions.

The median ground motions calculated from these five attenuation models are compared below for M 5.5 and M 7.0 earthquakes. Since three different distance measures are used in the five models, specific fault geometries were defined so as to make valid comparisons. Figure 5-7 compares the horizontal PGA attenuation for a vertical strike-slip fault at rock sites. Similarly, Figure 5-8 compares the horizontal PGA attenuation for a 45-degree dipping fault for sites over the hanging wall on rock. In both cases, the rupture for the M 7.0 event is assumed to rupture to the surface and to a depth of 12 km. For the M 5.5 event , a point source at a focal depth of 5 km is used. The distance measure used in these plots is the horizontal distance from the vertical projection of the top of the rupture.

For comparison of the vertical strike-slip case in Figure 5-7, the various attenuation models yield similar median ground motions for the 10-30 km distance range where the bulk of the data are available and the models all pass through the center of the data (Figure 5.5). At both large and small distances, the differences in the median ground motions become larger, reflecting the small amount of strong motion data in these distance ranges, with the exception of soil sites at small distances. This was affected mainly by a large number of recordings at short distances on soil sites and may lead to underestimate the true uncertainty in near fault ground motions on soil sites.

For comparison of the dipping reverse fault case, the differences in model predictions is larger than for the vertical strike-slip fault case. First of all, for the M 7.0 event, the effects of the hanging wall are apparent in the Boore and others (1997) and Abrahamson and Silva (1997) models. These two models account for differences in ground motions over the hanging wall and the footwall. The hanging wall effects show up as a bump in the attenuation (when plotted as a function of the horizontal distance from the top of the rupture). The models still have good agreement at distance of about 20 km (near the center of the data), but show large variations at short distances for rock sites, reflecting the small number of near-fault recordings on rock sites from reverse faulting events.

The 84$^{th}$ parcentile SA spectra for a M 7.0 vertical strike-slip earthquake at a distance of 10 km are shown in Figure 5-9. At all periods, the spectral values are within a factor of 2 of each other. The Spudich and others (1997) model for extensional tectonic regimes produces the smallest ground motions.

In general, PG&E has used the average of ground motions calculated from these attenuation models for seismic evaluation of its dams in the 1990's.

## 5.3 NEW-GENERATION-ATTENUATION MODELS (NGA)

For present review of PG&E dams the horizontal ground motion values (both PGA and SA) for the crustal sources are computed based on the recently developed suite of empirical attenuation

relationships (New-Generation-Attenuation models, NGA) under the auspices and guidance of the Pacific Earthquake Engineering Research Center (PEER)[1]. The objective of the NGA program was to develop a new set of comprehensive and broadly accepted ground motion attenuation models for the Western US. This program obtained agreement from the major researchers on a much larger, common data base that everyone now uses as the basis for individual relationships developed for estimating ground motions. Each of the 5 research teams, Campbell and Bozorgnia, Chiou and Youngs, Abrahamson and Silva, Boore and Atkinson, and Idriss, selected the portion of the data base that they believed to be most appropriate and developed a suite of ground motion relationships. The researchers then developed five NGA models concurrently to estimate potential ground motions. These models update the five major models that have been used in California and Western United States since the 1997. Many of the authors remain the same in both regression analyses:

| NGA 2007 | Late 1990s |
|---|---|
| Abrahamson and Silva (2007) | Abrahamson and Silva (1997);<br>Spudich and others (1996, 1997);<br>Abrahamson and Becker (1979) |
| Boore and Atkinson (2007) | Boore, Joyner and Fumal (1997) |
| Campbell and Bozorgnia (2007) | Cambell (1997); Cambell and Bozorgnia (2003) |
| Chiou and Youngs (2006) | Sadigh, Chang, Egan, Makdisi and Youngs (1997) |
| Idriss (2007) | Idriss (1994; 1996) |

Note: The 2007 NGA versions are finalized from and essentially the same as the earlier 2006 versions cited in the STID Chapter 5 reports for specific dams in the Mokelumne-Stanislaus region.

NGA developers consider the NGA models to be significant improvements over their previous models because the previous models used much smaller data sets and the data sets did not have as much review. In addition, the teams by working together have provided checks and peer reviews along the way. The results are 5 new-generation-attenuation (NGA) models that are peer-reviewed and will be published in Earthquake Spectra in March 2008. Each of these models use the greatly enhanced strong motion database, incorporate data with well-documented source and site parameters, and have a better basis in physics.

The PEER strong motion database contains 3551 3-component records from 173 shallow crustal

1 PEER stands for the Pacific Earthquake Engineering Research Center. The NGA program is funded by grants from CALTRANS, PG&E, California Energy Commission, and National Science Foundation through PEER. It was established in 2002 to obtain cooperation from the several researchers who had developed earlier relationships to agree on a new updated NGA database for their models. This program is essentially complete with the publication of five regression relationships.

earthquakes from tectonically active regions. It has a wide distribution of events both in magnitude (Mw 5 to 8) and in distance from the fault (0 to 200 km), as illustrated by the 6and Youngs (2007) database that is typical for the NGA Models (Figure 5-10). This database is significantly expanded both in the numbers of earthquakes and records than that used in the previous generation of attenuation models (Figure 5-11).

The important characteristics of the NGA Models, as summarized by Chiou and others (2004) and Power and others (2008), include:

1. A widely applicable magnitude range:
   Mw 5.0 to 8.5 for strike slip faults and
   Mw 5.0 to 8.0 for reverse faults,
2. Extended applicable range of distance from the fault source to 200 km, and in particular, coverage in the near-source (less than 20 kilometers) ground motions is significantly improved,
3. Data from all fault types, strike slip, reverse, and normal, are available.
4. Except for very soft soil, most soil conditions are included in the models (i.e., 180 m/sec $\leq$ Vs30).

Main characteristics of all the five models are tabulated below:

**Characteristics of the NGA Models**

| Effect | Predictors | Highlights |
|---|---|---|
| Magnitude | $M_w$ | No over-saturation of near-field motion with magnitude |
| Distance | $R_{rup}$ or $R_{jb}$ | Anelastic damping: Lg wave propagation |
| Hanging Wall | $R_{run}$, $R_{jb,}$ fault dip, | Higher ground motions on hanging wall |
| Fault Type | Style of faulting | Reverse > strike slip> normal |
| Depth to Fault Rupture | $Z_{Tor}$ | Not considered in previous models. |
| Soil Condition | $V_{S30}$, Depth to bedrock ($Z_{1.0}$, or $Z_{2.5}$) | Nonlinear soil response<br>Deep basin response |

(modified after Chiou, and others, 2004; Power and others, 2008)

**Model Soil Profile: $V_{S30}$ -** Four NGA models use $V_{S30}$ and one uses $V_{S30}$-based for soil classes. This removes ambiguity of the definition of 'rock' and the models are suitable for code application. This soil profile approach improves the past approach of previous models that used 'generic rock' with the following properties:

| | |
|---|---|
| Abrahamson and Silva (1997) | 550 m/sec? |
| Boore and others (1997) | 620 m/sec |
| Cambell and Borzorgnia (2003) | ~ 620 m/sec |

Sadigh and others (1997) 500 m/sec?

The direct modeling of non-linear soil response allows soil amplification as a function of PGA or spectral acceleration on rock, soil class $V_{S30,}$ and depth to bedrock, as shown in the sketch below:

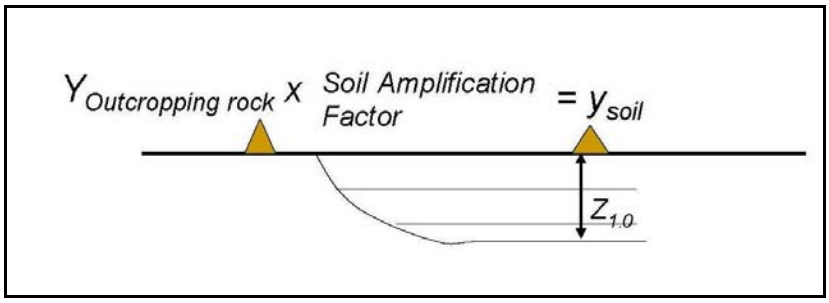


(from Chiou, and others, 2004; Power, and others, 2008)

Some NGA model developers have chosen to use a soil profile based on depth to bedrock to extend their relationships that are important for long-period motions. The definition of 'bedrock' used for $Z_{1.0}$ is Vs=1.0 km/sec and for $Z_{2.5}$ is Vs=2.5 km/sec. As shown in Figure 5-12, 1-sec SA is significantly amplified for Z1.0 > 600 m (right panel), but 0.01-sec SA is not affected (left panel).

**Fault Characteristics -** In the NGA models the median ground motions varies between different styles of faulting with reverse faulting larger than strike-slip faulting and strike slip larger that normal faulting. The amount of difference, however, varies among NGA models.

Hanging wall effects are also evident (Figure 5-13A) and apply to normal and reverse faulting. The effect is significant and period dependent, but is quite complex to model (Figures 5-13B and 5-13C).

Depth to the top of fault rupture also proves significant. As shown in Figure 5-14, the PGA amplification factor ranges from 1.0 to 1.7 for $Z_{Tor}$ > 10 km.

**Regression Analysis -** The following functional form is representative of what were used in the regression analysis by all modelers. Figure 5-15 shows a typical functional form for the NGA models. The similar functional forms were used by all modelers. But they varied the constants and selected slightly different subsets from the overall database. Details of the regression procedures and results are described in the papers authored by these modelers and to be published in a special issue of Earthquake Spectra on NGA models in March 2008.

**Comparison Among NGA Models -** Ground motions calculated from the NGA models compare each other with relatively minor differences. For example, Figure 5-16 illustrates the ground motions (SA) at $V_{S30}$ = 760 m/sec from the four models for a magnitude M7.5 event on a vertical strike-slip fault that reaches the surface. In this example the distance measures are equivalent and there are no hanging wall and depth-to-the-top-of-rupture effects.

**Comparison of NGA Models with 1997** - Attenuation Models – In general, the 2007 NGA

models will result in lower estimates of PGA and SA than the corresponding 1997 models for the same set of source and site parameters. For example, Figures 5-17 – 5-20.

## 5.4 GROUND MOTION METHODOLOGY FOR PG&E DAMS - 2007

The ground motions developed for the PG&E dams in the Mokelumne-Stanislaus hydro-electric system use the updated active fault map for source characterization. This includes the Quaternary fault digital data base developed by the U.S. Geological Survey, California Geological Survey, and Nevada Bureau of Mines and Geology and supplemented by the PG&E data on faults in Sierra Nevada that was updated in 2007 (U.S. Geological Survey, 2007). The seismic sources are then used in the new-generation-attenuation (NGA) models. The results from four NGA models are averaged to estimate potential ground motions at each dam. The models used are Campbell and Bozorgnia (2006; 2007), Chiou and Youngs (2006), Abrahamson and Silva (2007), and Boore and Atkinson (2007). The model developed by Idriss (2006; 2007) is not used because he presents fewer periods but no curve, limiting accuracy of interpolation between periods. The NGA models calculate generally lower ground motions than the older models for most periods in the spectra including the periods of interest for PG&E dams. All the NGA models directly differentiate between normal, strike slip, and reverse/thrust faulting. Thus the 20% reduction applied to the ground motions models used for PG&E dams in the past is not needed.

Median and 84$^{th}$ percentile horizontal ground motions (PGA and spectral accelerations) are computed for each significant seismic source from the four empirical attenuation relationships as discussed above. These computed horizontal PGA values and response spectra (5% spectral damping) are then averaged to represent the potential ground motions for review of each dam.

Figures 5-17 and 5-18 compare the attenuation curves of PGA and SA at periods equal to 0.2 and SA at periods equal to 1.0 and 3.0 seconds respectively on rock for strike-slip earthquakes (Abrahamson and Silva, 2007). It is evident that the NGA curves are below the 1997 models for all magnitudes above M = 6 over the whole distance range. Alternatively, Figures 5-19 and 5-22 compare the SA spectra on rock of strike-slip earthquakes with different magnitudes between the 1997 and 2007 attenuation models (Abrahamson and Silva, 2007) at distances 30 and 1 km, respectively. These figures show that the whole SA spectra are reduced for magnitudes greater than M = 6 at both distances.

## 5.5 COMPARISON OF THE 2007 NGA AND EARLIER GROUND MOTIONS REGRESSION MODELS USED FOR PG&E DAMS

To help interested readers to understand the marked changes in the estimates of ground motions over the past 15 years, we tabulate the variation of PGA for two typical dams (Table 5-1) to illustrate the changes in the estimated potential ground motions for two typical PG&E dams in the Sierra Nevada.

From Table 5.1 it is noticed that the estimated PGA values from the NGA models are smaller than previous estimates for both dams. The difference is apparent particularly between the 2002 and 2007 estimates, even though the potential earthquake magnitudes and distances are almost

the same. This is mainly due to the reduction of estimated ground motions by the NGA models.

For example, Figures 5-21 and 5-22 show the average and four individual SA spectra calculated from the 1997 and 2007 ground motion attenuation models, respectively, for a M7 strike-slip earthquake at 10 km on rock. It is found that the average PGA value is reduced from 0.35 g estimated by the 1997 attenuation models down to about 0.25 g estimated by the 2007 NGA models. Similar reduction is also apparent over the whole period range. Furthermore, the range of differences among the 2007 NGA models is significantly smaller than that of the 1997 attenuation models. These explain the large differences between the present and previous estimates of potential ground motions for PG&E dams, as exemplified in Table 5.1.

# 6.0 REFERENCES


Abrahamson, N.A., 1997, Updated attenuation relations for normal faulting events, given in Yucca Mountain Ground Motion Data Package #1, Department of Energy, Yucca Mountain Project.

Abrahamson, N.A., and Becker, A.M., 1997, Ground motion characterization at Yucca Mountain, Nevada, Report to the U.S. Geological Survey, October 13, 1997, Level 4 Milestone SPG28EM4, WBS Number 1.2.3.2.8.3.6.

Abrahamson, N. A. and Shedlock, K. M., 1997b, Overview: Seismological Research Letters, v. 68, p. 94-127.

Abrahamson, N.A. and Silva, W.J., 1997a, Empirical response spectral attenuation relations for shallow crustal earthquakes, Seismological Research Letters, 68, p. 94-127.

Abrahamson, N.A. and Silva, W.J., 2007, Abrahamson & Silva NGA Ground Motion Relations for the Geometric Mean Horizontal Component of Peak and Spectral Ground Motion Parameters: Draft Version 2, PEER Report 2007/0x, 354p.

Alt, J.N., Schwartz, D.P., and McCrumb, D.R., 1977, Earthquake evaluation studies of the Auburn Dam Area, regional geology and tectonics: (unpublished) report by Woodward-Clyde Consultants for the U.S. Bureau of Reclamation, v. 3., 118 p., 4 appendices.

ANSS, 2007, Advanced National Seismic System online catalog, http://quake.geo.berkeley.edu/cnss/catalog-search.html, accessed 3/13/2007.

Argus, D.F. and Gordon, R.G., 1991, Current Sierra Nevada-North America motion from very long baseline interferometry: Implications for the kinematics of the western United States: Geology, v.19, p. 1085-1088.

Argus, D.F. and Gordon, R.G., 2001, Present tectonic motions across the Coast Ranges and San Andreas fault system in central California: Geological Society of America Bulletin, v. 113, p. 1580-1592.

Bachman, S.B., 1978, Pliocene-Pleistocene break-up of the Sierra Nevada--White-Inyo Mountains block and formation of Owens Valley: Geology, v. 6, p. 461-463.

Bacon, C.R., Giovannetti, D.M., Duffield, W.A., Dalrymple, G.B., and Drake, R.E., 1979, Age of the Coso Formation, Inyo County, California: U.S. Geological Survey Bulletin 1527, 18 p.

Bailey, R.A., Dalrymple, G.B., and Lanphere, M.A., 1976, Volcanism, structure, and geochronology of Long Valley caldera, Mono County, California: Journal of Geophysical Research, v. 81, p. 725-744.

Bateman, P.C. and Wahrhaftig, C., 1966, Geology of the Sierra Nevada, California: in Bailey, E.H., ed., Geology of northern California, California Division of Mines and Geology Bulletin 190, p. 107-172.

Beanland, S. and Clark, M.M., 1994, The Owens Valley fault zone, eastern California, and surface rupture associated with the 1872 earthquake: U.S. Geological Survey Bulletin 1982, 29 p.

Bennett, R.A., Davis, J.L., and Wernicke, B.P., 1999, Present day pattern of Cordilleran deformation in the western United States: Geology, v 27, p. 317-374.

Bennett, R.A., Wernicke, N.A., Niemi, N.A., Freidrich, A.M., and Davis, J.L., 2003, Contemporary strain rates in the northern Basin and Range province from GPS data: Tectonics, 22(2), doi:10.1029/2001TC001355.

Berman, F.A., 1999, The paleoclimate and tectonic significance of the Bee Springs alluvial fan sequence, west central Inyo Mountains, east-central California [M.S. thesis]: Humboldt State University, 77 pp.

Biggar, N, Cluff, L.S. and Ewoldsen, H., 1978, Geologic and seismologic investigations, New Melones Dam project, California: report by Woodward-Clyde Consultants to U.S. Army Corps of Engineers, Sacramento, 246 p.

Birkeland, P.W., 1964, Pleistocene volcanism and deformation of the Truckee area, north of Lake Tahoe, California: Geological Society of America Bulletin, v. 74, p. 1453-1464.

Blackwelder, E., 1931, Pleistocene glaciation in the Sierra Nevada and Basin Ranges: Geological Society of America Bulletin, v. 42, p. 865-922.

Bolt, B. A. and Miller, R. D., 1975, Catalog of earthquakes in northern California and adjoining areas. 1 January 1910-31 December 1972, Seismographic Stations: University of California, Berkeley, California, p. 567.

Boore, D.M., Joyner, W.B., and Fumal, T.E., 1993, Estimation of response spectra and peak accelerations from western North American earthquakes: An interim report, U.S. Geological Survey Open-File Report 93-509, 72 p.

Boore, D.M., Joyner, W.B., and Fumal, T.E., 1994, Estimation of response spectra and peak accelerations from western North American earthquakes: An interim report Part 2. U.S. Geological Survey Open-File Report 94-127, 40 p.

Boore, D.M., Joyner, W.B., and Fumal, T.E., 1997, Equations for estimating horizontal response spectra and peak accelerations from western North American earthquakes: A summary of recent work, Seismological Research Letters, v. 68, 128-153.

Boore, D.M. and Atkinson, G.M., 2007, Boore-Atkinson NGA Ground Motion Relations for the Geometric Mean Horizontal Component of Peak and Spectral Ground Motion Parameters: PEER Report 2007/01, 234p.

Campbell, K.W., 1981, Near-Source Attenuation of Peak Horizontal Acceleration, Bull. Seism. Soc. Am. 71, 2039-2070.

Campbell, K.W., 1997, Empirical near-source attenuation relationships for horizontal and vertical components of peak ground acceleration, peak ground velocity, and pseudo-absolute acceleration response spectra: Seismological Research Letters, v. 68, p. 154-179.

Campbell, K.W., and Bozorgnia, 2003, Updated near-source ground motion (attenuation) relations for the horizontal and vertical components of peak ground acceleration and acceleration response spectra, Bull. Seism. Soc. Am., v. 93, 314-331.

Campbell, K.W. and Bozorgnia, Y., 2006, Campbell-Bozorgnia NGA empirical ground motion model for the average horizontal component of PGA, PGD and SA at selected spectral periods ranging from 0.01-10 seconds: draft manuscript, version 1.1, submitted for publication, 199p.

CDMG, 2000, digital Database of Faults form the fault activity map of California and adjacent areas, DMG CD 2000-006, California Department of Conservation Division of Mines and Geology.

Chiou, B. S.-J., Roblee, C., Abrahamson, N.A., and Power, M.S., 2004, The Research Program of "Next Generation of Ground-Motion Attenuation Models" (NGA) Proceedings of GeoTrans 2004 Conference, Los Angeles, California, pp768-777.

Chiou, B. S.-J., and Youngs, R.R., 2006, Chiou and Youngs PEER NGA empirical ground motion model for the average horizontal component of peak acceleration and , pseudo-spectral acceleration for selected spectral periods of 0.01-10 seconds: Interim report for US GEOLOGICAL SURVEY Review, June 14, 2006 (revised editorially July 10, 2006): draft manuscript submitted for publication, 219p.

Clark, L.D., 1960, Foothills fault system, western Sierra Nevada, California: Geological Society of America Bulletin, v. 71, p. 483-496.

Dames and Moore, 1993, Photogeologic and imagery analysis for the geologic and seismologic investigation, New Hogan Dam, Calaveras County, California: unpublished consulting report submitted to U.S. Army Corp. of Engineers, Sacramento, p. 51, 14 figures, 1 plate, 1 appendix.

dePolo, C.M., and Anderson, J.G., 2000, Estimating the slip rates of normal faults in the Great Basin, USA: Basin Research, v. 12, p. 227-240.

dePolo, D., Smith, K., Anooshehpoor, R., dePolo, C. and Priestley, K., 1995, Double Spring Flat Earthquake, western Nevada, 12 September 1994: American Geophysical Union, 1994 Fall Meeting abstracts, in 1995 Spring Meeting proceedings, supplement to *EOS*, S301.

dePolo, C.M., Anderson, J.G., dePolo, D.M., Price, J.G., 1997, Earthquake Occurrence in the Reno-Carson City Urban Corridor: Seismological Research Letters, v. 68, p. 401-412.

dePolo, C.M., 1998, A reconnaissance technique for estimating the slip rates of normal-slip faults in the Great Basin, and application to faults in Nevada, U.S.A.: University of Nevada Ph.D. Dissertation, 199 p.

Dixon, T.H, Miller, M., Farina, F., Wang, H., and Johnson, D., 2000, Present-day motion of the Sierra Nevada

block and some tectonic implications for the Basin and Range province, North American Cordillera. Tectonics 19:1, pp. 1-24.

Dokka, R.K. and Travis, C.J., 1990, The role of the Eastern California Shear Zone in accommodating Pacific-North American plate motion: Geophysical Research Letters, v. 17, n. 9, p. 1323-1326.

Frazer, W.A., and Howard, J.K., 2003, Ground Motion estimation procedures: California Division of Safety of Dams: Slide presentation 8/11/2003.

Gilbert, G.K, 1884, A theory of the earthquakes of the Great Basin, with a practical application: American Journal of Science – Third Series, v. XXVII, no. 157, p. 49-53.

Gillespie, A.R., 1982, Quaternary glaciation and tectonism in the southwestern Sierra Nevada, Inyo County, California [Ph.D. dissertation]: California Institute of Technology, 657 p.

Hamilton, D. H., Harlan, R.D., and Castle, J.A., 2005, Phase II, Seismic Fault Investigation for North Fork Stanislaus River Hydro Electric Development Project, FERC Project No. 2409-CA, and Donnells Project, FERC Project No. 2005-CA: unpub. Consulting report submitted to Northern California Power Agency and Tri-Dam Project, Murphys, California, 70 p., 3 tables, 18 figures, 11 plates.

Harden, D.H., 1998, *California Geology*: Prentice Hall, Inc., 479 p.

Idriss, I.M., 1978, Characteristics of Earthquake Ground Motions, Proc. ASCE Geotechnical Eng. Div. Specialty Conf. On Earthquake Engineering and Soil Dynamics, Vol. III, 1151-1265.

Idriss, I.M., 1994, Lecture notes: Part 1, Development of input motions; Part 2, Site reponse analyses: Workshop 1.a., Geotechnical Engineering, Advances in Earthquake Engineering Practice, University of California, Berkeley.

Idriss, I.M., 1996, Updated peak acceleration attenuation relation for rock, written communication, Sept. 1996.

Idriss, I.M., 2007, Empirical model for estimating the average horizontal values for pseudo-absolute spectral accelerations generated by crustal earthquakes, Volume I, Sites with Vs30=450 to 900 m/s: Interim issued for US GEOLOGICAL SURVEY review, 76p.

Jennings, C.W., 1975, Fault activity map of California and adjacent areas, with locations of recent volcanic eruptions: California Division of Mines and Geology geologic data map no. 6, scale 1:750,000 with explanatory text, 92 p.

Jennings, C.W., 1977, Geologic map of California; digital database: version 2.0 by Saucedo, G.J., Bedford, D.R., Raines, G.L., Miller, R.J., and Wentworth, C.M., 2000, California Geological Survey, scale: 1:750,000.

Jennings, C.W., 1994, Fault activity map of California and adjacent areas with explanatory text to accompany the fault map: California Division of Mines and Geology; Map No. 6, scale 1:750,000; 92 p.

Jones, L.M. and Dollar, R.S., 1986, Evidence of Basin-and-Range extensional tectonics in the Sierra Nevada: The Durwood Meadows Swarm, Tulare County, California (1983-1984): Bulletin of the Seismological Society of America, v. 76, p. 439-461.

Joyner, W.B. and Boore, D.M., 1981, Peak Horizontal Acceleration and Velocity from Strong-Motion Records Including Records from the 1979 Imperial Valley, California, Earthquake, Bull. Seism. Soc. Am. 71, 2011-2038.

Kent, G.M., Babcock, J.M., Driscoll, N.W., Harding, A.J., Dingler, J.A., Seitz, G.C., Gardner, J.V., Mayer, L.A., Goldman, C.R., Heyvaert, A.C., Richards, R.C., Karlin, R., Morgan, C.W., and Gayes, P.T., 2005, 60 k.y. record of extension across the western boundary of the Basin and Range province: Estimate of slip rates from offset shoreline terraces and a catastrophic slide beneath Lake Tahoe: Geological Society of America Geology, v. 33, No. 5, p. 365-368.

Lahren, M.M. and Schweickert, R.A., 1991, Tertiary brittle deformation in the central Sierra Nevada, California: Evidence for late Miocene and possibly younger faulting: Geological Society of America Bulletin, v. 103, p. 898-904.

Lueddecke, S.B., Pinter, N., and Gans, P., 1998, Plio-Pleistocene ash falls, sedimentation, and range-front faulting along the White-Inyo Mountains front, California: The Journal of Geology, v. 106, p. 511-522.

Muir, J., 1971, John Muir in Yosemite: Flying Spur Press, Yosemite, California, 48 p.

Nadin, E.S., 2007, Structure and history of the Kern Canyon fault system, southern Sierra Nevada, California: Ph.D. Thesis, California Institute of Technology, 266p. plus appendices and plate.

Nadin, E.S. and Saleeby, J.B., 2001, Relationship between the Kern Canyon fault (KCF) and the Proto-Kern Canyon fault (PKCF), southern Sierra Nevada, California: EOS, Transactions Norris, R.M., and Webb, R.W., 1990, *Geology of California*: John Wiley & sons, Inc. (second edition), 541 p.

National Geographic, 2004, California Map data discs 5 and 6: TOPO! Seamless USGS topographic maps on CD-ROM.

NCSN, 2007, Northern California Seismic Network online catalog, http://quake.geo.berkeley.edu/ncedc/catalog-search.html, accessed 3/13/2007.

Norris, R.M., and Webb, R.W., 1990, *Geology of California*: John Wiley & sons, Inc. (second edition), 541 p.

Page, W.D. and Sawyer, T.L., 2001, Use of geomorphic profiling to identify Quaternary faults within the Northern and central Sierra Nevada, California: in H. Ferriz, and R. Anderson, eds., Engineering Geology Practice in Northern California, California Geological Survey Bulletin 210/Association of Engineering Geologist Special Publication 12, p. 275-293.

Page, W.D., Unruh, J.R., Sawyer, T.L, and McLaren, M.K., in preparation, Tectonics of the Sierran microplate, California.

Petersen, M.D., Bryant, W.A., Cramer, C.H., Cao, T.C., Reichle, M.S., Frankle, A.D., Lienkaemper, J.J., McCrory, P.A., and Schwartz, D.P., 1996, Probabilistic seismic hazard assessment for the State of California: both—California Division of Mines and Geology Open-File Report 96-08 and U.S. Geological Survey Open-File Report 96-706, 31 p, plus 2 appendices.

PG&E Geoscience Department and Piedmont GeoSciences, 2003, Regional Geology, Seismicity, and General Ground Motion Considerations for the Drum/Spaulding Hydroelectric System, Placer and Nevada Counties, California, 14 p. plus attached figures and tables.

PG&E, 1988, Final report of the Diablo Canyon Long Term Seismic Program: Chapter 4, Characterization of Ground Motions, U.S. Nuclear Regulatory Commission, Docket Nos. 50-275 and 50-323, 81 p.

PG&E, 1989, Static and dynamic stability assessment, Ione Canal Dam; Section 2.0, Seismicity, seismic geology, and ground motion evaluations and Appendix A, Seismic Geology: report by Engineering Department, San Francisco: 15 p. plus appendix plus figures.

PG&E, 1990, Response to Question SSC 5 on the Final Report of the Diablo Canyon Long Term Seismic Program: submitted to the U.S. Nuclear Regulatory Commission, 15 p.

PG&E, 1994, Reconnaissance Report on the September 12, 1994 Double Spring Flat Earthquake, M 6.3 Douglas County, Nevada, 14p. plus figures.

PG&E, 1994a, Characterization of potential earthquake sources for, Ralston Afterbay Dam, State Dam No. 1030-4, FERC Project No. 2079: report to Placer County Water Agency, Foresthill, for the Federal Energy Regulatory Commission, 93 p.

PG&E, 1994b, Characterization of potential earthquake sources for Rock Creek (Drum) Dam: report to Division of Safety of Dams, Sacramento, 93 p.

PG&E, 1992, Supplement to characterization of potential earthquake sources, Lake Francis Dam: report to the California Division of Safety of Dams, v.1 and 2.

Piedmont GeoSciences and PG&E Geosciences Department, 2004, Regional geology, seismicity, and general ground motion considerations for the Merced, San Joaquin, and Kings Hydroelectric Systems: report for Hydro Generation Department, Pacific Gas and Electric Company, San Francisco: .33p plus tables and figures and appendices.

Piedmont GeoSciences and PG&E Geosciences Department, 2005, Regional geology, seismicity, and general ground motion considerations for PG&E dams, North Fork Feather River Region, FERC Projects 619, 803, 1962, And 2105, Butte and Plumas Counties, California: Report submitted to Hydro Generation Department,

Pacific Gas & Electric Co., 31 p., plus tables, figures, construction drawings, and appendices.

Power, M.S., Chiou, B.S.-J., Abrahamson, N.A., Bozorgnia, Y., Shantz, T., and Roblee, C. (2008), An Overview of the NGA Project, Special Issue of Earthquake Spectra on the NGA Project, Earthquake Engineering Research Institute, scheduled to be published in March, 2008).

Ramelli, A.R., Bell, J.W., dePolo, C.M., and Yount, J.C., 1999, large-magnitude, late Holocene earthquakes on the Genoa fault, west-central Nevada and eastern California: Bulletin of the Seismological society of America, v. 89, no. 6, p. 1458-1472.

Sadigh, K., Chang, C.-Y., Egan, J. A., Makdisi, F. and Youngs, R. R., 1997, Attenuation relationships for shallow crustal earthquakes based on California strong motion data: Seismological Research Letters, v. 68, p. 180-189.

Sauber, J., Thatcher, W., Solomon, S.C., and Lisowski, M., 1994, Geodetic slip rate for the Eastern California shear zone and the recurrence time of Mojave Desert earthquakes: Nature, v. 367, p. 264-266.

Savage, J.C., Lisowski, M., and Prescott, W.H., 1990, An apparent shear zone trending north-northwest across the Mojave Desert into Owens Valley, eastern California: Geophysical Research Letters, v. 17, no. 12, p. 2113-2116.

Sawyer, T.L., Wakabayashi, J., Page, W.D., Thompson, S.C., and Ely, R.W., 1993, Late Cenozoic internal deformation of the northern and central Sierra Nevada, California: A new perspective: EOS, Trans. Amer. Geophys. Union, v.74, no. 44, p. 609.

Schnabel, P.B., and Seed, H.B., 1973, Accelerations in rock for earthquakes in the western United States, Bull. Seism. Soc. Am., v. 63, 501-516.

Schwartz, D. P., Swan F. H., Harpster, R. E., Rogers, T. H., and Hitchcock, D. E., 1977, Surface faulting potential: Earthquake Evaluation Studies of the Auburn Dam Area, Volume 2: report by Woodward-Clyde Consultants to the U.S. Bureau of Reclamation, Denver; 135 p. plus appendices.

Schweickert, R.A. and Cowan, D.S., 1975, Early Mesozoic tectonic evolution of the western Sierra Nevada, California: Geological Society of America Bulletin, v. 86, no. 10, p. 1329-1336.

Seed, H.B., Ugas, C., and Lysmer, J., 1976, Site-Dependent Spectra for Earthquake-Resistant Design, Bull. Seism. Soc. Am. 66, 221-243.

Seed, H.B., and Idriss, I.M., 1982, Ground motions and soil liquefaction during earthquakes: *in* Engineering Monographs on Earthquake Criteria, Structural Design, and Strong Motion Records, Earthquake Engineering Research Institute, v. 5, 134 pages.

Slemmons, D.B., 1953, Fault map of the Walker Lake 1°X2° sheet: unpublished map compiled for Figures 3, 4, 5, 6 and 8 in Slemmons (1967), 1:250,000 scale map.

Slemmons, D.B., 1966, Cenozoic volcanism of the central Sierra Nevada, *in*, E.H. Bailey (ed.), Geology of Northern California: California Division of Mines and Geology Bulletin 190, pp. 199-208.

Slemmons, D.B., Jones, A.E., and Gimlett, J.I., 1965, Catalog of Nevada earthquakes, 1852-1960: Seismological Society of America Bulletin, v. 55, no. 2, p. 519-565.

Spudich, P., Fletcher, J.B., Hellweg, M., Boatwright, J., Sullivan, C., Joyner, W.B., Hanks, T.C., Boore, D.M., McGarr, A., Baker, L.M., and Lindh, A.G., 1996, Earthquake ground motions in extensional tectonic regimes, U.S. Geological Survey, Open File Report 96-292.

Spudich, P., Fletcher, J.B., Hellweg, M., Boatwright, J., Sullivan, C., Joyner, W.B., Hanks, T.C., Boore, D.M., McGarr, A., Baker, L.M., and Lindh, A.G., 1997, SEA96 - A new predictive relation for earthquake ground motions in extensional tectonic regimes: Seismological Research Letters, v. 68, p. 190-198.

Spudich, P., Joyner, W.R., Lindh, A.G., Boore, D.M., Margaris, B.M., and Fletcher, J.B., 1999, SEA99: a revised ground motion prediction relation for use in extensional tectonic regimes: Bulletin Seismological Society of America, v. 89, pp. 1156-1170.

Stockli, D.F., Surpless, B.E., and Dumitru, T.A., 2000, Late Miocene transition from east-west extension to right-lateral transtension in the central Walker Lane belt: Geological Society of America Abstracts with Programs, v. 32, p. A105.

Stover, C.W., and Coffman, J.L., 1993, Seismicity of the United States, 1568-1989 (Revised): U.S. Geological Survey Professional Paper 1527, p.417.

Swan, F.H., III, and Hanson, K., 1977, Quaternary geology and age dating, *in* Woodward-Clyde Consultants, Earthquake evaluation studies of the Auburn Dam area, v. 4: report for the U.S. Bureau of Reclamation, Denver, 83 p. plus appendices

Thatcher, W., Foulger, G., Julian, B., Svarc, J., Quilty, E., and Bawden, G., 1999, Present day deformation across the Basin and Range province, western United States: Science, v. 283, p. 1715-1718.

Toppozada T. R., Parke, D. L., and Higgins, C. T., 1978, Seismicity of California 1900-1931: California Division of Mines and Geology special Report 135, 39 p.

Toppozada, T.R., Real, C.R., and Parke, D.L., 1981, Preparation of isoseismal maps and summaries of reported effects for pre-1900 California earthquakes: California Division of Mines and Geology Open File Report 81-11 SAC, 182 p. plus attached figures.

Toppozada T. R., Real, C. R., and Parke, D. L., 1981, Preparation of isoseismic maps and summaries of reported effects for pre-1900 California earthquakes: California Division of Mines and Geology Open File Report 81-11 SAC, 182 p. plus attached figures.

Toppozada, T., Branum, D., Petersen, M., Hallstrom, C., Cramer, C. and Reichle, M., 2000, Epicenters of areas damaged by M>5 California earthquakes, 1800-1999, Map sheet 49, California Division of Mines and Geology.

U.S. Geological Survey, 2007, U.S. Geological Survey, California Geological Survey, and Nevada Bureau of Mines and Geology, Quaternary fault and fold database for the United States, accessed 2/1/2007, from US GEOLOGICAL SURVEY web site: http//earthquakes.usgs.gov/regional/qfaults/.

Unruh, J.R., 1991, The uplift of the Sierra Nevada and implications for late Cenozoic epiorogeny in western Cordillera: Geological Society of America Bulletin, v. 103, p. 1395-1404.

Unruh, J., Humphrey, J., and Barron, A., 2003, Transtensional model for the Sierra Nevada frontal fault system, eastern California: Geology, v. 31, no. 4, p. 327-330.

Vittori, E., Michetti, A.M., Slemmons, D.B., and Carver, G.A., 1993, Style of recent surface deformation at the south end of the Owens Valley fault zone, eastern California: Geological Society of America Abstracts with Programs, v. 25, n. 5.

Wagner, D.L., Jennings, C.W., Bedrossian, T.L., and Bortugno, E.J., 1981, Geologic Map of the Sacramento Quadrangle: California Division of Mines and Geology, Regional Geologic Map Series Map No. 1A, Scale 1:250,000.

Wakabayashi, J. and Sawyer, T.L., 2001, Stream incision, tectonics, uplift, and evolution of topography of the Sierra Nevada, California: Journal of Geology, vol. 109, p. 539-562.

Wakabayashi, J. and Smith, D. L., 1994, Evaluation of recurrence intervals, characteristic earthquakes and slip rates associated with thrusting along the Coast Range-Central Valley geomorphic boundary, California: Bulletin of the Seismological Society of America, v. 84, no. 6, pp. 1960-1969.

Wakabayashi, J., and Sawyer, T.L., 2000, Neotectonics of the Sierra Nevada-Basin and Range transition, California, with field trip stop descriptions for the northeastern Sierra Nevada: in Field Guide to the geology and tectonics of the northern Sierra Nevada, eds. E.R. Brooks and L.T. Dida, California Division of Mines and Geology Special Publication 122, p. 173-212.

Weldon, R.J. and Humphreys, H., 1986, A kinematic model of southern California: Tectonics, v. 5, p. 33-48.

Wells, D.L., and Coppersmith, K.J., 1994, New empirical relationships among magnitude, rupture length, rupture width, rupture area, and surface displacement: Seismological Society of America Bulletin, v. 84, no. 4, p. 974-1002, with tables and figures.

Wong, I. G. and Ely, R. W., 1983, Historical seismicity and tectonics of the Coast Ranges-Sierran Block boundary: implications to the 1983 Coalinga, California earthquake, *in* Bennett, J. H. and Sherburne, R. W., eds., The 1983 Coalinga, California earthquakes: California Division of Mines and Geology Special Publication 66, p. 98-104.

Wong, I. G., Ely, R. W., Killmann, A. C., 1988, Contemporary seismicity and tectonics of the northern and central Coast Ranges-Sierran block boundary zone, California: Journal of Geophysical Research, v. 93, no. B-7, p. 7813-7833.

Wong, I., and Dobler, M., 2004, Evaluation of background earthquake in the Sierra Nevada, California: report to PG&E Geosciences Department, 5 p. plus table and figures.

Woodward-Clyde Consultants, 1978, Significant faults and seismicity in the northern Sierra Nevada region of major PG&E dams: San Francisco, California, Woodward-Clyde Consultants, unpublished report for Pacific Gas and Electric Company, W.C.C. project no. 13890A-1050, 34 p.

# 7.0 TABLES

**TABLE 2-1**
**POTENTIAL SEISMIC SOURCES AND ESTIMATED MAXIMUM EARTHQUAKES FOR PG&E DAMS IN THE MOKELUMNE-STANISLAUS REGION, CALIFORNIA**

| **Potential Seismic Source** (Fault/Rupture Seg.) **Sense of Slip** (N-normal; RL-right lateral; LL-left lateral; L-lateral) **Tectonic Regime:** Trans - transpressional Ext - extensional | **Fault Activity[1]** **Vertical Separation Rate** (mm/yr) [long-term rate] **Recurrence Interval** | **Estimated Subsurface Rupture Length** (km) | **Estimated Maximum Earthquake Rupture Area Magnitude[2]** ($M_w$) (other) |
|---|---|---|---|
| **SIERRA NEVADA FRONTAL FAULT SYSTEM** | | | |
| Antelope Valley and West Walker fault zone<br>N<br>Ext. | Holocene & late Pleistocene[3]<br>0.4-0.7mm/yr[4]<br>1-2 mm/yr | 24-49[5] | 6.5-6.8 |
| Carson Range fz<br>N<br>Ext. | Holocene to l. Ceno.[6]<br>2-3 mm/yr[7]<br>≥1.4-1.7 ka[8] | 25-75[9] | 6.6-7.1<br>(7.2-7.5[10]) |
| *Genoa* | Holocene & late Pleistocene[11]<br>2-3 mm/yr[12]<br>≥1.4-1.7 ka[13] | 39-63[14] | 6.7-7.0 |
| *Genoa and Diamond Valley* | Holocene & late Pleistocene[15]<br>2-3 mm/yr[16]<br>≥1.4-1.7 ka[17] | 39-63[18] | 6.7-7.0 |
| *Folger Peak* | Holocene(?) to late Cenozoic[19]<br>[0.04-0.1][20]<br>-- | 22-31[21] | 6.5-6.7 |
| *Folger Peak, Arnot Creek and Disaster Creek* | Holocene(?) to late Cenozoic[22]<br>[0.04-0.1][23] | 22-31[24] | 6.5-6.7 |
| Millie Lake<br>N<br>Ext. | late Quaternary[25]<br>--<br>-- | 12[26] | 6.2 |

**TABLE 2-1**
**POTENTIAL SEISMIC SOURCES AND ESTIMATED MAXIMUM EARTHQUAKES FOR PG&E DAMS IN THE MOKELUMNE-STANISLAUS REGION, CALIFORNIA**

| **Potential Seismic Source** (Fault/Rupture Seg.) **Sense of Slip** (N-normal; RL-right lateral; LL-left lateral; L-lateral) **Tectonic Regime:** Trans - transpressional Ext - extensional | **Fault Activity[1]** **Vertical Separation Rate** (mm/yr) [long-term rate] **Recurrence Interval** | **Estimated Subsurface Rupture Length** (km) | **Estimated Maximum Earthquake Rupture Area Magnitude[2]** ($M_w$) (other) |
|---|---|---|---|
| Waterhouse Peak<br>N; LL(?)<br>Ext. | late & early Quaternary[27]<br>[0.7][28]<br>1000's yrs[29] | 18-31[30] | 6.4-6.7 |
| West Tahoe-Dollar Point<br>N<br>Ext | Holocene & early Q[31]<br>0.10-1.0[32]<br>-- | 56[33] | 7.0 |
| *West Tahoe, Quail Lake, Echo Summit* | Holocene & early Q.[34]<br>0.10-1.0[35]<br>-- | 19-43[36] | 6.4-6.8 |
| West Walker<br>N<br>Ext. | Holocene[37]<br>[<0.3-<0.5][38]<br>-- | 16-24[39] | 6.4-6.5 |
| **FAULTS WITHIN THE SIERRAN MICROPLATE** | | | |
| Dardanelles Cone<br>N<br>Ext. | late Cenozoic[40]<br>--<br>-- | 12-15[41] | 6.2-6.3 |
| Dorothy Lake<br>RL, N[42]<br>Ext. | late Cenozoic to Holocene[43]<br>[0.008-0.015][44]<br>-- | 13-22[45] | 6.3-6.5 |
| Douds Landing[46]<br>N (RL?)<br>Ext. | late Cenozoic[47]<br>[0.001][48]<br>-- | 11-19[49] | 6.2-6.3 |
| Gopher Gulch<br>N<br>Ext. | late Cenozoic[50]<br>[0.002-0.005][51]<br>-- | 14-22[52] | 6.3-6.5 |

**TABLE 2-1**
**POTENTIAL SEISMIC SOURCES AND ESTIMATED MAXIMUM EARTHQUAKES FOR PG&E DAMS IN THE MOKELUMNE-STANISLAUS REGION, CALIFORNIA**

| **Potential Seismic Source** (Fault/Rupture Seg.) **Sense of Slip** (N-normal; RL-right lateral; LL-left lateral; L-lateral) **Tectonic Regime:** Trans - transpressional Ext - extensional | **Fault Activity[1]** **Vertical Separation Rate** (mm/yr) [long-term rate] **Recurrence Interval** | **Estimated Subsurface Rupture Length** (km) | **Estimated Maximum Earthquake Rupture Area Magnitude[2]** ($M_w$) (other) |
|---|---|---|---|
| Icehouse<br>N<br>Ext. | late Cenozoic[53]<br>[>0.04-<0.06][54]<br>-- | 9-15[55] | 6.1-6.3 |
| Martell<br>N<br>Ext. | late Cenozoic[56]<br>0.02-0.06[57]<br>-- | 13[58] | 6.3 |
| McKays Point[59]<br>N, RL?<br>Ext. | late Cenozoic[60]<br>[0.008-0.009][61]<br>-- | 8-14[62] | 6.1-6.3 |
| North Fork Stanislaus[63]<br>N, LL?<br>Ext. | | | |
| *North Fork[64]* | late Cenozoic[65]<br>[0.008][66]<br>-- | 11-18[67] | 6.2-6.4 |
| *Stanislaus[68]* | late Cenozoic[69]<br>--<br>-- | 18[70] | 6.4 |
| Poorman Gulch<br>N, RL<br>Ext. | late Quaternary[71]<br>[0.006-0.024][72]<br>≥6.3-25 ka | 15-22[73] | 6.3-6.5 |
| Post Corral[74]<br>RL, N<br>Ext. | late Cenozoic[75]<br>[0.01-0.02][76]<br>-- | 12-20[77] | 6.2-6.5 |
| Red Peak fault zone<br>RL, N<br>Ext. | late Cenozoic[78]<br><0.1mm/yr<br>-- | 20-26 | 6.5-6.7 |

**TABLE 2-1**
**POTENTIAL SEISMIC SOURCES AND ESTIMATED MAXIMUM EARTHQUAKES FOR PG&E DAMS IN THE MOKELUMNE-STANISLAUS REGION, CALIFORNIA**

| **Potential Seismic Source** (Fault/Rupture Seg.) **Sense of Slip** (N-normal; RL-right lateral; LL-left lateral; L-lateral) **Tectonic Regime:** Trans - transpressional Ext - extensional | **Fault Activity[1]** **Vertical Separation Rate** (mm/yr) [long-term rate] **Recurrence Interval** | **Estimated Subsurface Rupture Length** (km) | **Estimated Maximum Earthquake Rupture Area Magnitude[2]** ($M_w$) (other) |
|---|---|---|---|
| Rawhide Flat East & West<br>N, RL?<br>Ext. | late Quaternary[79]<br>[E=0.001-0.004; W=0.002-0.008][80]<br>-- | 15[81] | 6.3 |
| Sunnybrook East<br>RL, N<br>Ext. | late Cenozoic[82]<br>[≤0.002][83]<br>-- | 7[84] | 6.0 |
| Youngs Creek<br>N, RL<br>Ext. | Quaternary?[85]<br>[0.0003-0.0015][86]<br>-- | 16-22[87] | 6.4-6.5 |
| **Background Earthquake**<br>(sources unknown)<br>Ext | Holocene<br>N/A<br>1000 yrs[88]<br>3000 yrs[89] | N/A | 5.8 |

Endnotes

[1] Late Cenozoic faults within the Sierra Nevada are considered to be "conditionally active" faults (i.e., potential seismic sources), as defined by the California Division of Safety of Dams (Frazer and Howard, 2003), unless demonstrated to have been inactive in the past 35,000 years.
[2] Maximum earthquake magnitudes are calculated using the empirical relationships of Wells and Coppersmith (1994) among subsurface rupture area and magnitude.
[3] Bryant (1983), Bryant (1984), USGS Internet Quaternary fault and fold database (USGS, 2007), CDMG (2000).
[4] Bryant (1984), dePolo (1998), dePolo and Anderson (2000)
[5] Based on data in PG&E Geosciences Department connecting the Antelope Valley and West Walker fault zones
[6] Ramelli and others (1999), USGS Internet Quaternary fault and fold database (USGS, 2007), CDMG (2000).
[7] Ramelli and others (1999).
[8] Ramelli and others (1999).
[9] Ramelli and others (1999).
[10] Ramelli and others (1999).
[11] Ramelli and others (1999), USGS Internet Quaternary fault and fold database (USGS, 2007), CDMG (2000).

**TABLE 2-1**
**POTENTIAL SEISMIC SOURCES AND ESTIMATED MAXIMUM EARTHQUAKES FOR PG&E DAMS IN THE MOKELUMNE-STANISLAUS REGION, CALIFORNIA**

---

[12] Ramelli and others (1999).
[13] Ramelli and others (1999).
[14] Ramelli and others (1999), USGS Internet Quaternary fault and fold database (2006), CDMG (2000), this study.
[15] Ramelli and others (1999), USGS Internet Quaternary fault and fold database (2006), CDMG (2000).
[16] Ramelli and others (1999).
[17] Ramelli and others (1999).
[18] Ramelli and others (1999), USGS Internet Quaternary fault and fold database (2006), CDMG (2000), this study.
[19] Based on data in PG&E Geosciences Department; Holocene inferred from helicopter observation of scarps on post-glacial deposits.
[20] Based on data in PG&E Geosciences Department.
[21] Based on data in PG&E Geosciences Department.
[22] Based on data in PG&E Geosciences Department; Holocene inferred from helicopter observation of scarps on post-glacial deposits.
[23] Based on data in PG&E Geosciences Department.
[24] Based on data in PG&E Geosciences Department.
[25] Based on data in PG&E Geosciences Department.
[26] Based on data in PG&E Geosciences Department.
[27] Based on USGS Internet Quaternary fault and fold database (USGS, 2007) and data in PG&E Geosciences Department.
[28] Based on geomorphic comparison with Carson Range fault zone.
[29] Based on data in PG&E Geosciences Department.
[30] USGS Internet Quaternary fault and fold database (2006), this study.
[31] Kent and others (2005); USGS Internet Quaternary fault and fold database (USGS, 2007).
[32] Kent and others (2005).
[33] USGS Internet Quaternary fault and fold database (2006), this study.
[34] Kent and others (2005); USGS Internet Quaternary fault and fold database (USGS, 2007).
[35] Kent and others (2005).
[36] USGS Internet Quaternary fault and fold database (2006), this study.
[37] Information is based on data in the files of PG&E Geosciences Department, San Francisco, California.
[38] Inferred from geomorphic comparison w/ other faults in Seirran Frontal fault zone.
[39] Based on data in the files of PG&E Geosciences Department and CDMG (2000).
[40] Based on data in the files of PG&E Geosciences Department and CDMG (2000).
[41] Based on data in the files of PG&E Geosciences Department and CDMG (2000).
[42] Based on data in Lahren and Schweickert (1991).
[43] Based on data in Lahren and Schweickert (1991).
[44] Based on data in Lahren and Schweickert (1991).
[45] Based on data in the files of PG&E Geosciences Department and CDMG (2000).
[46] New evidence by Hamilton and others (2005) casts uncertainty on the existence of fault.
[47] Based on data in the files of PG&E Geosciences Department.
[48] Based on data in the files of PG&E Geosciences Department.
[49] Based on data in the files of PG&E Geosciences Department and CDMG (2000).
[50] Based on data in Alt and others (1977), Woodward-Clyde Consultants (1978), Biggar, and others (1978), Dames and Moore (1993), and PG&E (1989).
[51] Based on data in Biggar and others (1987) and Woodward-Clyde Consultants (1978).
[52] Based on data in the files of PG&E Geosciences Department and CDMG (2000).
[53] Based on data in the files of PG&E Geosciences Department.
[54] Based on data in the files of PG&E Geosciences Department.
[55] Based on data in the files of PG&E Geosciences Department and CDMG (2000).
[56] Based on data in the files of PG&E Geosciences Department.

**TABLE 2-1**
**POTENTIAL SEISMIC SOURCES AND ESTIMATED MAXIMUM EARTHQUAKES FOR PG&E DAMS IN THE MOKELUMNE-STANISLAUS REGION, CALIFORNIA**

---

[57] Based on data Woodward-Clyde Consultants (1978) and Biggar and others (1978).
[58] Based on data in the files of PG&E Geosciences Department and CDMG (2000).
[59] New evidence by Hamilton and others (2005) casts uncertainty on the existence of fault.
[60] Based on data in the files of PG&E Geosciences Department.
[61] Based on data in the files of PG&E Geosciences Department.
[62] Based on data in the files of PG&E Geosciences Department and CDMG (2000).
[63] New evidence by Hamilton and others (2005) casts uncertainty on the existence of fault.
[64] New evidence by Hamilton and others (2005) casts uncertainty on the existence of fault.
[65] Based on data in the files of PG&E Geosciences Department.
[66] Based on data in the files of PG&E Geosciences Department.
[67] Based on data in the files of PG&E Geosciences Department and CDMG (2000).
[68] New evidence by Hamilton and others (2005) casts uncertainty on the existence of fault.
[69] Based on data in the files of PG&E Geosciences Department.
[70]Based on data in the files of PG&E Geosciences Department and CDMG (2000).
[71] Based on data in Alt and others (1977), Woodward-Clyde Consultants (1978), Biggar and others (1978), Dames and Moore (1993).
[72] Woodward-Clyde Consultants (1978) and Biggar and orthers (1978).
[73] Based on Dames and Moore (1993) and CDMG (2000).
[74] New evidence by Hamilton and others (2005) casts uncertainty on the existence of fault.
[75] Based on data in the files of PG&E Geosciences Department.
[76] Based on data in the files of PG&E Geosciences Department.
[77] Based on data in the files of PG&E Geosciences Department and CDMG (2000).
[78] Based on Slemmons (1953) and data in the files of PG&E Geosciences Department.
[79] Woodward-Clyde Consultants (1978), Biggar and others (1978), PG&E Geosciences Department.
[80] Woodward-Clyde Consultants (1978), Biggar and others (1978), PG&E Geosciences Department.
[81] Based on data in the files of PG&E Geosciences Department and CDMG (2000).
[82] Based on data in the files of PG&E Geosciences Department and Dames and Moore (1993).
[83] Based on data in the files of PG&E Geosciences Department.
[84] Based on data in the files of PG&E Geosciences Department and CDMG (2000).
[85] Based on data in Alt and others (1977), Woodward-Clyde Consultants (1978), Biggar and others (1978), CDMG (2000).
[86] Dames and Moore (1993); Woodward-Clyde Consultants (1978), Biggar and others (1978).
[87] Dames and Moore (1993).
[88] Appendix C, "Evaluation of Deterministic Background Earthquake in Sierra Nevada, California" in report entitled "Regional Geology, Seismicity, and General Ground Motion Considerations for the Feather River Hydroelectric System" (Piedmont GeoSciences and PG&E, April, 2004).
[89] Appendix C, "Evaluation of Deterministic Background Earthquake in Sierra Nevada, California" in report entitled "Regional Geology, Seismicity, and General Ground Motion Considerations for the Feather River Hydroelectric System" (Piedmont GeoSciences and PG&E, April, 2004).

CHECK END NOTES

**TABLE 5-1**
**COMPARISON OF 2007 NGA PEAK-GROUND-ACCELERATIONS ESTIMATES WITH EARLIER ESTIMATES FOR UPPER BLUE LAKE AND LYONS DAMS**

| POTENTIAL SEISMIC SOURCE | ESTIMATED MAXIMUM EARTHQUAKE and DISTANCE TO DAM | | | | | ESTIMATED PEAK GROUND ACCELERATIONS (g) | | | |
|---|---|---|---|---|---|---|---|---|---|
| | 1993 | 1997/99 | 2002 | 2007 | | 1992/93 | 1998/99 | 2002 | 2007 |
| **UPPER BLUE LAKE DAM** | | | | | | | | | |
| **Sierra Nevada Frontal fault system** | | | | | | | | | |
| Carson Range fault zone | Carson Valley 7.0 @ 10 km | Woodfords >6.6 @ 12 km | 6.6 to 7.1 @ 10km | 6.6 to 7.1 @ 10km | | 0.43 | Woodfords 0.36 | 0.41 to 0.46 | 0.33 to 0.38 [84th] |
| Waterhouse Peak fault | 6.5 @ ~2 km | 6.4 to 6.7 @ <0.4 to 8 km | 6.5 to 6.7 @ <0.4 to 8km | 6.4 to 6.7 @ <1 to 1.3km | | 0.3 | 0.34 to 0.57 [extension] | 0.35 to 0.57 [extension] | 0.14 to 0.39 |
| **LYONS DAM – Stanislaus River in the central Sierra Nevada** | | | | | | | | | |
| **Sierra Nevada Frontal fault system** | | | | | | | | | |
| West Walker | 7 to 7.5 @ 64km | 6.4 to 6.5 @ 64km | 6.4 to 6.5 @ 64km | 6.4 to 6.5 @ 65km | | 0.05 to 0.07 | 0.04 to 0.05 [84th extension] | 0.05 [84th extension] | 0.03 |
| Antelope Valley/West Walker | Not considered | Not considered | Not considered | 6.5-6.8 @ 65 to 75km | | -- | -- | -- | 0.07 [84th] |
| **Fault Sources within the Sierran microplate** | | | | | | | | | |
| Douds Landing fault | 6.3 to 6.5 @ 9km | 6.2 to 6. 4 @ 4 to 12km | 6.3 to 6.5 @ 9km | 6.3 to 6.5 @ 10km | | 0.28 to 0.33 | 0.30 to 0.33 1997 0.14 to 0.39 | 0.22 to 0.42 | 0.13 to 0.26 |
| **Background Earthquake** | | | | | | | | | |
| Background earthquake | 5 @ 5 to 15km | 5 @ 5 to15km | 5 @ 5 to 15km | 5.8 @ 15km (3000 year recurrence) | | 0.08 to 0.19 | 0.16 (extensional) | .06 to 0.16 (extensional) | 0.16 |

Note: Ground motions are median unless otherwise noted

# 8.0 FIGURES

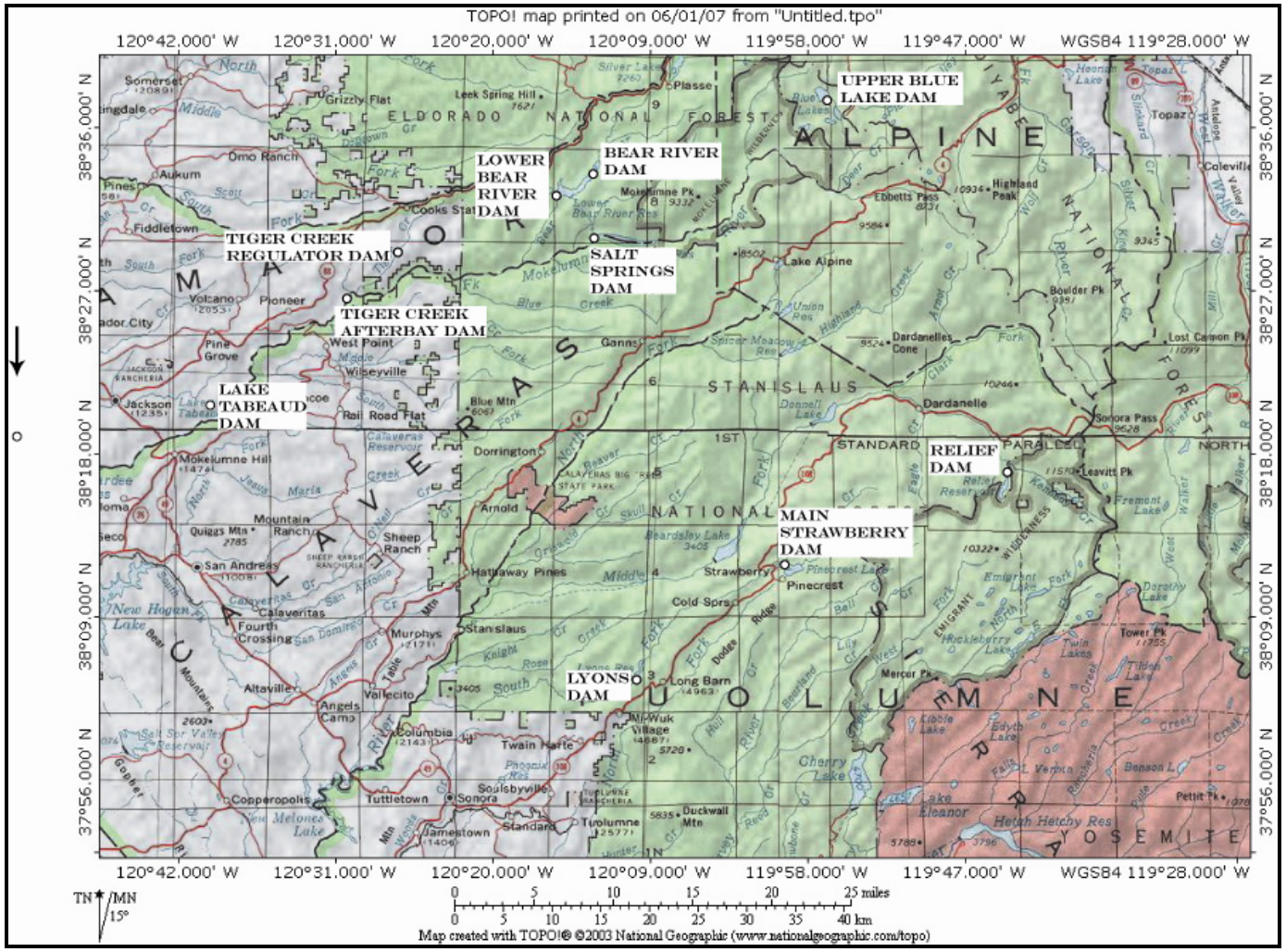


Base map from National Geographic, 2004

**FIGURE 1-1 MAIN PG&E DAMS IN THE MOKELUMNE-STANISLAUS REGION**

Mokelumne-Stanislaus Regional Report
PG&E Geosciences Department; October 28, 2007

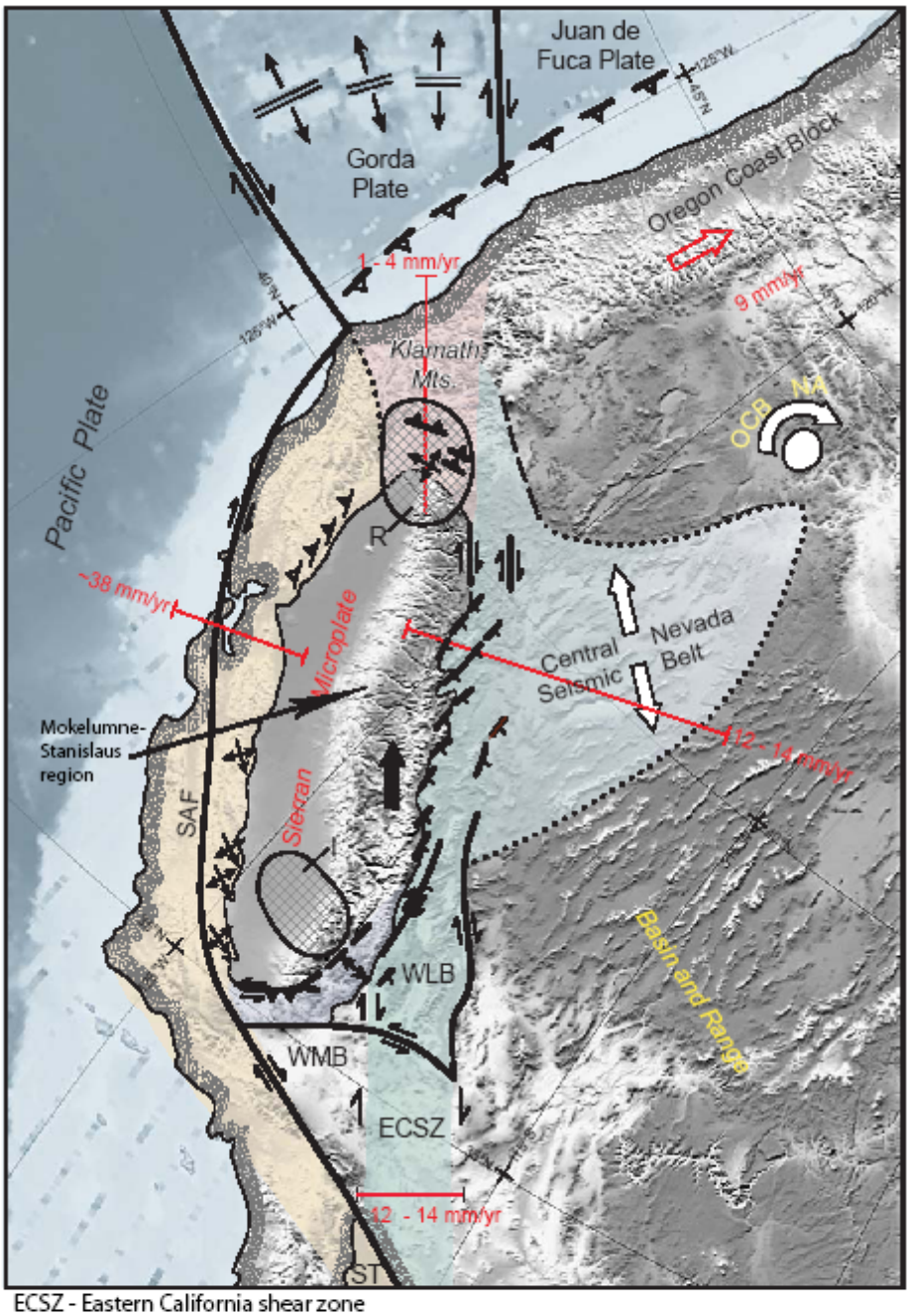


From Page and others (2007, in preparation)

**FIGURE 2-1 TECTONIC SETTING OF THE SIERRAN MICROPLATE**

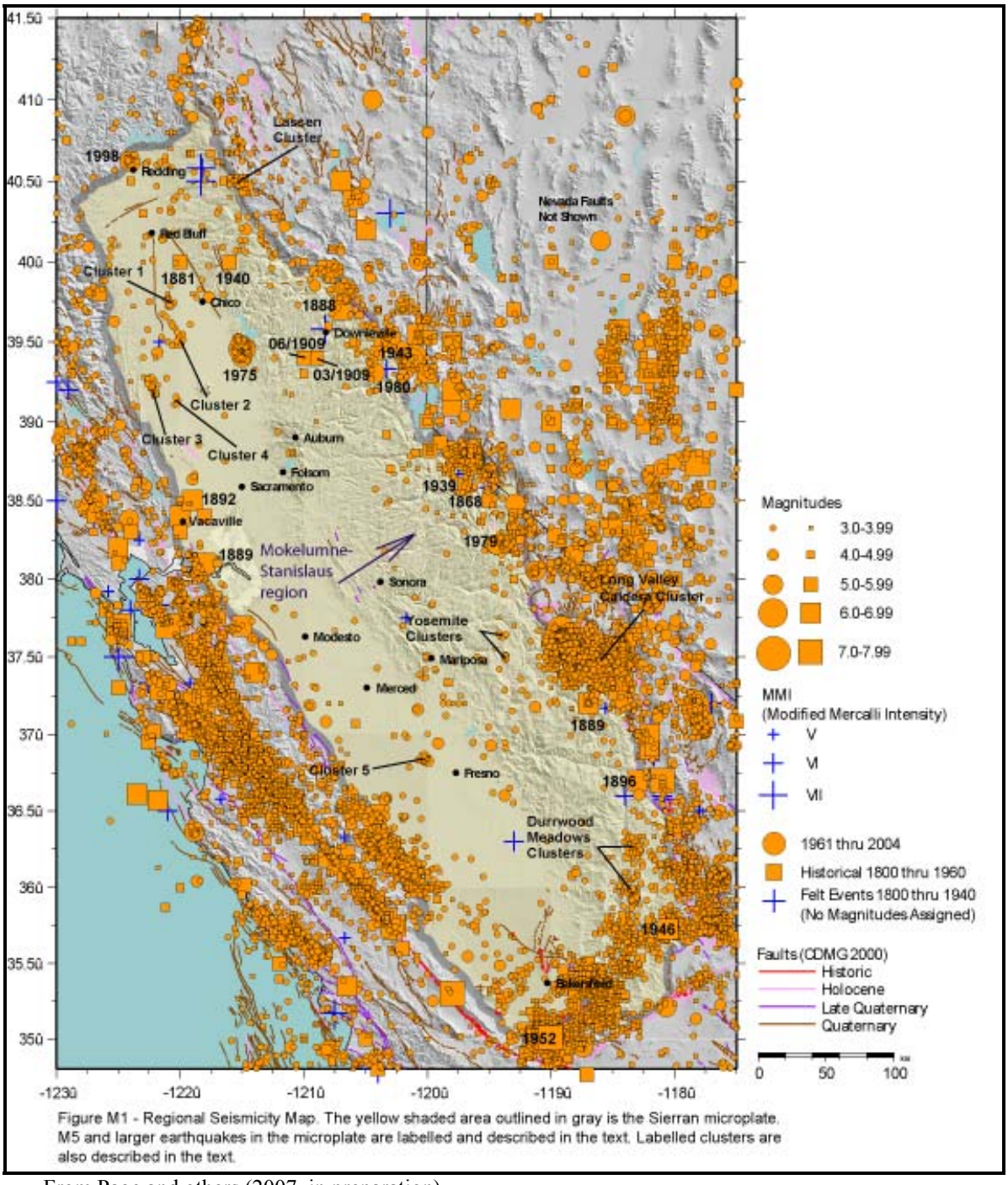


Figure M1 - Regional Seismicity Map. The yellow shaded area outlined in gray is the Sierran microplate. M5 and larger earthquakes in the microplate are labelled and described in the text. Labelled clusters are also described in the text.

From Page and others (2007, in preparation)

## FIGURE 2-2 SIERRAN MICROPLATE

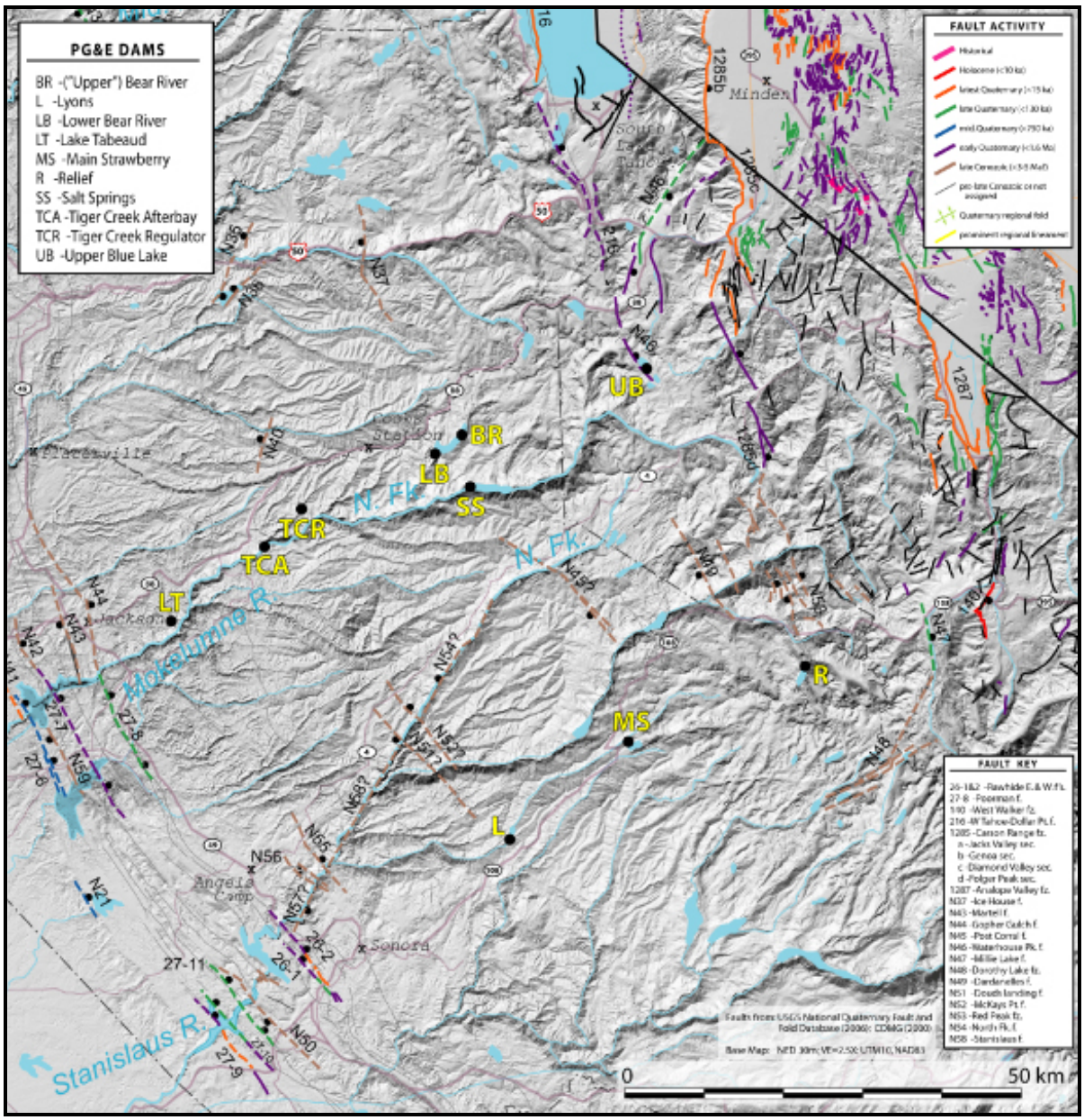

Figure by Piedmont GeoSciences

**FIGURE 2-3 QUATERNARY FAULTS IN MOKELUMNE-STANISLAUS REGION**

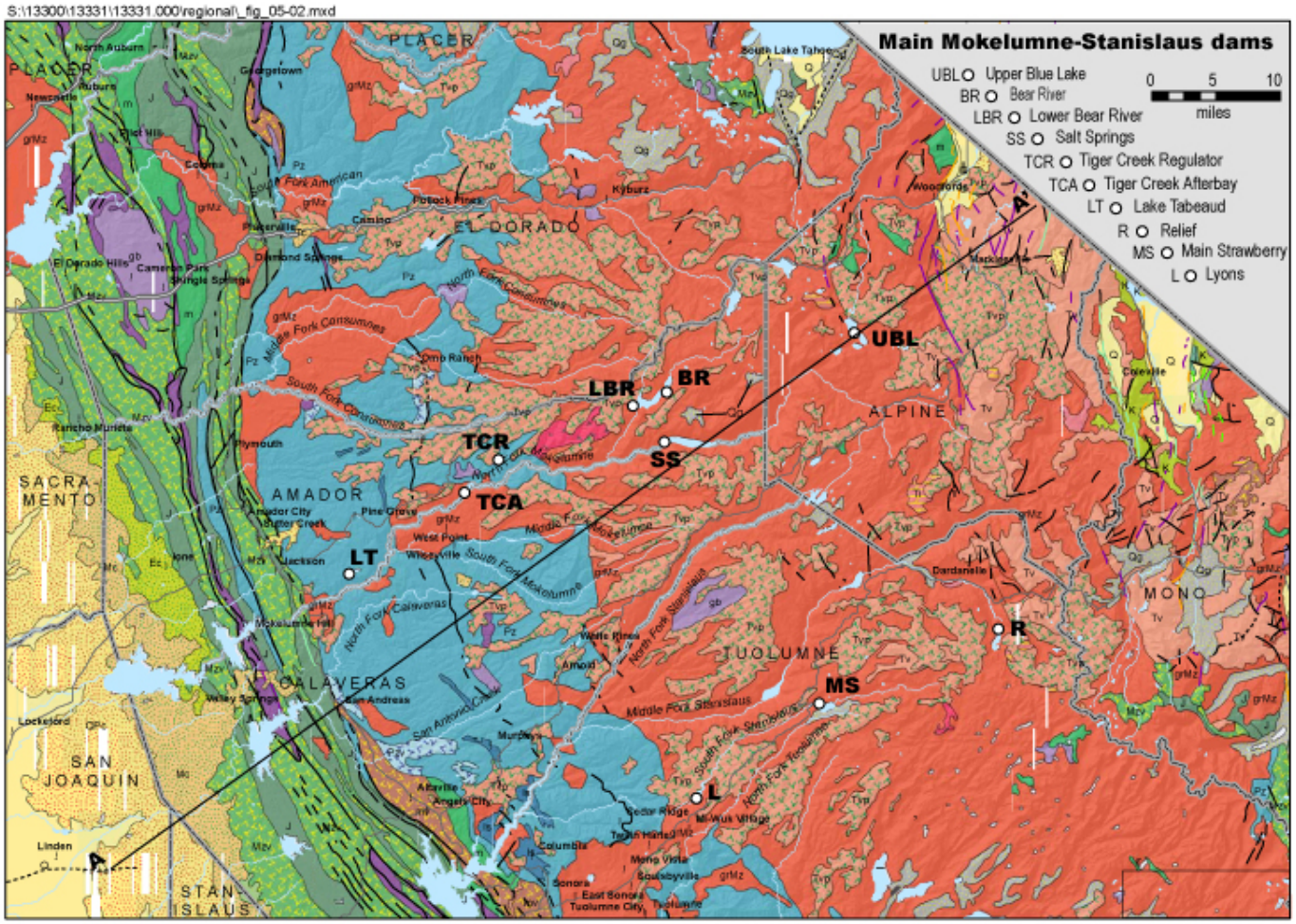


Figure by Geomatrix - modified from Jennings (1977); see Figure 3-2 for explanation of geologic units and cross section A-A'

## FIGURE 3-1 REGIONAL GEOLOGY OF THE MOKELUMNE–STANISLAUS REGION

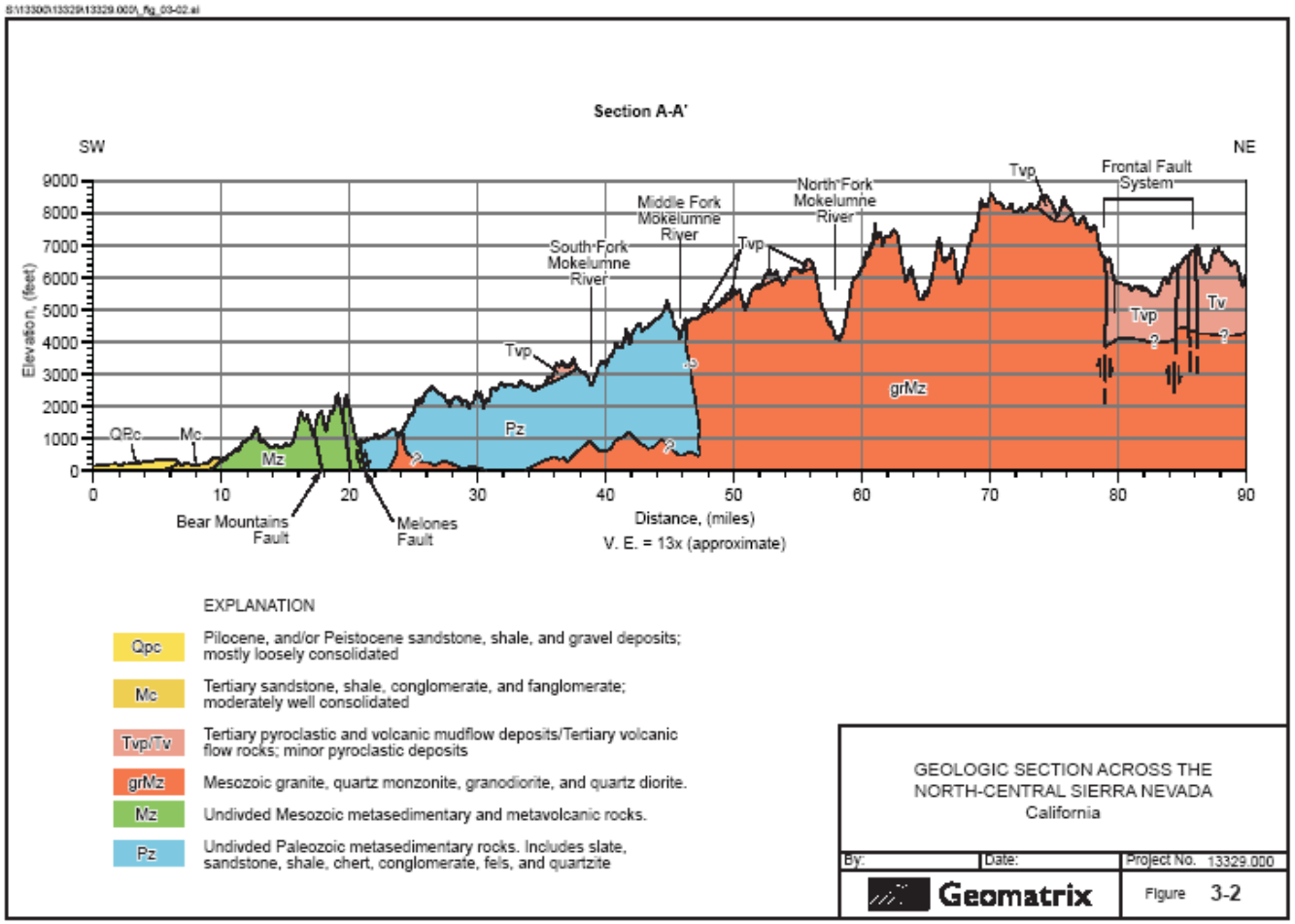


Figure by Geomatrix - modified from Jennings (1977

**FIGURE 3-2 REGIONAL GEOLOGIC CROSS SECTION OF MOKELUMNE-STANISLAUS REGION.**

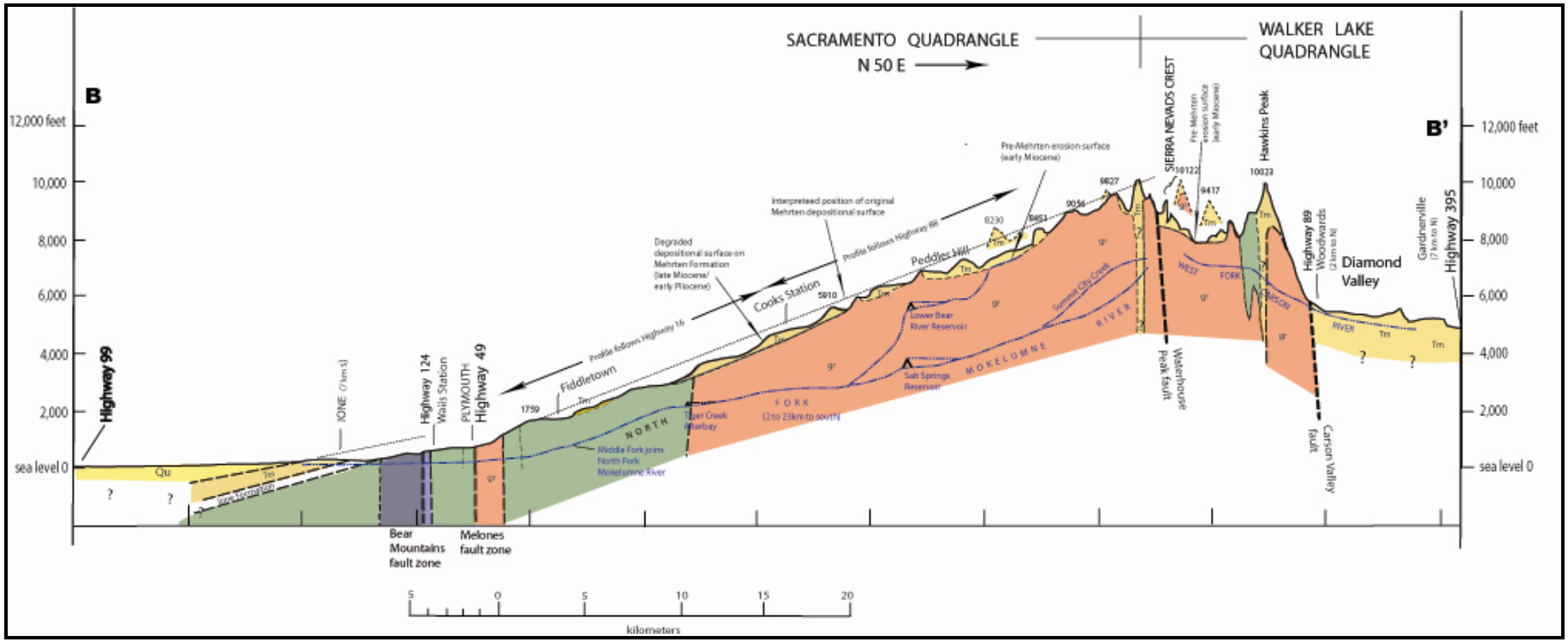


Profile follows the divide between the Mokelumne and Consumnes rivers from the Central Valley to the Sierra Nevada crest and then projects down the east escarpment of the range. The divides are projected perpendicular to the line of projection. V=10.6 H

**FIGURE 3-3 GEOMORPHIC PROFILE ACROSS THE SIERRA NEVADA NORTH OF MOKELUMNE RIVER**

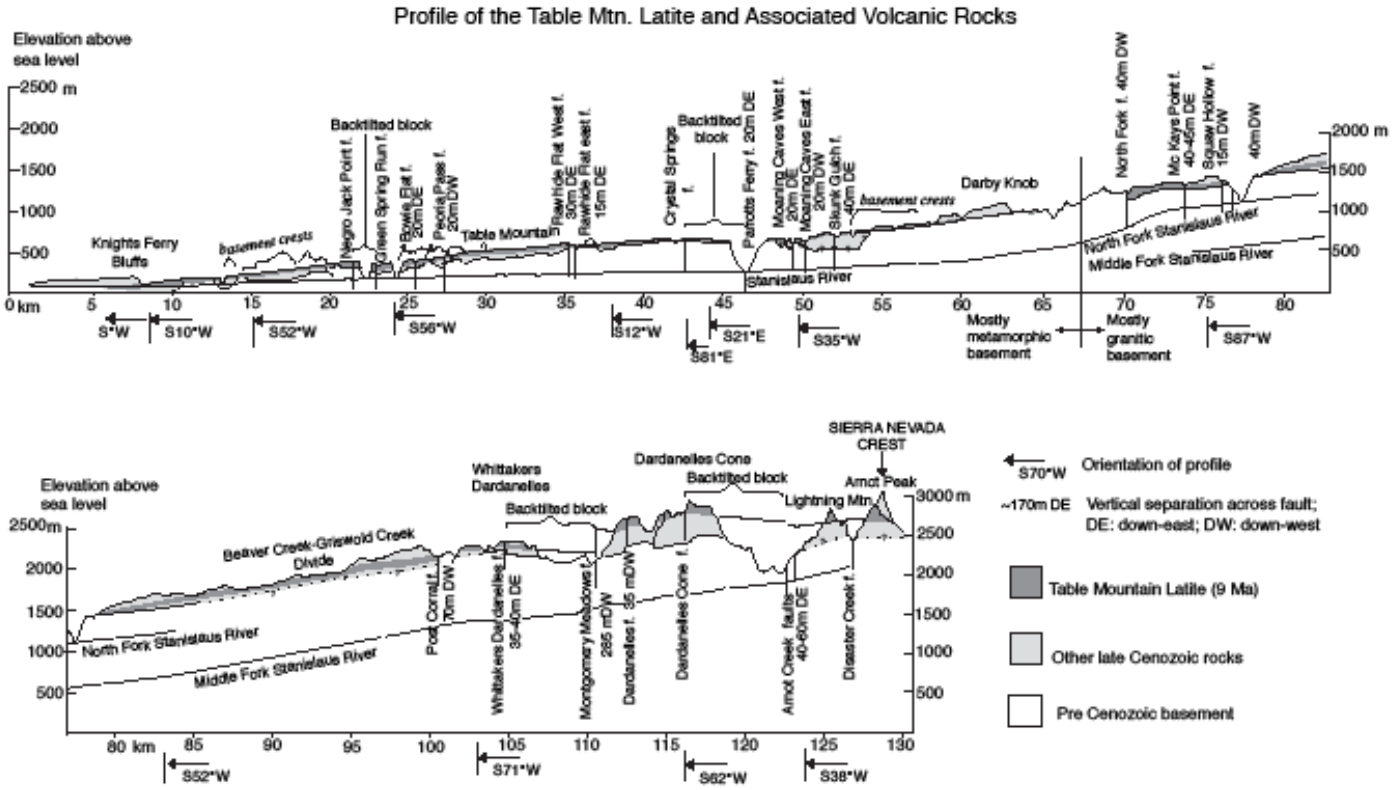


Depository Figure 4. Profile of the Table Mountain Latite and related volcanic rocks. 5X vertical exaggeration. Adapted from Wakabayashi and Sawyer (2000).

From Wakabayashi and Sawyer, 2001. Profile extends from the Central Valley at Knights Ferry in the Stanislaus watershed to the Sierra Nevada crest.

**FIGURE 3-4 GEOMORPHIC PROFILE ON THE TUOLUMNE TABLE MOUNTAIN LATITE**

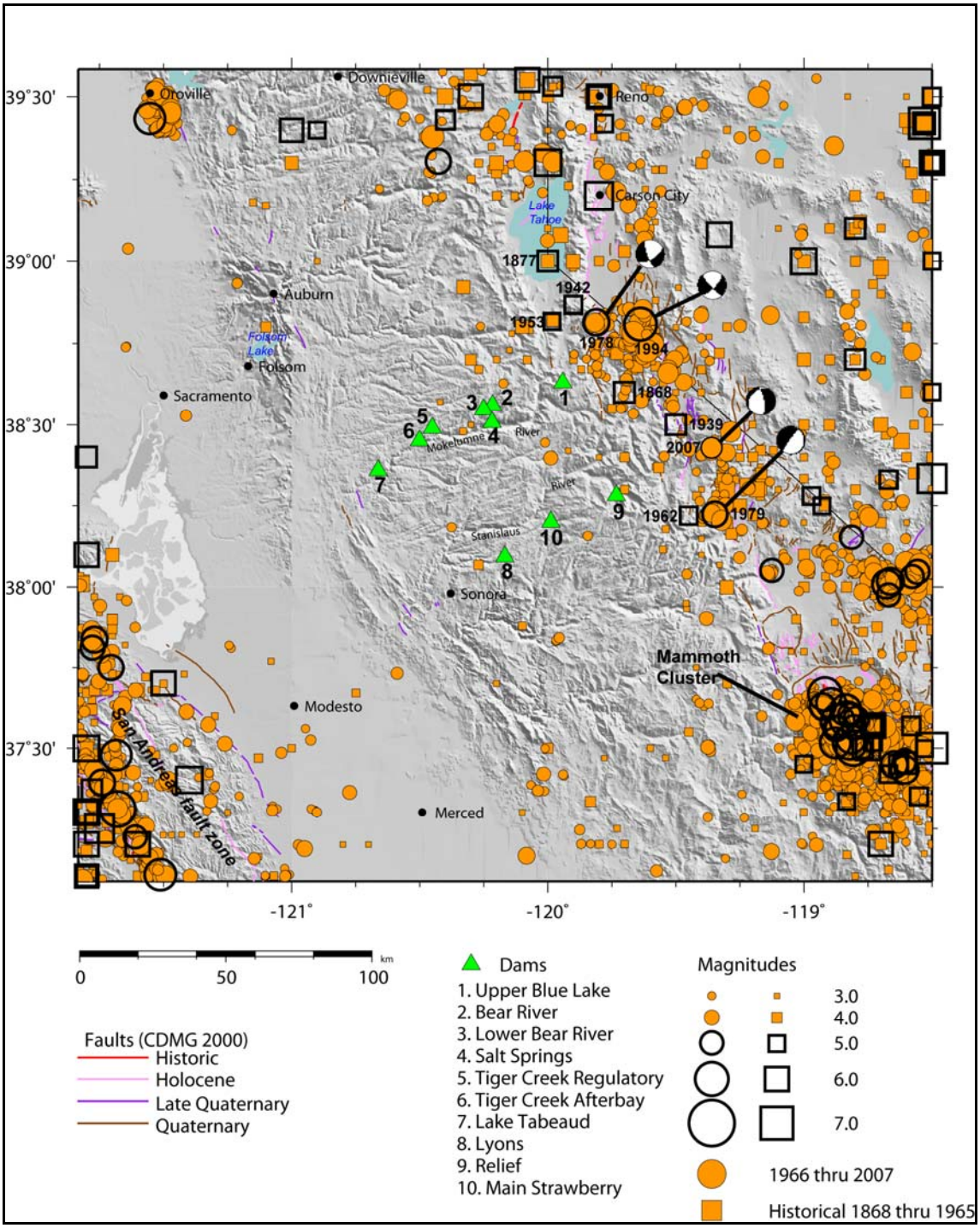


Magnitude 3 and greater earthquakes from 1868 through 2007 and selected focal mechanisms plotted (NCSN, 2007). The region is includes an area approximately 100 kilometers of the Mokelumne and Stanislaus River Dams.

**FIGURE 4-1 SEISMICITY IN MOKELUMNE-STANISLAUS REGION**

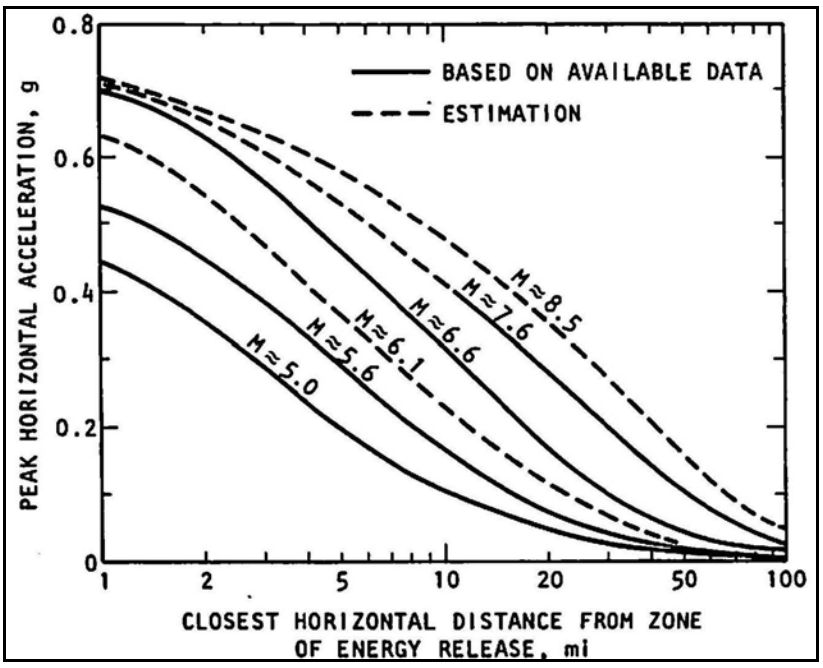


**FIGURE 5-1 AN EXAMPLE OF PGA ATTENUATION CURVES DEVELOPED IN THE 1980'S (Seed and Idriss, 1982)**

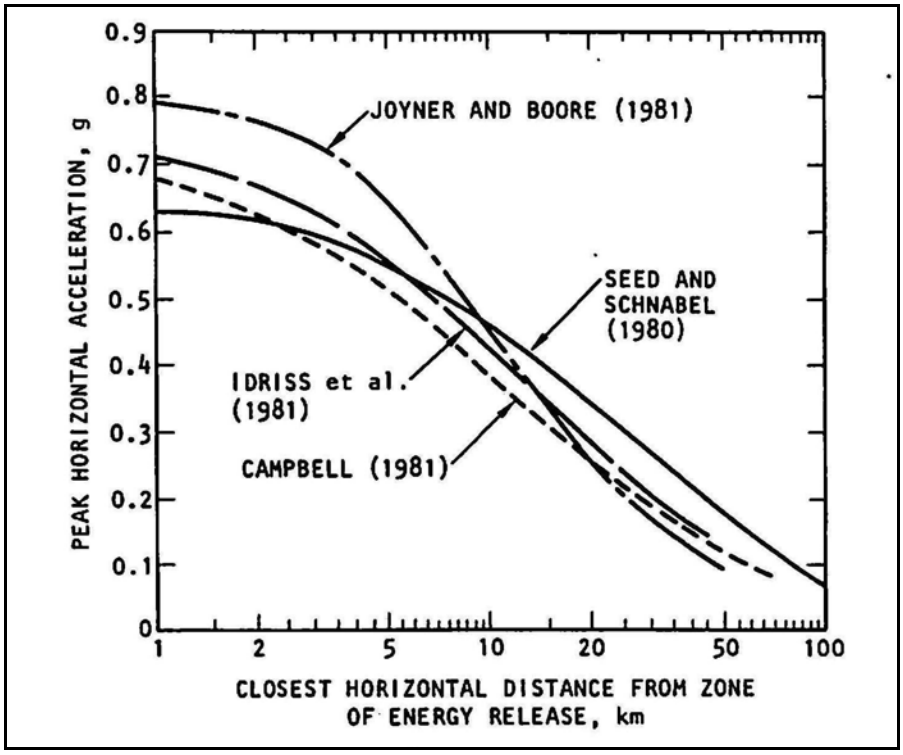


**FIGURE 5-2 COMPARISON OF PGA ATTENUATION CURVES DEVELOPED IN THE 1980'S (Seed and Idriss, 1982)**

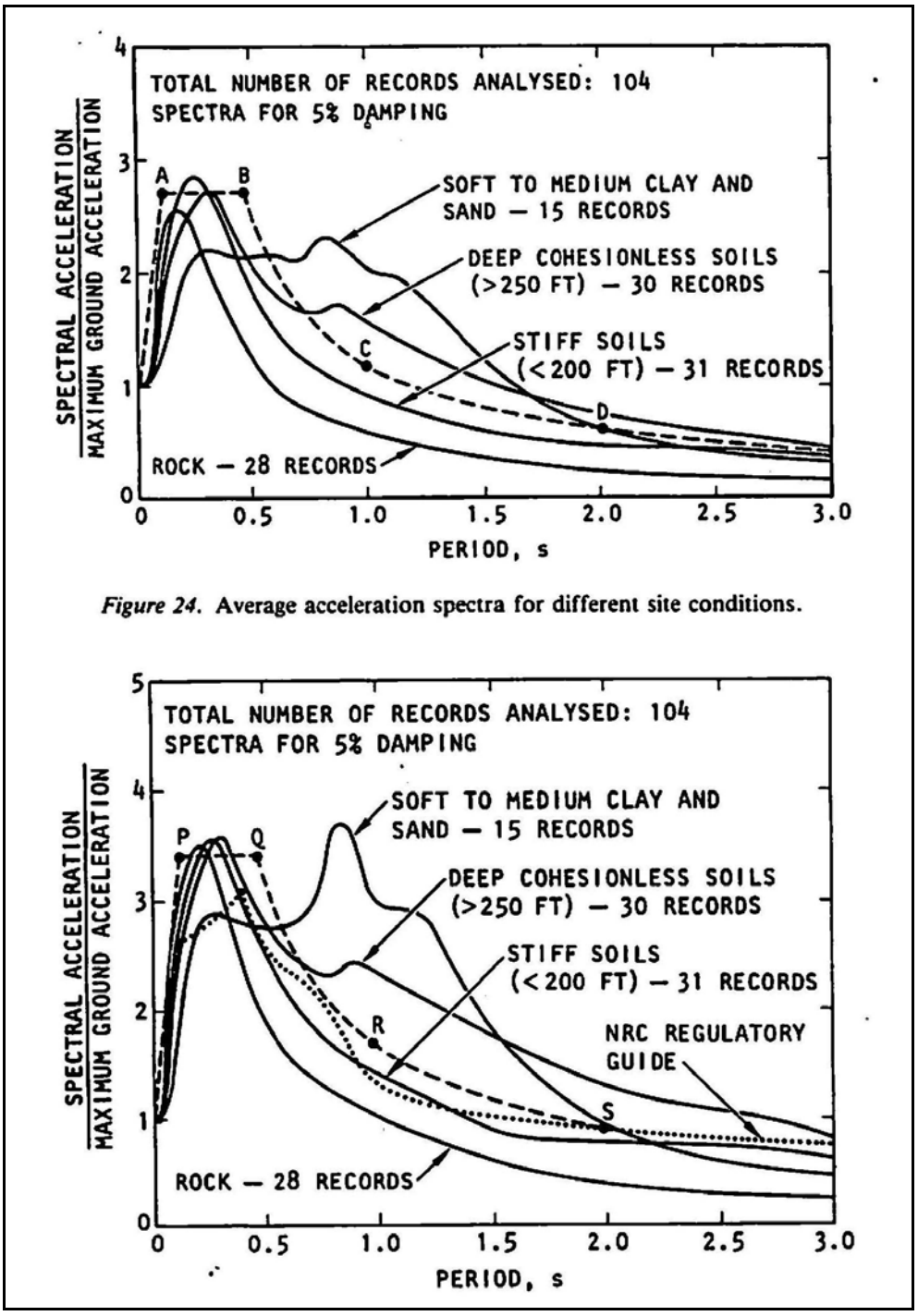


*Figure 24.* Average acceleration spectra for different site conditions.

**FIGURE 5-3 OBSERVED SITE-DEPENDENT SA SPECTRAL SHAPES: MEDIAN (TOP), 84TH PERCENTILE (BOTTOM) (Seed and Idriss, 1982)**

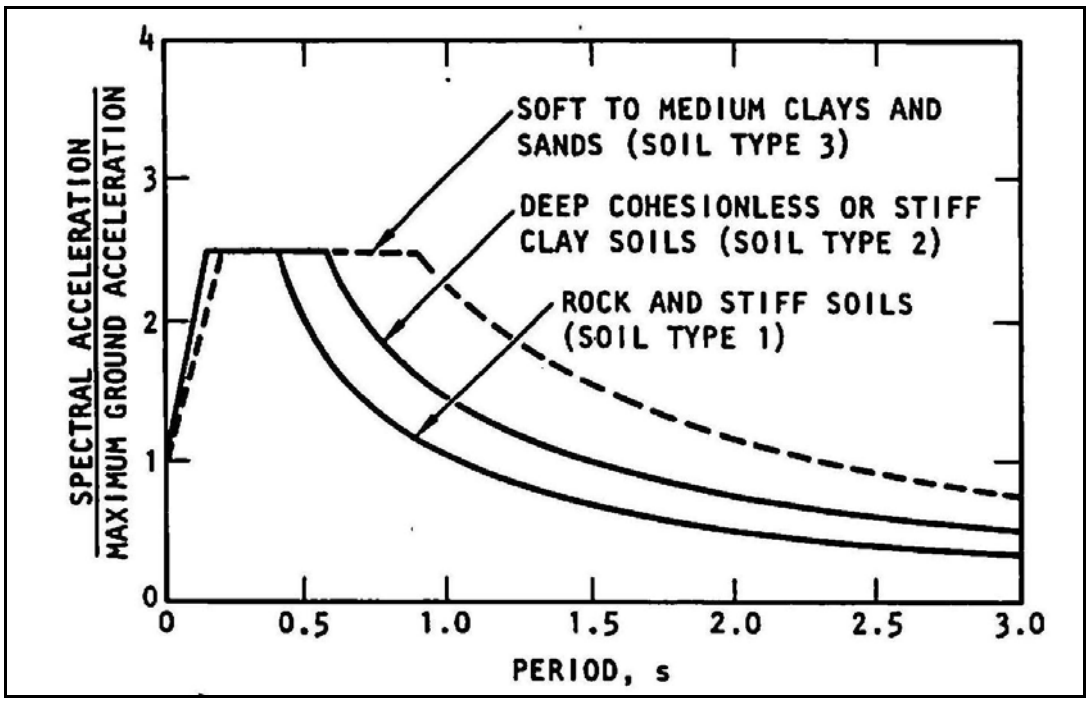


**FIGURE 5-4 SITE-DEPENDENT DESIGN SPECTRAL SHAPES FOR BUILDING CODES (Seed and Idriss, 1982)**

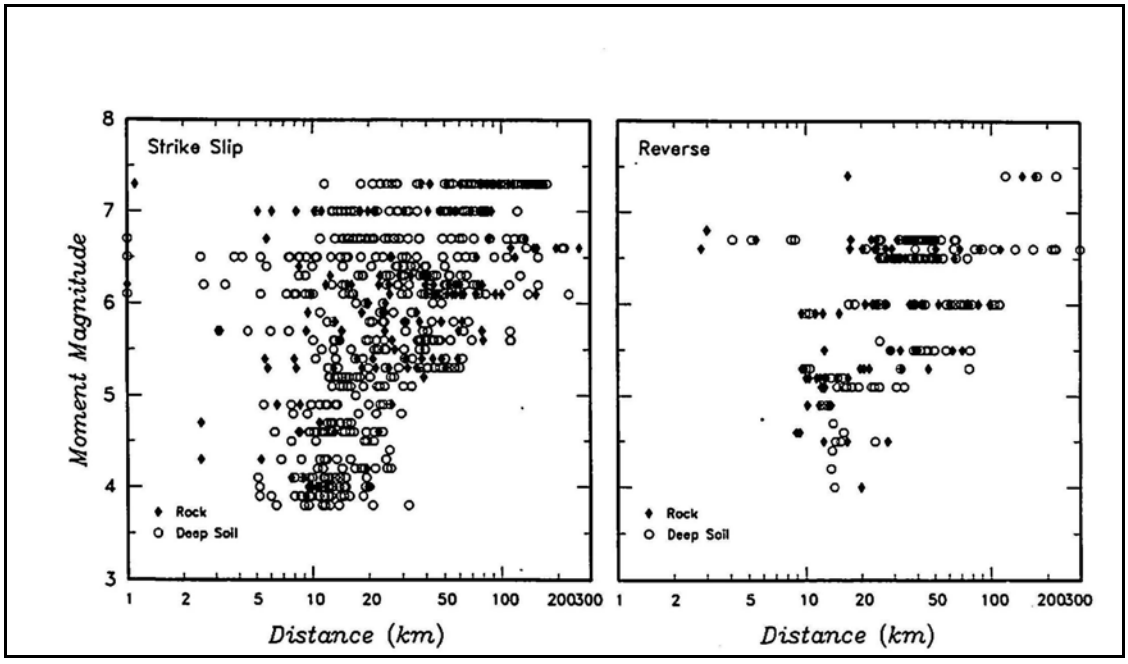


**FIGURE 5-5 TYPICAL STRONG MOTION DATABASE USED IN THE 1997 GROUND MOTION ATTEUATION MODELS (Sadigh and others, 1997)**

**TABLE 2A.**
**Summary Information on Attenuation Relationships**
**Shallow Crustal Earthquakes in Active Tectonic Regions**

| Model | Period Range (sec) | Comp | Site Conditions | Model Parameters[1] |
|---|---|---|---|---|
| Abrahamson & Silva | 0.0–5.0 | Ave H, V | Rock, Deep Soil | $M$, $r_{rup}$, $F_1$, HW |
| Boore, Joyner, & Fumal | 0.0–2.0 | Ave H | $V_s$ in top 30 m | $M$, $r_{jb}$, $F_2$ |
| Campbell | 0.0–4.0 | Ave H, V | Hard Rock, Soft Rock, Soil | $M$, $r_{seis}$, $F_2$, D |
| Sadigh *et al.* | 0.0–4.0 | Ave H | Rock, Deep Soil | $M$, $r_{rup}$, $F_1$, HW |
| Spudich *et al.* | 0.0–2.0 | Ave H | Rock, Soil | $M$, $r_{jb}$ |
| Idriss | 0.0–5.0 | Ave H | Rock/Stiff Soil, Deep Soil, Soft-Soil | $M$, $r_{rup}$, $F_1$ |

1. Model Parameters:
   $F_1$ = 1 for reverse, 0.5 for reverse/oblique, 0 otherwise;
   $F_2$ = 1 for reverse or reverse/oblique, 0 otherwise;
   $HW$ = 1 for sites over the hanging wall, 0 otherwise
   $D$ = depth to basement rock at the receiver (km)

**FIGURE 5-6 SUMMARY OF PARAMETERS USED IN THE 1997 GROUND MOTION ATTENUATION MODELS (Abrahamson and Shedlock, 1997)**

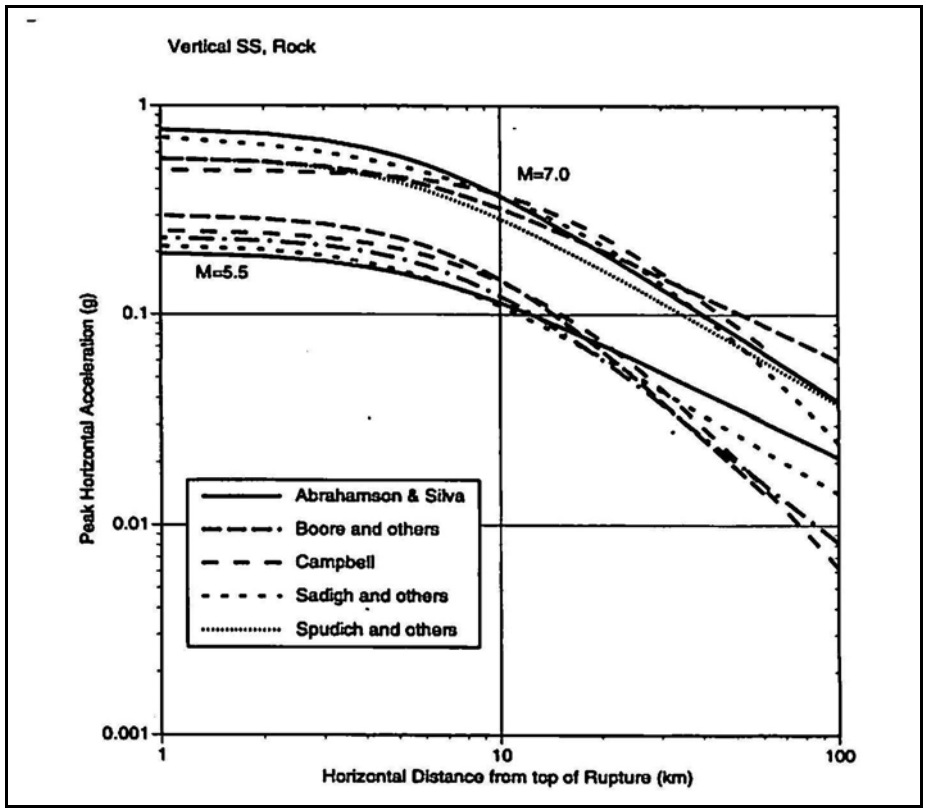


**FIGURE 5-7 COMPARISON OF PGA ATTENUATION ON ROCK FOR STRIKE-SLIP FAULTING (Abrahamson and Shedlock, 1997)**

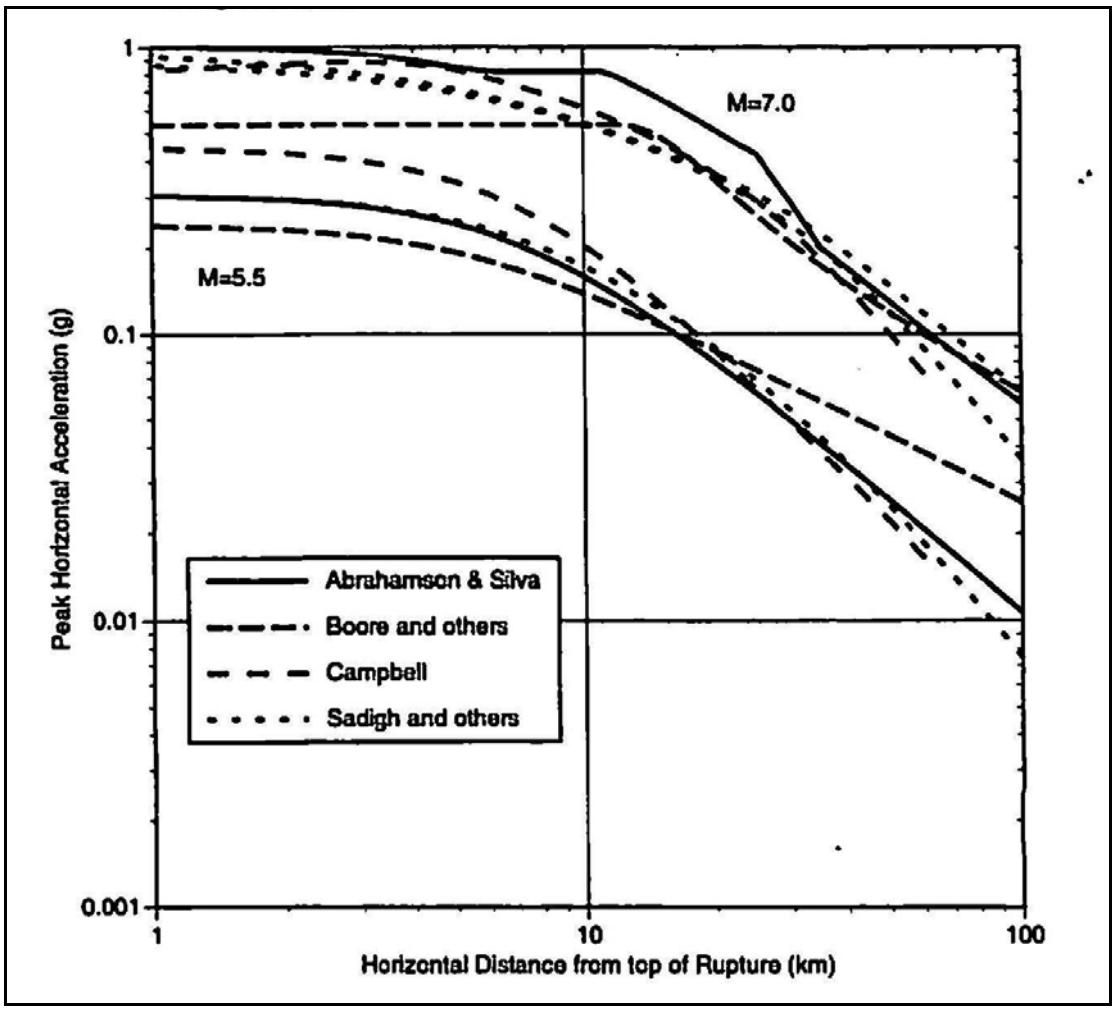


45 degrees RV, rock

**FIGURE 5-8 COMPARISON OF PGA ATTENUATION ON ROCK FOR REVERSE FAULTING (Abrahamson and Shedlock, 1997)**

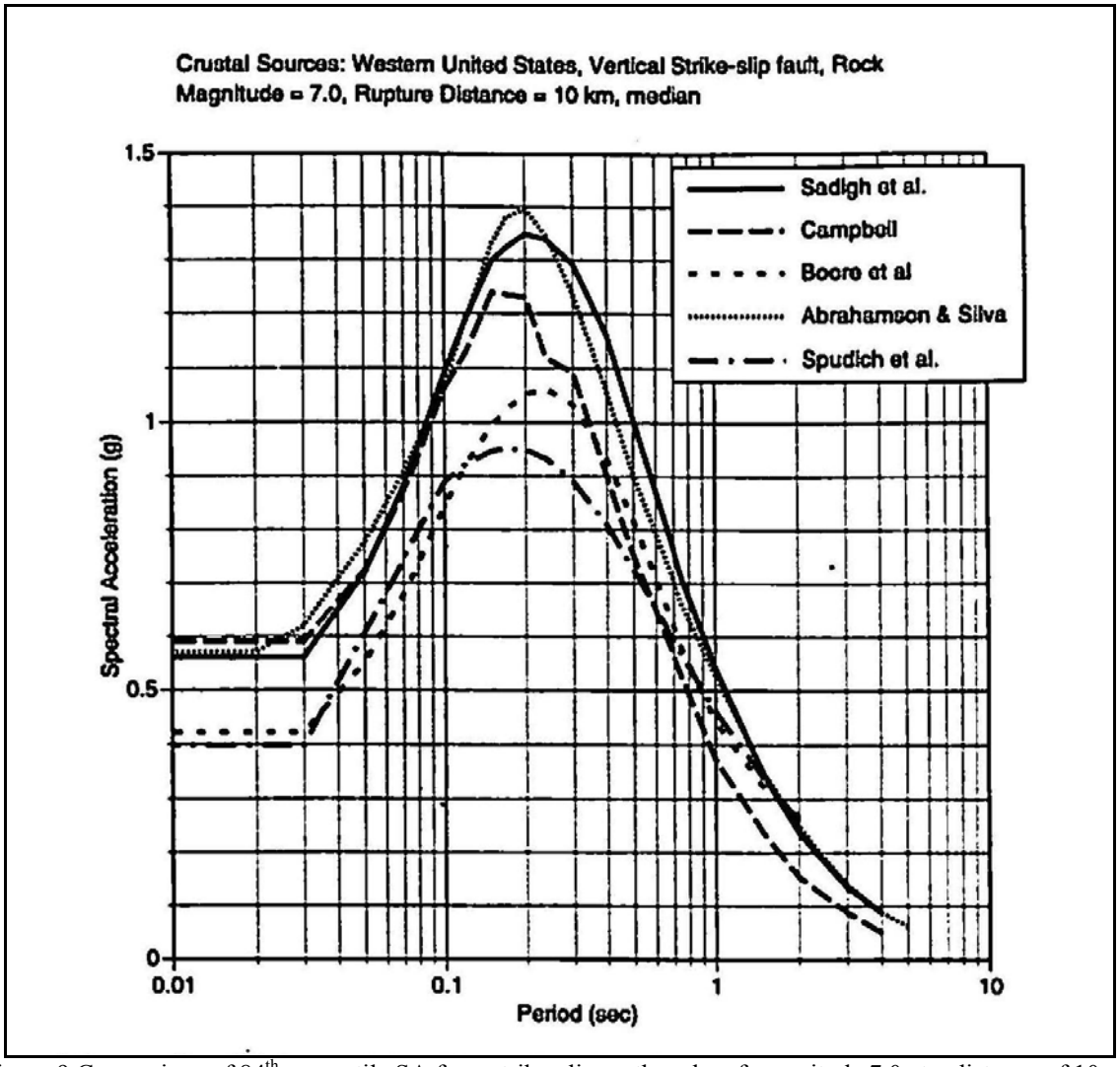


[Figure 9 Comparison of 84th percentile SA for a strike-slip earthquake of magnitude 7.0 at a distance of 10 kilometers in an active tectonic region. At most periods, the spectral values are within a factor of 1.5 of each other.]

**FIGURE 5-9 COMPARISON OF 84th SA SPECTRA AMONG FIVE 1997 GROUND MOTION ATTENUATION MODELS (Abrahamson and Shedlock, 1997)**

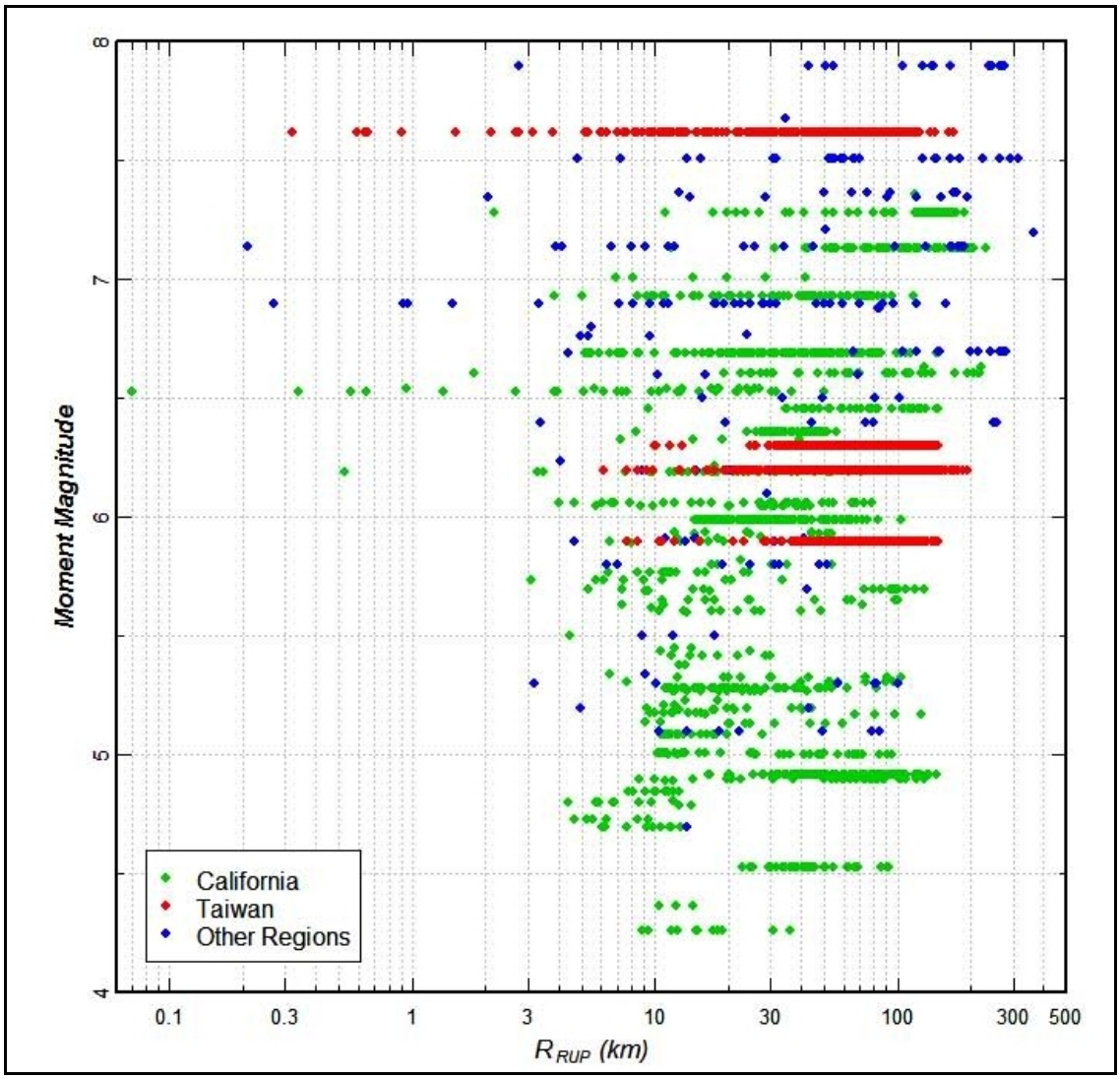


**FIGURE 5-10 STRONG MOTION DATA BASE USED IN NGA MODELS (Chiou and Youngs, 2006)**

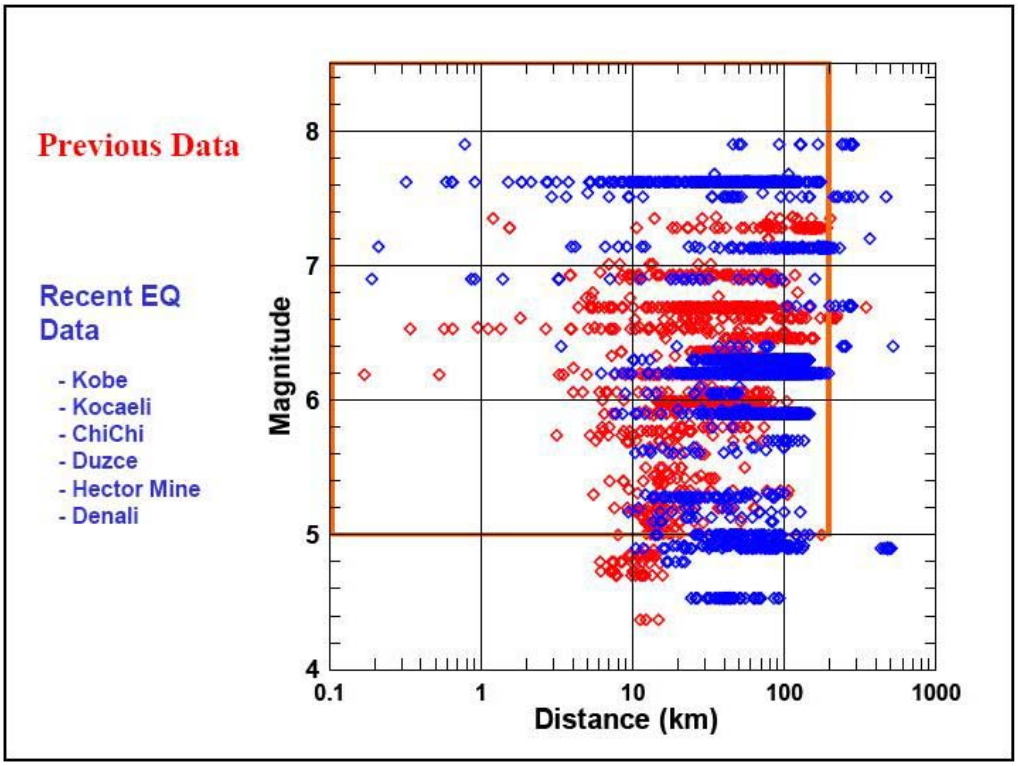


**FIGURE 5-11 COMPARISON OF THE NGA STRONG MOTION DATABASE WITH PREVIOUS DATA (Chiou and others, 2004; Power and others, 2008)**

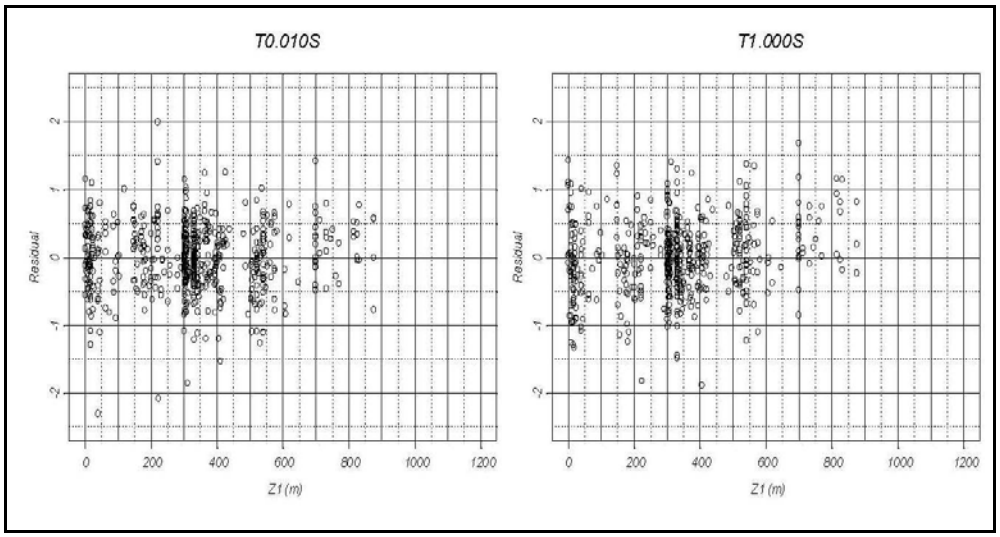


**FIGURE 5-12 EFFECTS OF DEPTH-TO-BEDROCK ON GROUND MOTIONS (Chiou and Youngs, 2006)**

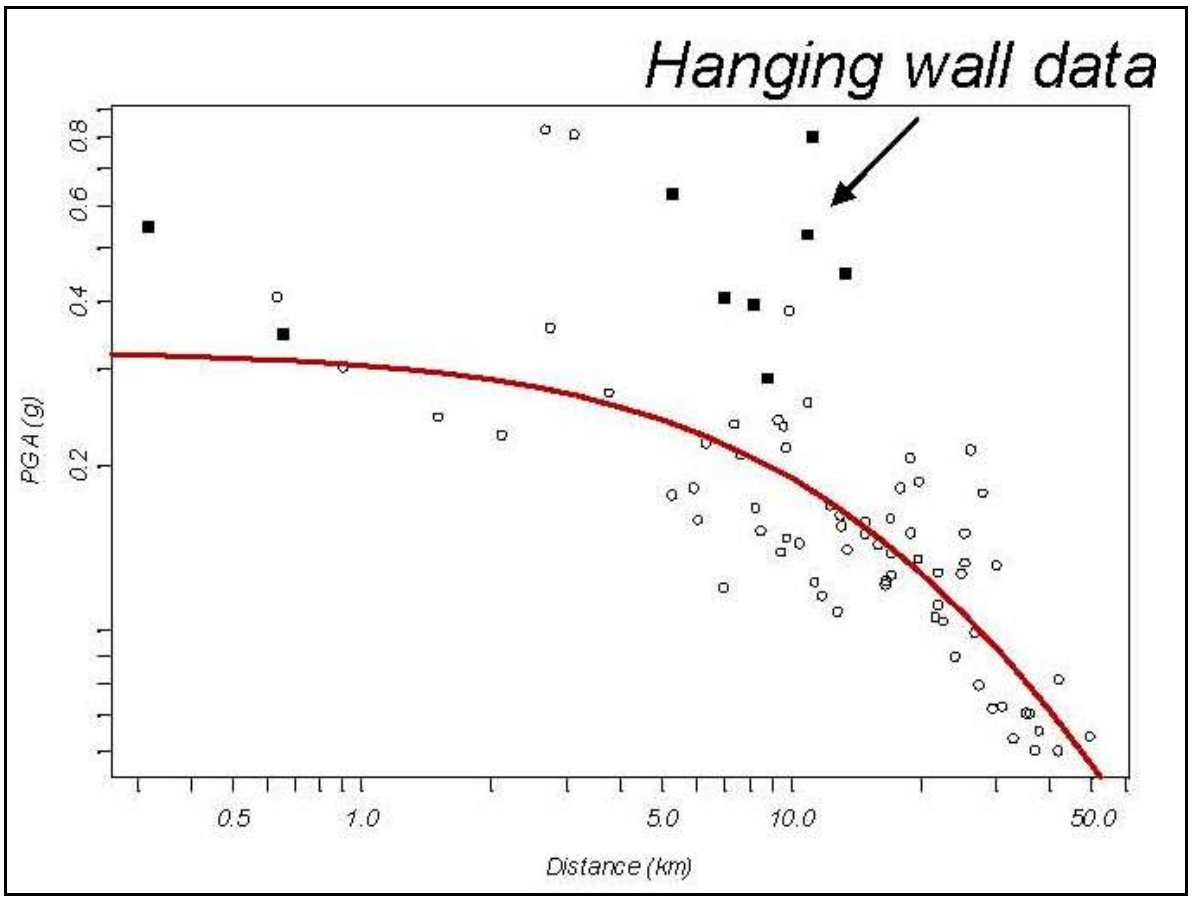


**FIGURE 5-13A OBSERVED HANGING WALL EFFECTS (Abrahamson and Silva, 2007)**

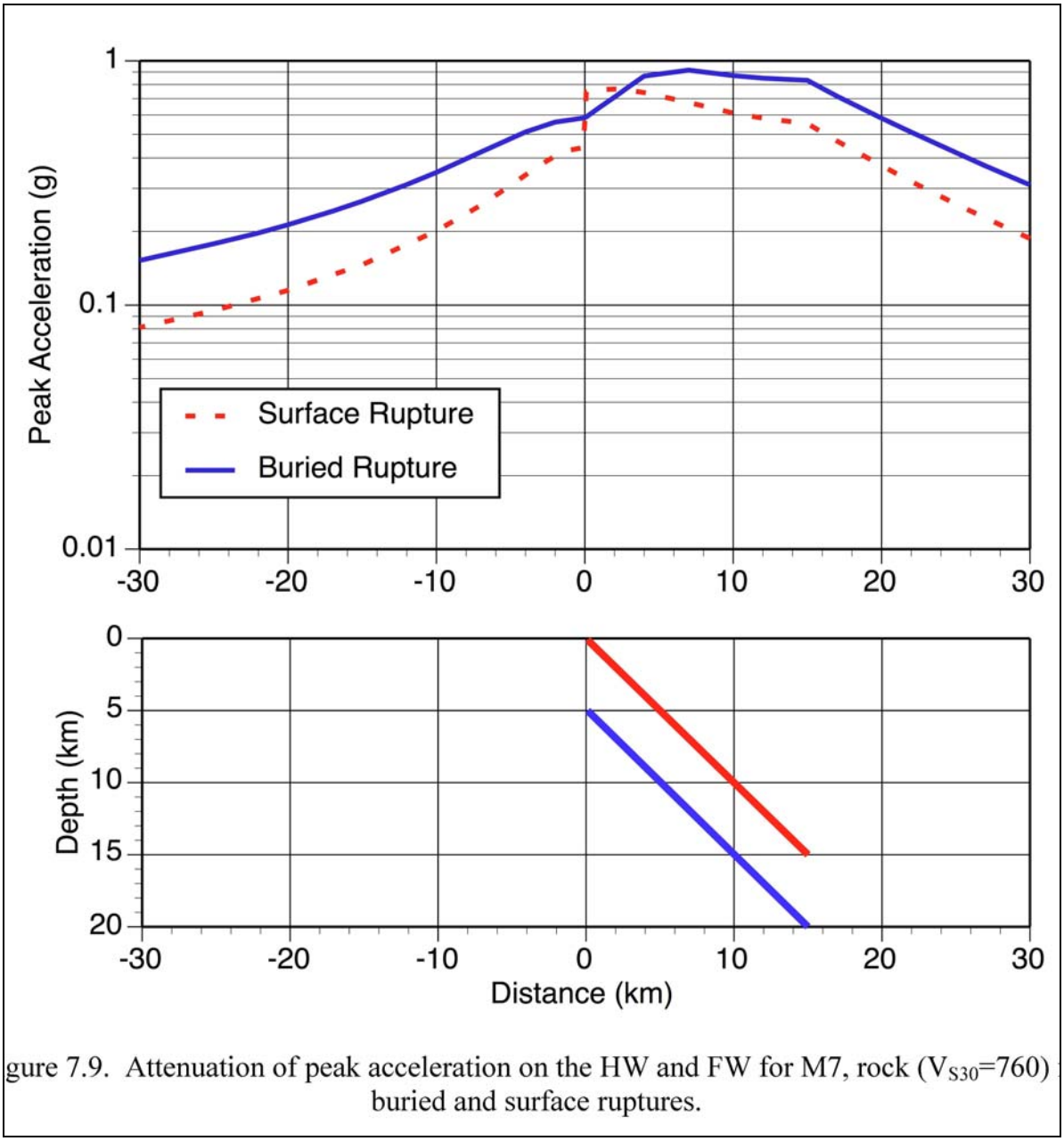


gure 7.9. Attenuation of peak acceleration on the HW and FW for M7, rock ($V_{S30}$=760) buried and surface ruptures.

**FIGURE 5-13B MODELING OF THE HANGING WALL AND FOOTWALL EFFECTS ON PGA ATTENUATION (Abrahamson and Silva, 2007)**

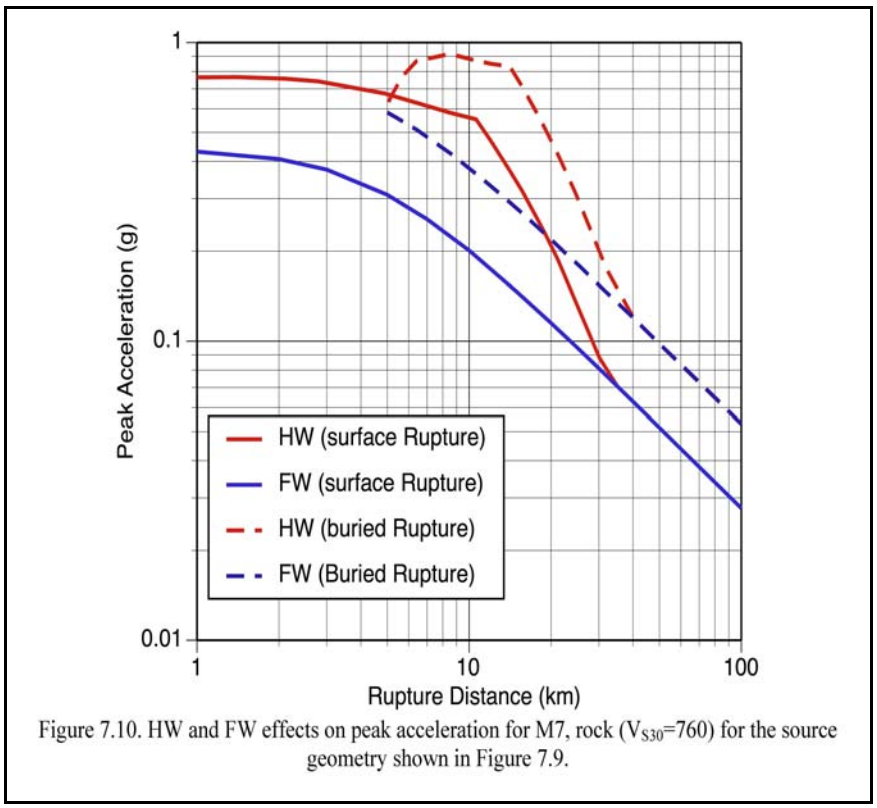


Figure 7.10. HW and FW effects on peak acceleration for M7, rock ($V_{S30}$=760) for the source geometry shown in Figure 7.9.

**FIGURE 5-13C HANGING WALL AND FOOTWALL EFFECTS ON PGA ATTENUATION (Abrahamson and Silva, 2007)**

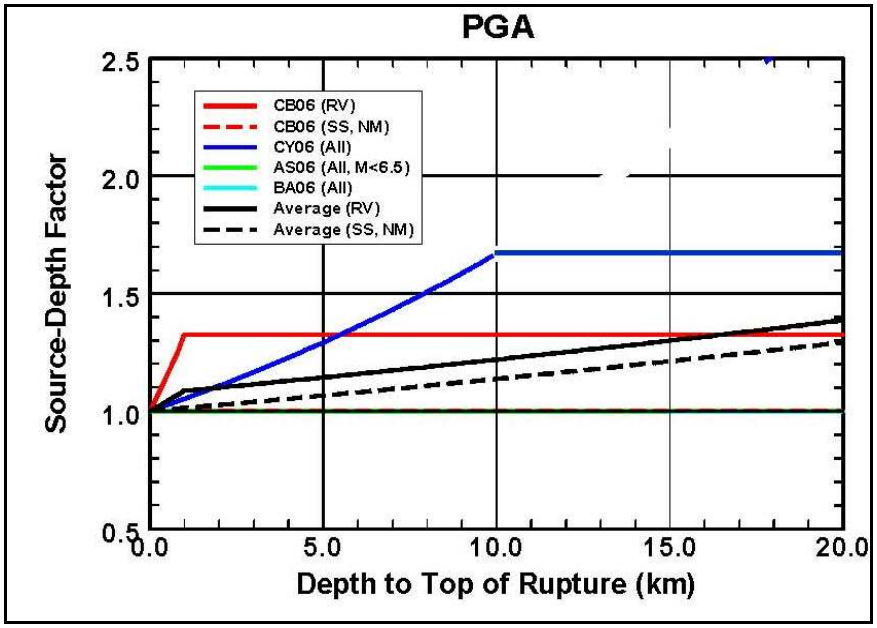


**FIGURE 5-14 PGA AMPLIFICATION FACTOR VERSUS DEPTH-TO-TOP-OF-RUPTURE (Abrahamson and Silva, 2007)**

## MODEL PARAMETER DEVELOPMENT

The general form of the ground motion model used to assess the model parameters is shown in Equation (16):

$$ln[y_{Surface}] = ln[y_{1130}] + f_{Site} + \sigma \cdot z_{ij}$$

$$ln[y_{1130}] = c_1 + f_{Source} + f_{Path} + f_{HW} + \tau \cdot z_i$$

$$f_{Source} = c_2(\mathbf{M}-6) + \left(\frac{c_2 - c_3}{c_n}\right) \times ln\left[1 + exp\{c_n(c_{\mathbf{M}} - \mathbf{M})\}\right] + c_{1a}F_{RV} + c_{1b}F_{NM} + c_7(Z_{TOR} - 4)$$

$$f_{Path} = c_4\, ln\left[R_{RUP} + c_5\, cosh\{c_6\, max(\mathbf{M} - c_{HM}, 0)\}\right] + (c_{4a} - c_4) \times ln\left[\sqrt{R_{RUP}^2 + c_{RB}^2}\right] + \left[c_{\gamma 1} + c_{\gamma 2} / cosh\{max(\mathbf{M} - c_{\gamma 3}, 0)\}\right] \times R_{RUP}$$

$$f_{HW} = c_9\, cos^2(\delta) \times tanh(R_{RUP}/2) \times \frac{tan^{-1}\left\{\frac{W\, cos(\delta)}{2(Z_{TOR}+1)}\right\}}{\pi/2} \times \left\{1 - \frac{R_{JB}}{R_{RUP} + 0.001}\right\}$$

$$f_{Site} = \phi_1\, min\left\{ln\left[\frac{V_{S30}}{1130}\right], 0\right\} + b_{Site}\, ln\left[\frac{exp\{ln[y_{1130}]\} + \phi_4}{\phi_4}\right]$$

$$b_{Site} = \phi_2 \times \left[exp\{\phi_3(min(V_{S30}, 1130) - 360)\} - exp\,\phi_3(1130 - 360)\right] \qquad (16)$$

**FIGURE 5-15 TYPICAL FUNCTIONAL FORM USED FOR THE NGA MODELS (Chiou and Youngs, 2006)**

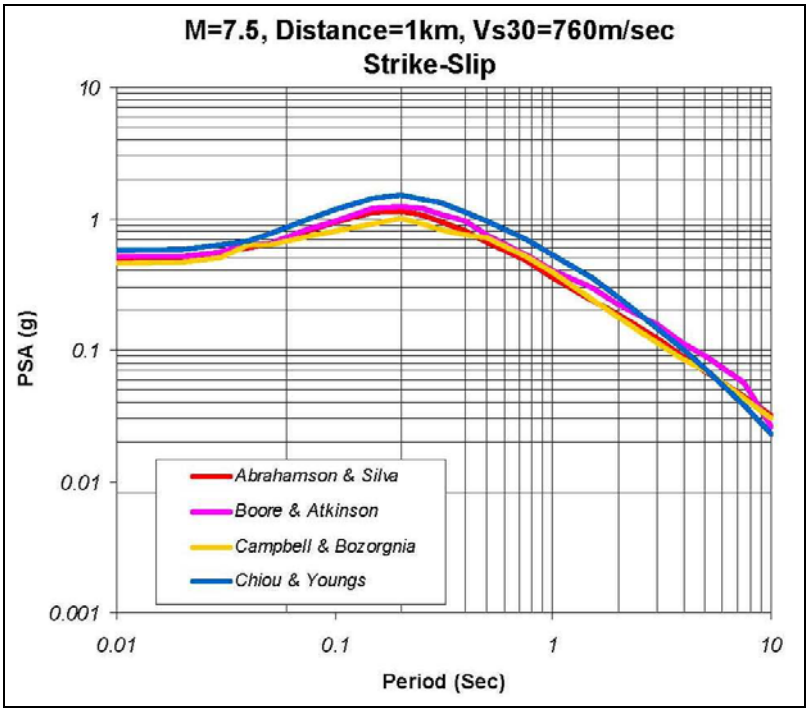


**FIGURE 5-16 COMPARISON OF GROUND MOTIONS FOR FOUR NGA MODELS (Chiou and others, 2004; Power and others, 2008)**

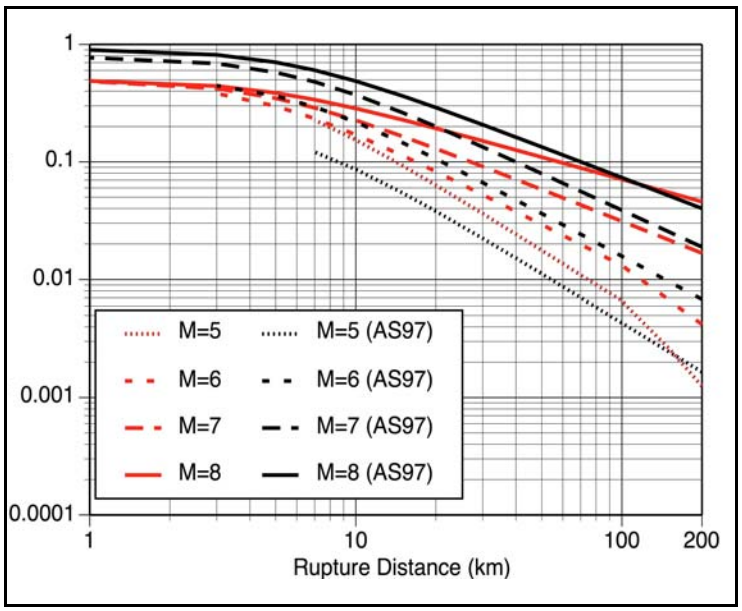


PGA vs. rupture distance for strike slip earthquakes on rock sites Vs=760 m/sec

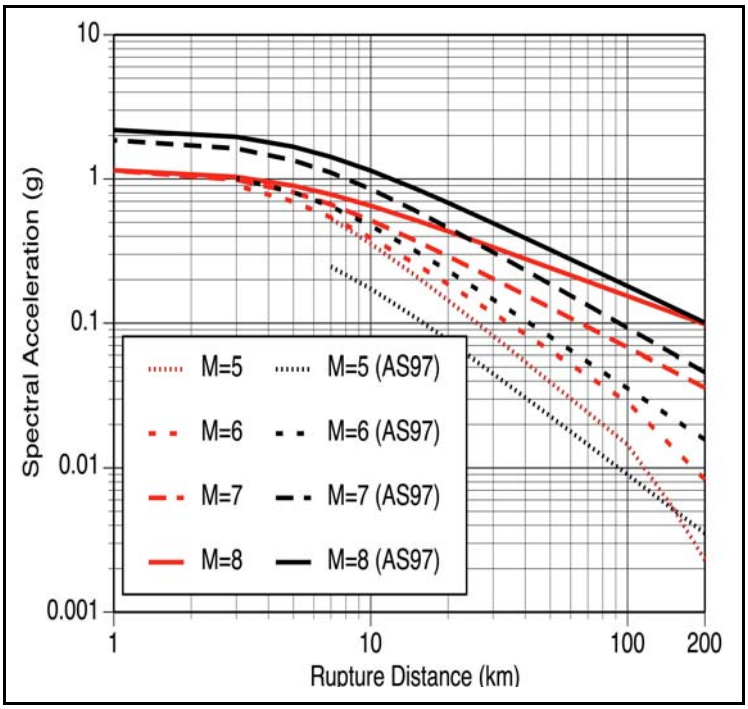


Spectral acceleration vs. rupture distance scaling at T=0.2 seconds for strike slip earthquakes on rock sites Vs=760 m/sec

**FIGURE 5-17 COMPARISON OF PGA (TOP) AND SA (T=0.2 SEC) (BOTTOM) ATTENUATION CURVES USED BY ABRAHAMSON AND SILVA IN 2007 AND 1997**

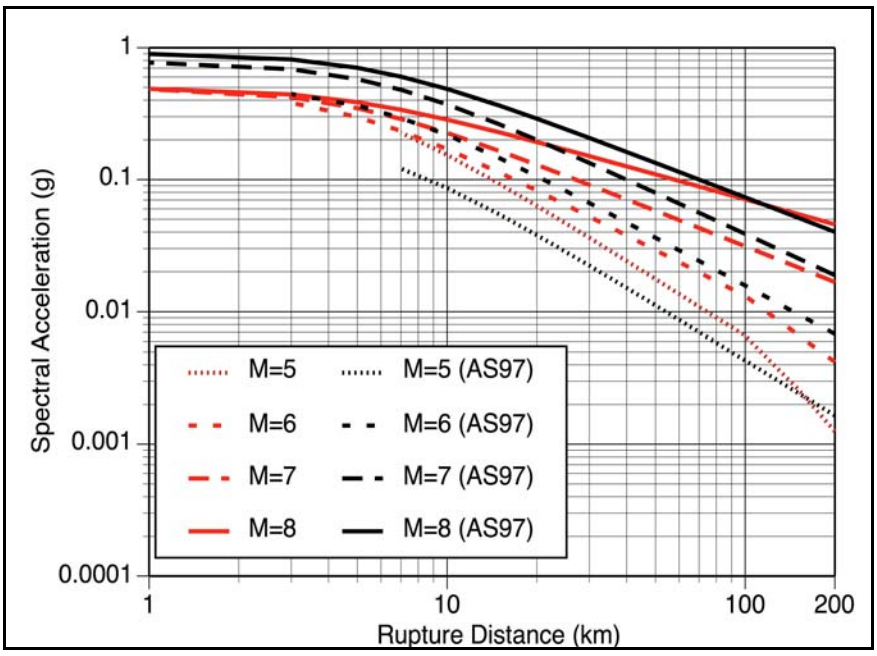


T=1 seconds for strike slip earthquakes on rock sites Vs=760 m/sec

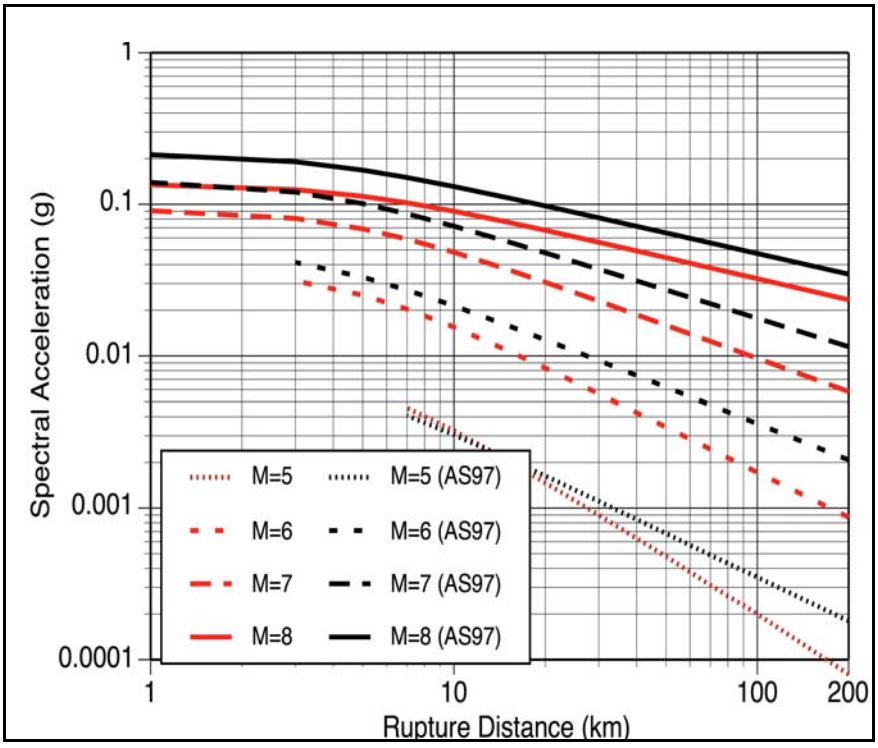


T=3 seconds for strike slip earthquakes on rock sites Vs=760 m/sec

**FIGURE 5-18 COMPARISON OF SA (T=1 [TOP] AND 3 SEC [BOTTOM]) ATTENUATION CURVES USED BY ABRAHAMSON AND SILVA IN 2007 AND 1997**

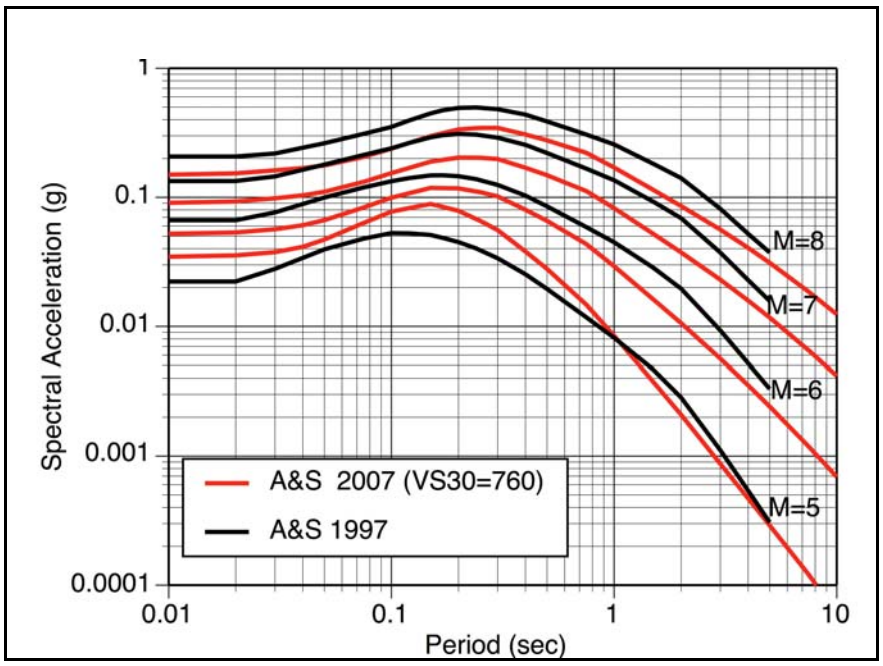


Rock sites Vs30=760

**FIGURE 5-19 COMPARISON OF SA SPECTRA AT 30 KM USED BY ABRAHAMSON AND SILVA IN 2007 AND 1997**

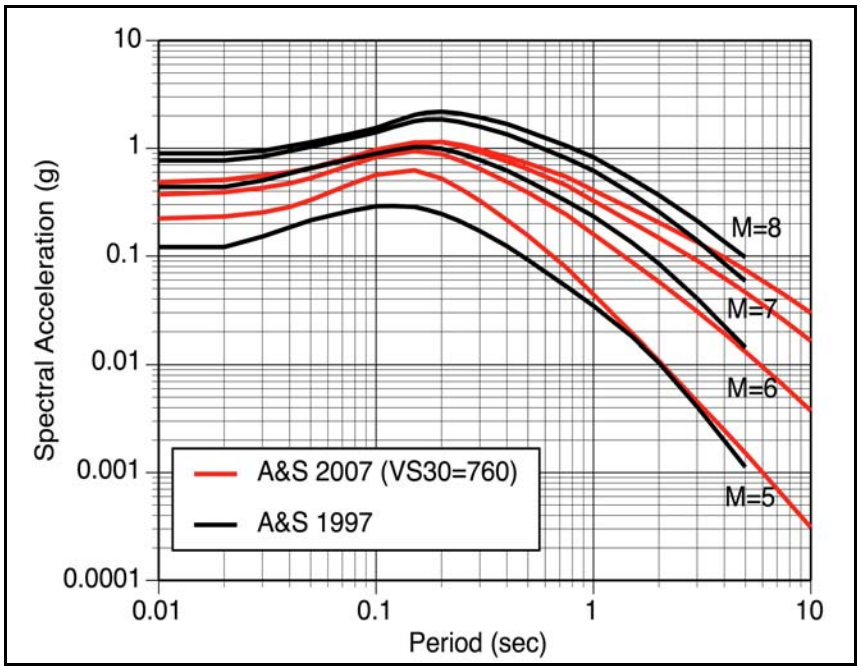


Rock sites Vs30=760 m/sec

**FIGURE 5-20 COMPARISON OF SA SPECTRA AT 1 KM USED BY ABRAHAMSON AND SILVA IN 2007 AND 1997**

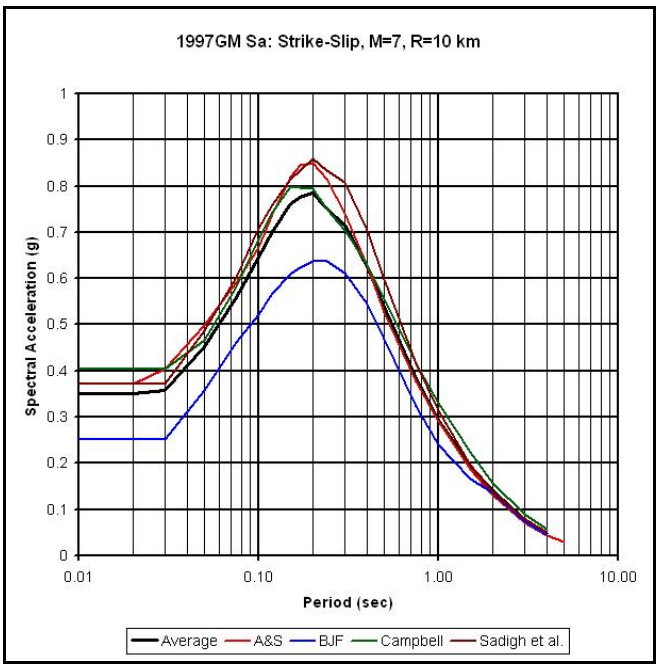


**FIGURE 5-21FOUR SA SPECTRA FROM THE 1997 GROUND MOTION ATTENUATION MODELS AND THEIR AVERAGE FOR A STRIKE-SLIP EARTHQUAKE AT 10 KM ON ROCK**

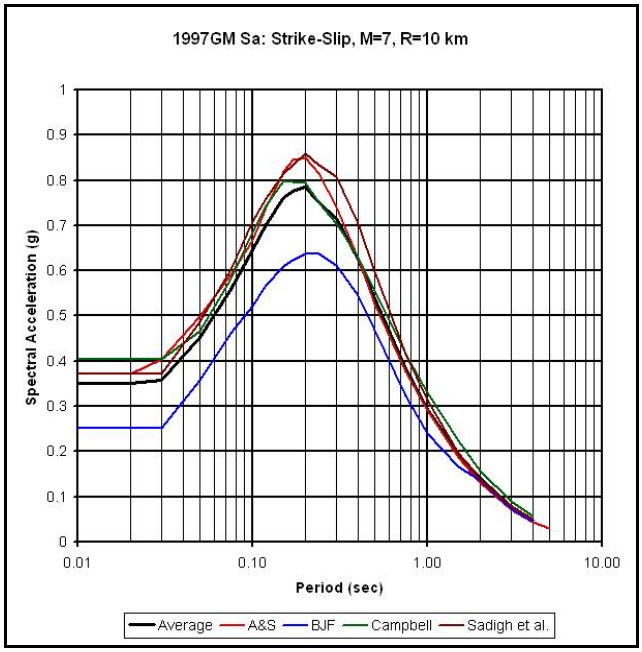


**FIGURE 5-22 FOUR SA SPECTRA FROM THE 1997 GROUND MOTION ATTENUATION MODELS AND THEIR AVERAGE FOR A STRIKE-SLIP EARTHQUAKE AT 10 KM ON ROCK**

# 9.0 APPENDIX

# APPENDIX A

# DESCRIPTION OF FAULTS IN THE MOKELUMNE-STANISLAUS REGION

## INTRODUCTION

The faults that are considered potential seismic sources for the dams in the Mokelumne and Stanislaus river hydroelectric systems are described in this appendix. Most, but not all, of these potential seismic sources exhibit evidence of activity in the late Cenozoic (past 3 to 5 million years) and as such are considered potentially active for this report. Some have evidence of activity in the late Quaternary (past 100,000 years) or the Holocene (past 10,000 years). The bedrock faults that show no evidence of displacements in the late Cenozoic are not described, with the exception of the prominent regional bedrock lineament along the Stanislaus River. The references are listed at the end of the appendix.

The map of the faults and the table summarizing the important information for characteristics are presented in the Sections 7 and 8 of this report.

## SIERRA NEVADA FRONTAL FAULT SYSTEM

### Antelope Valley Fault Zone

The Antelope Valley fault zone is comprised of predominately northwest-striking, east-dipping faults that bound the eastern side of the steep escarpment west of Topaz Lake (Curtis, 1951; Bryant, 1983a; Dohrenwend, 1982). Quaternary, including Holocene, offsets have been demonstrated along much of its length. The Antelope Valley fault zone is generally at the piedmont/range front contact, but geomorphic expression is discontinuous northwest of Topaz Lake. Topaz Lake itself occupies a large closed depression that lies adjacent to the fault zone and the base of a 700-m-high escarpment delineating the fault zone. The cumulative vertical displacement across the fault zone is between 600 and 1,200 m (Halsey, 1953 in Bryant, 1983a).

The Antelope Valley fault zone is characterized by a prominent 670-m-high east-facing escarpment with "wine-glass" shaped drainage canyons and a well defined break in slope at the base (Bryant, 1983a). Discontinuous scarps on alluvium range from 4 to 7 m high and have scarp slopes as steep as 32° (Bryant, 1984). Faults on the eastern side of Antelope Valley generally lack geomorphic evidence of down-to-the-west Holocene displacement (Bryant, 1984).

Bryant (1984) estimated a vertical slip rate of 0.4 mm/yr based on a fault scarp on alluvium thought to be 3 ka (age inferred by Borchardt, 1984, personal communication., in Bryant, 1984) based on soil development. dePolo (1998) and dePolo and Anderson (2000) calculated a preferred vertical slip rate of 0.73 mm/yr for the fault, based on an data presented by Bryant

(1984).

In this analysis we consider that the Antelope Valley fault zone ruptures in combination with the West Walker fault zone to the south. The basic premise being that the rugged terrain between these two fault zone has not been mapped in detail, they are roughly connected by a linear canyon along the West Walker River that could be masking fault continuity, and the recency and geomorphic expression of the West Walker fault zone suggest that it may rupture in combination with another fault or fault zone in the region. The length of a combined rupture along the Antelope Valley-West Walker fault zones is estimated to be 24 to 49 kilometers.

**Carson Range Fault Zone**

The Carson Range fault zone in westernmost Nevada and the easternmost California is one of the most active faults of the Sierra Nevada frontal fault system. The fault zone is expressed as a major range-front fault bounding the eastern front of the Carson Range southward from the Truckee River at Reno, Nevada, across the California-Nevada border in Carson Valley, to near Woodsfords, California. This fault zone or a related zone of late Cenozoic faults crosses the Sierra Nevada crest south of Ebbetts Pass, and continues across the upper part of the Stanislaus River drainage to southwest of Sonora Pass in the vicinity of Relief Reservoir. South of the crest, the geomorphic expression of the fault zone is significantly less prominent. For example, the fault zone is commonly delineated by linear drainage valleys (erosional features) in this area, rather than by precipitous range fronts with large fault facets (i.e., primary tectonic geomorphology) that characterize the fault zone to the north. The marked change in geomorphic expression results from a decrease in the amount of cumulative late Cenozoic displacements along the fault zone and extensive glacial erosion. Overall the fault zone is characterized by down-to-the-east normal displacement.

The well expressed northern Carson Range fault zone has been subdivided into six fault sections based on patterns and, in some cases, recency of faulting. From north to south the sections are: the 23-kilometer-long Mt. Rose section, the 16-kilometer-long Washoe Valley section, the 20-kilometer-long Carson City section (Ramelli and others, 1994), the 7.5-kilometer-long Jacks Valley section, the 18 kilometer-long Carson Valley or Genoa section (Ramelli and others, 1999), the at least 17-kilometer-long Diamond Valley section (Ramelli and others, 1999). Although these sections may represent earthquake-rupture segments (i.e., individual earthquake sources), the two most recent earthquakes apparently ruptured the southern five sections in a single very large earthquake approximately 550 years ago (Ramelli and others, 1999). Further south, Ramelli and others (1999) refer to a generalized Sierra section. We refer to this section as the Folger Peak section. The 22- to 31-kilometer-long Folger Peak section is comprised of the Arnot Creek and Disaster Creek faults.

In previous analyses, we had assumed that the Carson Range fault zone continued south of the Folger Peak section, as the "Relief section", to the vicinity of Relief Dam. However, based on our recent helicopter reconnaissance flight (15 June 2007), there appears to be a lack of continuity between the Folger Peak section and what was previously considered to be the Relief section. Recent geologic studies of the late Cenozoic volcanic stratigraphy between the Clark

and Middle forks of the Stanislaus River by Rood and others (2004), however, have confirmed many of the late Cenozoic faults originally mapped by (Slemmons, 1966) along the northern approximately half of the former Relief section. Although, recent field mapping by Hamilton and others (2005) report no evidence for the existence of the Relief fault within Mesozoic granitic bedrock in the vicinity of Relief Dam (described below). Thus, we herein consider the Folger Peak section to be the southernmost of the Carson Range fault zone. As described in a following sections, the former "Relief section" is no longer consider to be part of the Carson Range fault zone, but to be a separate fault zone, the "Red Peak" fault zone (described below).

The Diamond Valley section is the southernmost confirmed Holocene fault in the Carson Range fault zone (Clark and others, 1984; Smith, 1984; Bell, 1984; Ramelli and others, 1994; 1999). The Diamond Valley section extends from the Nevada-California state line at Jobs Creek southward through Woodfords, and west of Markleeville, to Indian Creek (Ramelli and others, 1999). Evidence for multiple Holocene displacements along this section include beveled fault scarps on Holocene alluvium up to 9 meters high, progressively higher scarps on each of four successively older Holocene terraces, and scarps as high as 16 meters on a late Tioga (10,000 to 13,000 years BP) outwash terraces (Clark and others, 1984; Ramelli and others, 1994). Based on these relationships, Ramelli and others (1994) interpreted three to four faulting events in the Holocene, each producing about 3 meters of vertical displacement. Clark and others (1984) estimated a slip rate of 0.7 to 1.6 mm/yr (1 mm/yr preferred) based on the offset of the late Tioga outwash terraces. These data are the basis for the State of California to identify this part of the Carson Range fault zone as a Holocene fault under the Alquist-Priolo Earthquake Hazard Zones Act (Smith, 1984; Jennings, 1994).

The Diamond Valley section appears to be associated with a cluster of recent (1970-1992) earthquakes. The largest earthquake was a $M_L$ 5.2 event in September 1978 (Sommerville and others, 1980). The focal mechanism for this event and another event in the cluster show steeply east-dipping nodal planes characterized by right-oblique-normal displacements. Hypocenter depths in this region range from less than one kilometer to as deep a 15 kilometers, with 90 percent of the events located above 10 kilometers (Martinelli, 1989).

The 1994 $M_W$ 6.1 Double Springs earthquake occurred 12 kilometers east of the Diamond Valley section, apparently on a northeast-striking concealed fault; the preliminary estimate of $M_W$ 6.3 was revised downward according to data obtained via the Internet from the U.S. Geological Survey's National Earthquake Information Center. The earthquake was strong enough to trigger the strong motions instruments at the Salt Springs Dam (Page and Others, 1994).

In addition to the Diamond Valley section, we consider in our maximum earthquake analysis the possibility that this section ruptures with one or more to the north, as possibly occurred during the two most recent paleoearthquakes. This scenario yields a rupture length of 25 to 75 kilometers (Ramelli and others, 1999). The southern section, Folger Peak, which appear to be part of the Carson Range fault zone, is herein considered as an independent potential seismic source.

## Folger Peak Section

The Folger Peak section extends southward from Diamond Valley, across the crest of the Sierra Nevada where helicopter reconnaissance suggests the presence of a Quaternary fault-bounded basin (data in G&E Geosciences Department files), and possibly splitting along Arnot and Disaster creeks (i.e., along the Arnot Creek and Disaster Creek faults) to the Clarks Fork of the Stanislaus River, a distance of 22 to 31 kilometers.

## "Relief Section"

See Red Peak fault zone (below).

### Millie Lake Fault

The "Millie Lake fault" is in northeastern Mono County 7 kilometers east of Sonora Pass and. The northerly striking fault has down-to-the-east normal offset. The fault was mapped by Dohrenwend (1982) along the West Walker River in the vicinity of State Route 108 as juxtaposing Quaternary alluvium on the east against bedrock on the west. South of the highway, Dohrenwend mapped the fault as having abrupt, steep, and well-defined fault scarps. Based on aerial reconnaissance, PG&E (data in PG&E Geosciences files) extended the fault further south where it apparently controls the course of the river. North of the highway, Dohrenwend mapped the fault along a prominent topographic lineament associated with features indicative of Quaternary fault activity. This part of the fault is shown on the Fault Activity Map of California (Jennings, 1994) as a Quaternary fault. PG&E (data in PG&E Geosciences files) extended the fault to the northeast across Wall Creek to Silver Creek and suggested evidence of late Quaternary activity. Along projection of this part of the fault, Dohrenwend mapped another Quaternary fault that borders the east side of a broad ridge-crest saddle, west of Lost Cannon Peak. This fault is not considered to be part of the Millie Lake fault however, because its geomorphic expression suggests down-to-the-west vertical displacement, rather than down to the east. The Millie Lake fault is about 12 kilometers long.

### Waterhouse Peak Fault

The Waterhouse Peak fault is in the northeastern corner of Alpine County, 12 kilometers southeast of South Lake Tahoe (Schweickert and others (2000) referred to this fault as the Jobs Canyon fault. The northern termination of the fault is at the Carson Range fault zone (Stewart and others, 1982; Ramelli and others, 1994, 1999; Schweickert and others, 2000) and coincides with the boundary between the Carson Valley section to the north and the Diamond Valley section to the south. The fault follows Jobs Canyon to the southwest and crosses the crest of the Carson Range west of Jobs Peak and east of Freel Peak. Near Freel Peak the fault reportedly forms scarps in "modern valley alluvium" (Schweickert and others, 2000), which likely means post-glacial. The fault forms the linear escarpment along the abrupt western border of Hope Valley, where it is locally expressed by spring alignments and vegetation lineaments. Hope Valley appears to be a glacially scoured graben, bordered on the east by discontinuous north-striking faults having an antithetic structural relationship to the Waterhouse Peak fault. The Waterhouse Peak fault extends southward along the base of this prominent escarpment to State

Highway 89 east of Carson Pass, where the fault may end. Between Waterhouse Peak and the pass located to the south, there appears to be two main fault traces; one near the base of the escarpment and a western fault trace delineated by a broad bench on the escarpment on which Scotts Lake is located. Jennings (1994) depicts the western trace to be a short Quaternary fault. To the south of the pass, this compound character of the escarpment continues, but Pleistocene alpine glaciers have strongly modified the escarpment.

The western fault trace may continue south of Carson Pass along the upper part of the glacially-embayed compound escarpment (Jennings, 1994). A discontinuous topographic lineament marked by an alignment of cirque headwalls and ridge-top saddles possibly delineates this fault to the vicinity of Lower Blue Lake, where the range-front relief diminishes. This fault may continue southward along the linear reach of Blue Creek through Clover Valley. The Waterhouse Peak fault is geomorphically well-defined from the near the crest of the Carson Range to State Highway 89 at Carson Pass, a distance of approximately 18 kilometers. If the fault extends south of Lower Blue Lake along the upper reach of Blue Creek, then the total fault length would be approximately 31 kilometers.

The Waterhouse Peak fault was first recognized as a late Quaternary fault by Woodward-Clyde Consultants (1978) in a report to PG&E. Geomorphic evidence for late Pleistocene to possibly Holocene displacements on the Waterhouse Peak fault include, vegetation lineaments, alignments of springs, the apparent beheaded character of Grass Lake Creek at Luther Pass (Woodward-Clyde Consultants, 1978), and reportedly scarps on "modern" alluvium (Schweickert and others, 2000). The structural association and apparent influence on the segmentation behavior of the Carson Range fault zone, also is consistent with late Quaternary activity on this fault. The extreme northern end of the Waterhouse Peak fault and a 5-kilometer-long section at Carson Pass, along with a 2-kilometer-long section of the antithetic fault zone in northern Hope Valley were mapped as Quaternary faults by Dohrenwend (1982) and by Stewart and others (1982). Between Carson Pass and Luther Pass, Jennings (1994) shows the Waterhouse Peak and antithetic faults as not having experienced displacements during the Quaternary. There is a distinct absence of recent microearthquakes (1970-1992) in the vicinity of the Waterhouse Peak fault (Martinelli, 1989).

**West Tahoe-Dollar Point Fault Zone**

The West Tahoe-Dollar Point fault zone bounds the western margin of the Lake Tahoe basin in eastern Placer and El Dorado counties. The two principal faults in this zone are the West Tahoe fault and, its northern extension, the Dollar Point fault. The West Tahoe fault, as defined herein, is actually a fault zone that includes the offshore West Tahoe fault and related onshore faults, the Quail Lake and Echo Summit faults. The West Tahoe fault zone extends north-northwestward from south of Echo Summit, near U.S. Highway 50, to McKinney Bay (Lindgren, 1897; Hawkins and others, 1986; PG&E, 1991a; Schweickert and others, 2000). The West Tahoe fault is delineated by a 450-meter-high east-facing escarpment that is characterized by 30° slopes beneath Lake Tahoe (Hyne and others, 1972; Gardner and others, 1999). Displacement on this fault zone is normal, down to the east. To the south, the Echo Summit fault terminates three kilometers south of Echo Summit, or slightly south of southernmost point

on the fault as mapped by Lindgren (1897). Southward along the same trend, another fault continues to the vicinity of Round Lake, but because the sense of displacement is down to the west, rather than down to the east, it is not considered to be an extension of the West Tahoe fault zone.

The Dollar Point fault is separated from the north end of the West Tahoe fault by a 4-kilometer-wide right step beneath McKinney Bay. The fault extends north from this point in the subsurface to Carnelian Bay, where it comes onshore and bounds the east edge of Dollar Point. Further north, the Dollar Point fault extend along the eastern fronts of Mt. Watson, Mt. Pluto, and Lookout Mountain as an oversteepened bedrock escarpment. On the eastern flank of Lookout Mountain, the north-striking Dollar Point fault intersects the linear, northwest-striking Truckee fault zone of Olig and others (2005). Movement on the Dollar Point fault is normal, down to the east.

Geomorphic and bathymetric evidence of late Quaternary activity along the West Lake Tahoe-Dollar Point fault zone includes scarps on late Pleistocene to Holocene lake sediment on the floor of Lake Tahoe, scarps on Tioga moraines and on “modern” (i.e., post-glacial) valley alluvium (Schweickert and others, 2000), geomorphic anomalies (e.g., saddles, scarp-like irregularities) on late Pleistocene lateral glacial moraines, and linear vegetation patterns (PG&E, 1991). However, in the Echo Summit area, Tahoe and Tioga lateral moraines reportedly conceal the southern part of the fault zone (e.g., Loomis, 1983; Hawkins and others, 1986), but breaks in the moraine crests observed during reconnaissance flights suggest post-glacial displacement (data in PG&E Geosciences files). The base of Myers Grade is a "rather gentle, concave-upward slope" which "is not suggestive of recent (i.e., post-glacial) fault movement" (Hawkins and others, 1986).

Hawkins and others (1986) indicate that two earthquakes (M = 4.2 and 2.0) may have occurred on the West Tahoe fault (events #1 and #31 in their Figure 4-6) suggesting evidence of contemporary fault activity. The down-to-the-east focal planes for both earthquakes provide strikes that are within 10° of the strike of the West Tahoe fault. When projected along the focal planes to the surface from the inferred hypocenter, the events plot within 5 kilometers of the fault trace. They suggested that a correlation between these events and the fault is possible given the uncertainties associated in the focal plane orientation, hypocenter depths, and the dip of the West Tahoe fault.

Based on their structural association, common sense of vertical displacement, and similar geomorphic/bathymetric expression, the West Tahoe and Dollar Point faults probably reflect a single, significant seismic source. The length of the West Tahoe fault zone was estimated to be 36 kilometers by Hawkins and others (1986). The Dollar Point fault has a mapped length of 21 kilometers (Schweickert and others, 2000). The entire length of the West Tahoe-Dollar Point fault zone is about 56 kilometers. For the purpose of estimating a maximum earthquake magnitude for the zone, we have assumed that the West Tahoe-Dollar Point fault zone ruptures in its entirety. We also consider that the 4-kilometer-wide right step between the West Tahoe and Dollar Point faults forms a rupture-segment boundary. Thus our analysis suggests ruptures from 19 to 43 kilometers long along the southern section (West Tahoe, Quail Lake, and Echo

Summit faults).

The U.S. Bureau of Reclamation (Hawkins and others, 1986) considered the West Tahoe fault and the North Tahoe fault, more than 5 kilometers to the east (Schweickert and others, 2000), as possibly a single arcuate fault, based in part on the first geophysical surveys of the lake bottom (Hyne and others, 1972). They characterized this fault system as having a combined rupture length of 56 kilometers. However, recent high-resolution bathymetry of the floor of Lake Tahoe (Gardner and others, 1999) clearly show that the West Tahoe-Dollar Point fault zone is separated from the North Tahoe fault, or the North Tahoe-Incline Village fault zone of Lahren and others (1999), by a greater than 5-kilometer-wide right step (Schweickert and others, 2000). Based on the historical world-wide earthquake record stepovers of this width have a strong tendency to arrest earthquake ruptures, suggesting that these fault zones are separate seismic sources (Knuepfer, 1989). The earthquake-rupture scenario of Hawkins and others (1986) is not included in the present study, because of the historical earthquake data and because their rupture length is equal to that of our maximum earthquake-rupture length for the West Tahoe-Dollar Point fault zone, which is also closer to PG&E dams in the region. In their evaluation of potential hazards of future large tsunamigenic earthquakes within the Tahoe basin, Ichinose and others (2000) also did not consider the West Tahoe-Dollar Point fault zone as rupturing coseismically with the North Tahoe-Incline Village fault zone.

Lahren and others (1999) suggested that "large (M7) earthquakes can be expected along active faults in the [Tahoe] basin in the future" but did not specifically assign this magnitude estimate to the West Tahoe-Dollar Point fault zone. However, Ichinose and others (2000) developed an earthquake scenario ("scenario B") that involved a 48-kilometer-long rupture along the West Tahoe-Dollar Point fault zone. They assumed an average slip of 2.83 m and a down-dip fault width of 17 kilometers. These assumed faulting parameters yields a scenario-earthquake magnitude of $M_w$=7.2 (Ichinose and others, 2000).

To date, the slip rate on the West Tahoe-Dollar Point fault zone is unknown. However, the high-resolution bathymetry of Lake Tahoe shows that the relief across the fault zone and its geomorphic expression are generally similar to that of the Carson Range fault zone. Therefore, based on this general comparison, we assign a slip rate of 0.1 to 1 mm/yr for the West Tahoe-Dollar Point fault zone.

Based on our analysis of the above information, we conclude that West Tahoe-Dollar Point fault zone is a major Holocene-active fault zone over most of its length.

**West Walker Fault**

The West Walker fault is in northeastern Mono County 13 kilometers east of Sonora Pass. The north- to north-northeast-striking fault has down-to-the-east normal offset. The fault extends along the base of the range front west of Hardy Station from at least the Little Walker River on the south, across State Route 108 and U.S. 395, to a point about 7 kilometers north of the intersection of these two highways, a minimum distance of 16 kilometers. Along most of this section, alluvium on the east is juxtaposed by late Quaternary faulting against bedrock on the west (Dohrenwend, 1982). South of the Little Walker River to near Buckeye Creek,

Dohrenwend (1982) mapped prominent topographic lineaments in bedrock. These lineaments and additional lineaments to the southeast, between Buckeye Creek and Eagle Creek, were mapped and interpreted by PG&E (data in PG&E Geosciences files) to be the southern continuation of the fault based on aerial reconnaissance. Thus, the West Walker fault appears to extend for a distance of 24 kilometers.

Evidence for late Quaternary activity includes steep well- to very-well-defined fault scarps, a possible groundwater barrier, and offset glacial moraine crests and till (Halsey, 1953; Clark, 1967, 1972, 1975; Dohrenwend, 1982; Bryant, 1983a). South of Junction Reservoir, the fault offsets a Tioga moraine crest along a 6- to 7-meter-high fault scarp with a maximum slope angle of 35°. North of the reservoir there is a 6-meter-high scarp on Tioga-age till (Clark, 1975; Bryant, 1983a). The Tioga-stage glaciation occurred about 13,000 to 20,000 years ago. Assuming that these scarp heights approximate the vertical offset on the fault, then these data suggest vertical slip rates of 0.3 to 0.5 mm/yr. However, the height of fault scarps on sloping geomorphic surfaces (e.g., moraine crests) are greater than the actual vertical offset on the fault, thus, these are maximum late Quaternary slip rate estimates. Evidence of Holocene fault activity includes undissected scarps, scarps and scarplets on Holocene alluvium, vertically offset drainages, a trough and linear depressions along the base of the scarp (Bryant, 1983a) and multiple-event(?) offsets of latest Pleistocene glacial deposits. Based on these features the fault was zoned as a Holocene-active fault under the Alquist-Priolo Earthquake Hazard Zone Act (Bryant, 1983a) and shown on the Fault Activity Map of California as a Holocene fault (Jennings, 1994).

In this analysis we consider that the West Walker fault zone ruptures in combination with the Antelope Valley fault zone to the north. The basic premise being that the rugged terrain between these two fault zone has not been mapped in detailed, they are roughly connected by a linear canyon along the West Walker River that could mask fault continuity, and the recency and geomorphic expression of the West Walker fault zone suggest that it may rupture in combination with another fault or fault zone in the region. The length of a combined rupture along the West Walker-Antelope Valley fault zones is estimated to be 24 to 49 kilometers.

## FAULTS WITHIN THE SIERRAN MICROPLATE

### Faults between the Sierra Nevada Frontal fault system and the Foothills fault system

#### Dardanelles Cone Fault

The Dardanelles Cone fault is in northeastern Tuolumne County about 17 kilometers south-southwest of Ebbetts Pass. The fault which borders the western front of Dardanelles Cone is characterized by down-to-the-west offset of the thick Tertiary volcanic section that makes up Dardanelles Cone. The fault cuts the Cretaceous granodiorite of Kinney Lakes (Huber, 1981) and the overlying late Cenozoic volcanic section (data in PG&E Geosciences files).

The Dardanelles Cone fault was inferred by PG&E (data in PG&E Geosciences files) based on a geomorphic profile (or shallow cross section) drawn on the late Cenozoic volcanic section.

The fault is delineated by an anticlinal gradient change which is shown by the contact between the Relief Peak Formation and the overlying Table Mountain Latite. The gradient of the contact is 53 m/km to the west on the southwest side of the fault, and 13 m/km to the east on the northeast side.

The Dardanelles Cone fault was subsequently confirmed by detailed mapping of the Tertiary volcanic stratigraphy by Rood and others (2004). This mapping shows that the Tertiary Mehrten Formation thickens westward from 60 to 200 m across the fault.

The Dardanelles Cone fault appears to extend from the Middle Fork Stanislaus River, along the front of the Dardanelles Cone to The Dardanelles northward to Highlands Creek, based on analysis of aerial photographs. To the south the fault may cross the west end of the divide between the Clark Fork Stanislaus River and the Middle Fork, and continue along a linear reach of this drainage to near Eagle Creek. The fault is considered to be 12 to 15 kilometers long.

**Dorothy Lake Fault Zone**

The Dorothy Lake fault zone is astride the crest of the Sierra Nevada and 18 kilometers south of Sonora Pass. Three principal faults, the Upper Twin Lake, Dorothy Lake, and Summit Meadow faults (from south to north), form the Dorothy Lake fault zone. These faults cut metasedimentary rock of the Snow Lake pendant and Jurassic to Cretaceous plutonic rock and have generally reactivated basement structures. Late Cenozoic displacement is right lateral with a normal component (Lahren and Schweickert, 1991). The Dorothy Lake fault zone may be structurally associated with the West Walker River fault zone and/or the Millie Lake fault, based on the distributed pattern of faulting, although further work would be needed to confirm this association.

The northeast-striking fault zone was mapped by Lahren and Schweickert (1991) as extending from at least Lower Twin Lake on the southwest to at least Cinko Lake on the northeast, a distance of 12 kilometers. Topographic expression of the fault zone on aerial photographs continues southwest to Huckleberry Lake. To the northeast the fault zone may continue along a linear tributary to the West Fork of the West Walker River, west of Hidden Lake. The fault is delineated by linear stream channels, glacially scoured valleys, and small escarpments at the base of ridges (Lahren and Schweickert, 1991).

Evidence for late Cenozoic displacement on the Dorothy Lake fault zone includes right-lateral offsets of an 8.8-million-year-old hornblende andesite dike. The dike is separated in a dextral sense 70 meters on the Grizzly fault and approximately 64 meters on the Dorothy Lake fault (Lahren and Schweickert, 1991). These data yield long-term right-lateral separation rates as much as 0.008 mm/yr on individual faults and 0.015 mm/yr across the fault zone. Lahren and Schweickert (1991) postulated Holocene displacement on the fault zone based on “steps” and “flat linear depressions” that they observed on post-glacial talus and alluvium. Alternatively, they proposed that these features may result from solifluction processes (i.e., mass wasting). Our (W.D. Page and T.L. Sawyer) field and aerial reconnaissance in 1992 of the Dorothy Lake fault zone found that the topographic features on post-glacial deposits to be discontinuous, and that the steps faced in opposite directions over short distances. We concluded that the

"Holocene fault features" were depositional pro-talus ramparts (talus deposited across snow accumulated at the base of steep slopes) and topographic lineaments resulting from thin alluvial sheets deposited in a draping manner on linear bedrock structures scoured and accentuated by Pleistocene glaciers. Hence, we conclude that the Dorothy Lake fault zone has been active in the late Cenozoic and probably in the Pleistocene, but not in the Holocene.

The Dorothy Lake fault zone extends at least from near Upper Twin Lake to near Cinko Lake, a distance of about 13 kilometers, and possibly to west of Hidden Lake, a distance of about 22 kilometers.

**Douds Landing Fault**

The suspected Douds Landing fault appears to cross the North Fork Stanislaus River about 6 kilometers south of Arnold, California. The northwest-striking fault is inferred to cut Mesozoic granitic and Paleozoic metasedimentary rock and the overlying volcanic stratigraphy. The strike of the fault appears to be approximately perpendicular to the intrusive contact between the granitic rock and the metasedimentary rock (Wagner and others, 1981), but parallel to the regional structural grain exhibited by the metasedimentary basement. Displacement on the fault is normal, down to the southwest.

Possible evidence for late Cenozoic displacement on the Douds Landing fault was initially inferred by PG&E (data in PG&E Geosciences files) from the abrupt western termination of the Table Mountain Latite on the divide between the North Fork of the Stanislaus River and Love Creek to the north. However, this termination appears to delineate the margin of a paleo-channel, backfilled with the latite. The western margin of the inferred paleo-channel coincides with the inferred Douds Landing fault, suggesting the paleo-drainage may have preferentially eroded along the fault. East of Douds Hill, the base of the Mehrten Formation appears in the field to be vertically separated about 6 meters down-to-the-southwest.

Between Douds Hill and State Highway 4 to the northwest, the fault is moderately to weakly expressed by ridge-crest benches and short linear drainages that are generally aligned. Features indicative of late Cenozoic faulting are not obvious along the projection of the fault northwest of the highway. On the divide between the Middle and North forks of the Stanislaus River, the fault is moderately defined by aligned benches on the ends of bedrock ridges, ridge-crest saddles, and a west-facing escarpment at McCormic Meadows. Southeast of the canyon of the Middle Fork the fault appears to be moderately expressed by a short west-facing escarpment west of Mount Knight, linear drainages, and ridge-crest saddles. The alignment of these features can be traced to Rose Creek but are not apparent farther to the southwest on Grant Ridge.

However, Hamilton and others (2005) recently reported that the suspected Douds Landing fault was not encountered in Collierville Power Tunnel, which crosses the inferred fault trace, based on geologic logs of the tunnel. Their field mapping in the area shows that a previously mapped remnant of Mehrten Formation does not exist. This remnant was used on the regional profile that PG&E constructed and from which inferred the existence of the Douds Landing fault.

The existence of the Douds Landing fault may be in question, but until further field work can be completed, it is considered to be a potential seismic source. The fault is inferred to extend from State Highway 4 to the Middle Fork of the Stanislaus River, a distance of 11 kilometers. The fault may continue southeast to near Grant Ridge, for a total distance of about 19 kilometers.

**Ice House Fault**

The Ice House fault is a suspected late Cenozoic fault located in central El Dorado County. The fault appears to strike across the South Fork of the American River and Peavine Ridge and extend northward to near Ice House Reservoir. The fault transects Mesozoic granitic rock and may locally coincide with a contact between granitic rock and metasedimentary rock of the Paleozoic Shoo Fly Complex (Wagner and others, 1981).

The suspected Ice House fault was identified by PG&E (data in PG&E Geosciences files) from a down-to-the-west step on the Mehrten Formation that caps Peavine Ridge, 5 kilometers south of Ice House Reservoir. The inferred vertical separation on the surface of the Mehrten Formation at this locality is between 200 and 320 meters, depending on the surface-gradient projections across a 5-kilometer gap in remnants of the formation. The base of the formation is separated about 225 meters at this locality. Assuming that displacement on the Ice House fault began concurrently with the onset of Sierra Nevada uplift, about 3 to 5 million years ago (Unruh, 1991), than these data yield long-term slip rates ranging from 0.04 to 0.1 mm/yr. Our reconnaissance mapping of the base of the formation suggests the remnants may be channeled in a Miocene paleo-valley. If there was a meandering paleo-valley filled by the Mehrten Formation at this location, than the apparent vertical separation could be explained by the channel meandering around a paleo-highland in the granitic basement, rather than by down-to-the-west displacement on the suspected fault. However, based on the amount of vertical separation and the gradient of the Mehrten Formation surface (5 to 20 m/km), the meandering length of the postulated paleo-valley would have had to have been 10 to 16 kilometers, or more, in a horizontal distance between Mehrten remnants. This seemingly requires the presence of a large paleo-highland (e.g., Tunnel Hill in the American River drainage), for which there is scant evidence in the modern landscape. Nevertheless, this possibility, plus the long projection distance, make the Ice House fault a suspected late Cenozoic fault.

The northerly strike of the Ice House fault is constrained by the truncation of the broad (approximately 1.3 kilometers wide) Mehrten-Formation remnant on Peavine Ridge. North of Peavine Ridge and on trend with this apparently truncated remnant is a linear west-facing escarpment, extending north to Ice House Reservoir near Jones Place. To the south of Peavine Ridge, there are aligned west-facing topographic steps, and a linear gully that extends the fault south of the South Fork American River canyon where the fault appears to follow a straight reach of Alder Creek. North of Jones Place and south of the linear stream reach, geomorphic expression diminishes and the fault appears to die out.

The suspected Ice House fault is inferred to be at least 9 kilometers long. The geomorphic lineaments associated with the fault suggest a total fault length of as much as 15 kilometers.

**McKays Point Fault**

The suspected McKays Point fault crosses the North Fork Stanislaus River east of McKays Point, 5 kilometers east of Arnold. The fault appears to follow a northwest-striking intrusive contact between Mesozoic granitic rock on the northeast and Paleozoic metasedimentary rock on the southwest (Wagner and others, 1981). The fault is characterized by down-to-the-east normal displacement and, based on the northwest strike (i.e., sub-parallel to the Poorman Gulch fault), we infer a subordinate right-lateral component. The fault was identified by PG&E (data in PG&E Geosciences files) based on stratigraphic and geomorphic evidence, which was the basis for showing it as a late Cenozoic fault on the Fault Activity Map of California (Jennings, 1994).

Possible evidence for late Cenozoic displacement on the McKays Point fault includes down-to-the-east vertical separation of the approximately 9 million year old Table Mountain Latite and the overlying Mehrten Formation, which is about 4.6 million years old, or older. This offset is marked by an east-facing geomorphic step on the top of the latite near McKays Point, about 5 kilometers east of Arnold. Across the fault the contact between the top of the latite and the base of the overlying Mehrten Formation exhibits 40 to 45 meters of down-to-the-northeast vertical separation. Field inspection confirmed the vertical separation of the latite east of McKays Point. PG&E (data in PG&E Geosciences files) infers a long-term vertical separation rate of 0.008 to 0.009 mm/yr based on these data.

However, Hamilton and others (2005) report that rather than vertical separation of the base of the Mehrten Formation, this relief results from erosion of the Table Mountain latite prior to burial by Mehrten deposits. They also reported that the fault was not encountered in the Beaver Creek Diversion tunnel, or in the foundation of Beaver Creek Diversion Dam. Although the tunnel appears to cross the fault the dam foundation may not. More work is needed to completely discount the McKays Point fault as a potential seismic source.

The suspected fault has moderate geomorphic expression delineated by linear stream reaches, and aligned ridge-top saddles and benches. The fault extends from the Middle Fork of the Stanislaus River, northwest across the divide between the Middle Fork and North Fork, along the east side of McKays Point and continues to near Summit Level Ridge, about 4 kilometers north of Arnold. Exposures of the Mehrten Formation on the south side of Summit Level Ridge do not reveal evidence for late Cenozoic displacement on the projection of the fault, based on examination of aerial photographs. The McKays Point fault is geomorphically expressed between the Middle Fork of the Stanislaus River and Summit Level Ridge, a distance of 8 to 14 kilometers.

### Post Corral Fault

The suspected Post Corral fault is in northeastern Tuolumne County, approximately 4 kilometers west of Donnell Lake. The Post Corral fault appears to follow the northwest-striking uppermost reach of Shoofly Creek and to cross the divide between the Middle Fork Stanislaus River and Highland Creek, west of Whittakers Dardanelles. The fault transects basement mapped as Cretaceous granitic rock by Wagner and others (1981).

The fault is inferred from a 70 meter down-to-the-west vertical separation of the top of the Table Mountain Latite across the valley of Shoofly Creek, southwest of Whittakers Dardanelles. The fault was first identified by PG&E (data in PG&E Geosciences files) based on this geomorphic anomaly. Assuming that movement on the fault began concurrently with the onset of Sierra Nevada uplift, about 3 to 5 million years ago (Unruh, 1991), than these data yield a late Cenozoic slip rate of 0.014 to 0.023 mm/yr.

However, recent mapping by Hamilton and others (2005) indicates that there is no remnant of the Table Mountain Latite east of the fault as show on the PG&E regional profile, which was based on published small-scale mapping. Further they found no offsets in the field but did identify a paleo-channel at the inferred fault. Further field work in needed to discount the Post Corral fault at this time.

The fault appears to be delineated by a prominent northwest-striking topographic lineament that passes through a 2.5-kilometer-wide gap between latite outcrops. The fault may extend southward into the Middle Fork Stanislaus River canyon, where its geomorphic expression is lost. To the north, the fault may be delineated by a linear reach of Highland Creek into the North Fork Stanislaus River canyon. The fault appears to cross the canyon near Big Meadow Campground and follow a southwest-facing escarpment into the upper reaches of Blue Creek, in the Mokelumne River drainage. The Post Corral fault is estimated to be 12 to 20 kilometers long based on air-photo analysis.

**Red Peak fault zone**

Slemmons (1953) originally mapped several late Cenozoic normal faults between the Clark and Middle forks of the Stanislaus River. Recent studies of the late Cenozoic volcanic stratigraphy in this region by Rood and others (2004) have confirmed many of these previously mapped faults. We informally refer collectively to these late Cenozoic faults as the "Red Peak fault zone". The extent of two of these mapped faults mapped is about 12 kilometers, the minimum rupture length considered in our analysis. PG&E in earlier analyses proposed that the bedrock lineaments (delineated by linear stream reaches, short east-facing escarpments, canyon-wall benches, and ridge-top saddles[data based on helicopter reconnaissance in PG&E Geosciences files]) that project southward to west of Relief Reservoir may be the continuation of the late Cenozoic faults. However, south of the Middle Fork late Cenozoic deposits are sparse and the activity of the fault is unknown.

In our previous analysis of potential seismic sources in the region, we considered that these late Cenozoic faults, as well as, the once inferred "Relief fault" to the south, made up the "Relief" or southernmost section of the Carson Range fault zone. However observations made during our 15 June 2007 helicopter reconnaissance flight indicate a lack of continuity and magnitude of late Cenozoic faulting southward from near the crest of the Sierra Nevada. Thus, the Red Peak fault zone is herein considered to be separate potential seismic source from the Carson Range fault zon.

Geomorphic features in Mesozoic granitic terrane, linear escarpments and drainage valleys and aligned hillside benches, once formed the basis for inferring the presence of the Relief fault.

However, Hamilton and others (2005) recently examined bedrock exposures in the vicinity of Relief Dam and found no evidence of late Cenozoic faulting. Many of the geomorphic features once used to infer the existence of the Relief fault are parallel or subparallel to prominent joint sets in bedrock and none cross late Cenozoic deposits, based on our recent helicopter reconnaissance. With this new information we now discount the existence of the Relief fault.

Without further evidence to evaluate the Quaternary activity of the Red Peak fault zone, we consider it to be a potential seismic source having a rupture distance of 15 to 26 kilometers.

**Stanislaus Fault Zone**

The inferred Stanislaus fault zone coincides with parts of the Stanislaus River canyon that form the most continuous and prominent linear drainage in the Sierra Nevada . The drainage trends N35°E for a distance of 50 kilometers from near Columbia on the southwest to near Ganns on State Highway 4 on the northeast. The linearity of this drainage suggests a structural control, possibly by a left-oblique-slip fault zone; the sense of lateral slip is inferred from the northeast strike, which is sub-parallel to the Dog Valley fault, the source of the $M_L$ 6.0 Truckee earthquake of 1966 (Hawkins and others, 1986), and from the opposing senses of vertical separation at different points along the fault zone (data in PG&E Geosciences files). The linear drainage is very prominent on the digital relief maps, as well as on small scale topographic maps (e.g., 1;250,000 Sacramento quadrangle). We assume that several transverse faults (e.g., McKays Point, Douds Landing, Skunk Gulch, and Moaning Caves east and west fault) divide the fault zone into three earthquake rupture segments, from southwest to northeast: the Parrotts Ferry, Stanislaus, and North Fork faults. The two closest faults to the PG&E project dams in the Mokelumne-Stanislaus river drainages, the Stanislaus and North Fork faults, are described below as potential seismic sources, although their existence as late Cenozoic structures has been recently questioned.

***Stanislaus Fault*** **-** The Stanislaus fault is inferred from the linearity of the North Fork Stanislaus River extending from the Skunk Gulch fault near the intersection of the North Fork with the South Fork Stanislaus River northeast to the Douds Landing fault, where the fault apparently terminates. The northeast end of the fault is 5 kilometers south of Arnold. Late Cenozoic displacement is suspected on the Stanislaus fault because of its apparent structural association with other faults in the zone having suspected late Cenozoic offsets (e.g., Parrotts Ferry and North Fork faults). The Stanislaus fault about 18 kilometers long.

***North Fork Fault*** **-** The northeast-striking North Fork fault is 7 kilometers east of Arnold and cuts Mesozoic granitic rock, but does not correspond with a previously mapped bedrock fault (Wagner and others, 1981). The fault is interpreted as coinciding with the North Fork Stanislaus River from the McKays Point fault on the southwest to near Ganns on the northeast. In addition to this straight river reach.

The North Fork fault was inferred by PG&E (data in PG&E Geosciences files) from the discordant elevation of the top of the Table Mountain Latite on either side of the North Fork Stanislaus River about 7 kilometers south of Dorrington. The distribution of latite outcrops shown on Wagner and others (1981) was refined by reconnaissance geologic mapping and

aerial photograph interpretation. The top of the latite appears to be vertically separated about 30 to 40 meters, down to the northwest, across the canyon. However because of the relatively wide spacing between the latite remnants, normal faulting and/or tectonic warping may account for this vertical separation. The fault is also marked by a change in the gradient of the latite of about 8 m/km. Specifically, the contact between the latite and the overlying Mehrten Formation slopes 33 m/km to the southwest on the east side of the North Fork fault. Whereas, the exhumed surface on the latite slopes 25 m/km to the southwest on the west side of the fault. These data were the basis for considering the North Fork as a late Cenozoic fault by Jennings (1994).

However, Harlan and others (2005) recently argued that both the vertical separation and the change in gradient of the volcanic stratigraphy result from the PG&E regional profile crossing from one paleo-channel to a different paleo-channel as it crossed the North Fork canyon. They do report that major bedrock joints exposed in the foundation of McKays Point Dam, which is astride the North Stanislaus River, frequently exhibited striations (orientation not specified). At present additional field work is needed before the inferred North Fork fault can be discounted.

The length of the North Fork fault is poorly constrained. The fault is considered to terminate at the McKays Point fault on the southwest. The northeast end of the fault is assumed to be marked by a change in the trend of the North Fork canyon from northeast to east-northeast, which occurs 3 kilometers southwest of Ganns. The assumed length of the North Fork fault is 11 to 18 kilometers.

## Reactivated Faults in Foothills Fault System

### Gopher Gulch Fault

The north- to northwest-striking Gopher Gulch fault is in southwestern Amador County, 2 kilometers east of Sutter Creek. The fault appears to coincide with the western tectonic contact of the Calaveras Complex (Wagner and others, 1981). The fault is delineated by prominent topographic lineaments that consist of straight steam reaches, ridge-top saddles, spring lines, and tonal lineaments. Three of these lineaments coincide with fracture zones in the Mehrten Formation (Alt and others, 1977; PG&E, 1989; Dames and Moore, 1993; Bill Frazer, oral communication, 1993). The lineaments extend from north and east of Plymouth southeastward to Jackson and continue southward along Murphy Gulch and Hunt Gulch to the Mokelumne River (Dames and Moore, 1993). The north end of the fault is poorly defined, because this lineament zone intersects the prominent north-trending lineament defined by Big Indian Creek and the eastern front of Logtown Hill, which extends continuously along State Highway 49 to near El Dorado, California. For this evaluation, we assume that the change in the trend of lineaments at Plymouth, from north-northwest to northward, marks the north end of the Gopher Gulch fault. The south end of the fault appears to die out at the Mokelumne River approximately where the late Cenozoic Poorman Gulch fault ends to the north.

Evidence for late Cenozoic displacements on the Gopher Gulch fault includes fracture zones, geomorphic anomalies (“steps”) and stratigraphic offsets in the Mehrten Formation. For example east of Sutter Creek, Woodward-Clyde Consultants (1978) found fractures in the

Mehrten Formation that were interpreted to be associated with the Gopher Gulch fault by PG&E (1989). Dames and Moore (1993) identified down-to-the-east steps between geomorphic surfaces on the Mehrten Formation coincident with the fracture zones north of Jackson. A geomorphic profile across the Gopher Gulch fault indicates a 15-m-high, down-to-the-east step on the Mehrten Formation on the divide between the North Fork of Jackson Creek and Sutter Creek, near the town of Sutter Creek (data in PG&E Geosciences files). Associated with this step is a 14 m/km (shallowing to the west) change in the gradient of the Mehrten geomorphic surfaces. Bill Frazer of the California Division of Safety of Dams (oral communication, 1993) observed a one meter down-on-the-east separation of a resistant unit in the Mehrten Formation, between outcrops about 5 meters apart, in a saddle on a Mehrten-capped ridge north of Gopher Gulch, about 1.8 kilometers northeast of Sutter Creek.

The belt of lineaments that delineate the Gopher Gulch fault extends from near Plymouth on the north to the Mokelumne River (i.e., the Poorman Gulch fault) on the south, for a distance of 14 kilometers to possibly 22 kilometers. Dames and Moore (1993) assumed a maximum rupture length of 16 kilometers along the Gopher Gulch fault, and concluded that the evidence for Quaternary displacements on the fault is inconclusive. The California Division of Mines and Geology considers this to be a late Cenozoic fault (Jennings, 1994), based on data provided by PG&E (data in PG&E Geosciences files). In this analysis we consider a 14- to 22-kilometer-long rupture on the Gopher Gulch fault.

**Martell Fault**

The Martell fault passes one kilometers west of Jackson, through Martell, California. Late Cenozoic activity is suspected on the fault (Jennings, 1994) based on data provided by PG&E (data in PG&E Geosciences files). The Martell fault was considered to be part of the late Cenozoic Gopher Gulch fault zone by Dames and Moore (1993). Although both faults strike north-northwest and are only 2 to 3 kilometers apart, the Martell fault is associated with a west-facing monocline whereas the Gopher Gulch fault is associated with down-to-the-east normal displacement. We thus consider the Martell fault to be a separate potential seismic source.

The fault appears to coincide with a contact between metavolcanic rock of the Jurassic Logtown Ridge Formation and metasedimentary rock of the Jurassic Mariposa Formation (Wagner and others, 1981). The Martell fault was first identified as a potential seismic source by PG&E (data in PG&E Geosciences files), based on geomorphic profile analysis of the Mehrten Formation. Across the fault, the profile shows a monoclinal gradient change of 16 m/km on the Mehrten surfaces on the divide between Sutter Creek to the north and Jackson Creek to the south. The geomorphic surface east of the inferred fault slopes westward at 13 m/km, whereas the surface to the west of the fault slopes 29 m/km to the west. There appears to no or little (less than 15 meters) vertical separation associated with the gradient change. The base of the Mehrten Formation across this geomorphic anomaly was mapped by Taliaferro and others (1950), which also shows a similar gradient change, but no definitive vertical separation.

However, the gradient change may result from non-tectonic processes. For example, if the westward-flowing lahars of the Mehrten Formation were deposited in a draping manner over

pre-existing topography, perhaps created by differential erosion along the bedrock contact, than both the base and surface of the formation might display monoclinal geometries. We conservatively assume however that the gradient change of the Mehrten Formation results from late Cenozoic displacement on the Martell fault, rather than to deposition processes.

The suspected fault is constrained to strike between north and northwest by the distribution of Mehrten Formation remnants. Although several well-defined topographic lineaments pass through the area of the gradient change, the most prominent lineament coincides with the basement contact. This lineament is inferred to delineate the fault. The lineament is defined by hillside benches, linear drainage valleys and broad ridge-top saddles. It trends N25W from Sutter Creek to Jackson Creek but continues along a N7W trend to south of the Mokelumne River. The expression of the lineament diminishes in the vicinity of the town of Sutter Creek suggesting that the fault dies out to the north. The lineament follows School Land Gulch into the canyon of the Mokelumne River and may continue southward to Big Dome, where it appears to die out.

The suspected Martell fault extends between Sutter Creek and Jackson Creek, and may extend south of the Mokelumne River, for a total fault length of about 13 kilometers.

**Poorman Gulch Fault**

The Poorman Gulch fault is in northwestern Calaveras County, between the Mokelumne River and the South Fork of the Calaveras River. This fault and the Gopher Gulch fault are aligned with each other and coincide with the same bedrock shear zone, the Melones fault zone. The north end of the Poorman Gulch fault was postulated to connect with the south end of the Gopher Gulch fault and, thus, form the Poorman Gulch fault zone by PG&E (1989). The lack of geomorphic expression of Quaternary fault features between these faults (and along the Gopher Gulch fault), however suggests that they are separate late Cenozoic structures. The north-northwest-striking Poorman Gulch fault is characterized by down-to-the-east normal displacement. The rake of slickensides on fault planes of the Poorman Gulch fault (Woodward-Clyde Consultants, 1978) suggests a possible subordinate right-lateral component.

The Poorman Gulch fault coincides with the main trace of the Melones fault zone which separates slate and massive greenstone of the Jurassic Mariposa Formation on the west from phyllite of the late Paleozoic Calaveras Complex on the east (Wagner and others, 1981). The Poorman Gulch fault is associated with prominent topographic lineaments extending from the Mokelumne River southward to the South Fork of the Calaveras River where their geomorphic expression diminishes. The fault appears to die out south of San Andreas, California. The fault is delineated by straight stream segments, including Murphys Gulch, Poorman Gulch and Chili Gulch, ridge-crest-saddles, and hillside benches.

Evidence of late Cenozoic displacement along the Poorman Gulch fault was first postulated by Goldman (1964) based on analysis of structural contours drawn on the base of the Mehrten Formation, and later confirmed by Woodward-Clyde Consultants (Alt and others, 1977; Woodward-Clyde, 1978; Biggar and others, 1978). The fault offsets a belt of Tertiary deposits on the Mokelumne River-Calaveras River divide. Woodward-Clyde Consultants (1978)

measured 27.4 meters (±1.5 meters) down-to-the-east vertical separation of the base of the 4.6-million-year-old Mehrten Formation across the Poorman Gulch fault, based on field mapping and a level-line survey. The 23-million-year-old Chili Hill Tuff member of the underlying Valley Springs Formation was shown to be separated 61 to 76 meters across the fault based on detailed field mapping and topographic surveys.

Dames and Moore (1993) discovered an additional zone of displacement about one kilometer east of the Poorman Gulch fault, where a wedge of Mehrten Formation appears to have been down-faulted against the Calaveras Complex. Profile B-B' in their report shows on the order of 110-meters of down-to-the-east deformation across the Poorman Gulch fault and additional displacement zone (their Figure 6). The down-faulted wedge is close to a 4.6-million-year-old, post-Mehrten dacite intrusion (Bartow and others, 1981) and, therefore, Dames and Moore suggested that this vertical deformation could be associated with warping during intrusion of the dacite.

PG&E (data in PG&E Geosciences files) re-plotted the Woodward-Clyde Consultants (1978) survey data on the base of the Chili Hill Tuff to reevaluate the amount of post-Valley-Springs vertical separation because their projection plane was not oriented perpendicular to the strike of the Poorman Gulch fault, and several of the Chili Hill Tuff remnants were projected as much as 1.5 kilometers. This section is oriented perpendicular to the fault, so that projection distortions are minimized. The total vertical separation of the base of the Chili Hill Tuff is approximately 84 meters. The amount of vertical separation of the base of the Mehrten Formation across the fault was unchanged because the original data was plotted without projection distortions.

Therefore, the total vertical separation of the Mehrten Formation across the entire one-kilometer width of the Poorman Gulch fault zone is estimated to be about 110 meters. Part of the vertical separation (roughly 83 meters) may be due to warping associated with the emplacement of a dacite intrusion (Dames and Moore, 1993). Therefore, the rate of vertical separation on the fault zone between 23 million years ago and 4.6 million years ago was about 0.005 mm/yr, whereas in the past 4.6 million years the rate ranges from 0.006 to 0.024 mm/yr.

Evidence for late Quaternary displacement on the Poorman Gulch fault was identified in three exploratory trenches excavated in the Mehrten Formation by Woodward-Clyde Consultants (1978; Biggar and others, 1978). The trenches exposed a zone of shearing up to 6 meters wide, that contained slickensided and polished vein-quartz and planes on metamorphic rock. In the first trench (Mother Lode trench 1) landslide debris obscured the trench relationship, but a paleosol ("paleo B horizon") appeared to be truncated by down-to-the-east displacement on the primary fault planes. The paleo B horizon is interpreted to be at least 100,000 years old (Woodward-Clyde Consultants, 1978). Two additional trenches excavated at this site were located by tracing a 8-centimeter-high scarplet northward from the first trench. The presence of this subtle geomorphic feature suggests Holocene fault displacement or perhaps soil expansion likely within a clay gouge unit (R8), possibly similar to the pseudo-mole tracks along faults near Healdsburg, California (Malone and others, 1992). In Mother Lode trenches 2 and 3, two colluvial units (S2 and S3) were faulted down to the east. The associated fault planes in trench 2 were traced to within approximately 70 centimeters of the land surface, where they were

overlain by surficial unit S1 (e.g., Figure A. 19 of Biggar and others, 1978). Although this overlying unit thickens above the fault, no shears were found within the unit. The age of unit S2 is unknown, but may be younger than 35,000 years old (Biggar and others, 1978). Based on a reconstruction of soil types across the fault, Woodward-Clyde Consultants (1978) inferred that the most recent event may have produced 15 centimeters of vertical displacement (their Figure C.4A-33); which is the maximum estimated for a single-event displacement on other faults of the Foothills fault system near the proposed Auburn Dam by Woodward-Clyde Consultants (1978) and at the lower limit (15 to 40 cm) on the Dewitt fault north of Auburn (PG&E, 1994c; Schwartz and others, 1996).

Bryant (1983) conducted a brief field reconnaissance of the Mother Lode trench site, after it was reclaimed, and found no geomorphic evidence of Holocene faulting along the Poorman Gulch fault. Bryant postulated that the scarplet northwest of trench 1 may have been formed by soil creep, but that it was probably destroyed by the clean-up operations. Bryant concurred with the conclusion of Woodward-Clyde Consultants, that the Poorman Gulch fault is a late Pleistocene fault (Bryant, 1983; Jennings, 1994).

If we assume that (1) the long-term vertical separation rate of 0.024 mm/yr adequately characterizes the contemporaneous activity on the Poorman Gulch fault and (2) the fault produces characteristic displacements of 15 centimeters per event, then a recurrence interval of about 6300 years is suggested. However, this recurrence interval estimate seems too short, based on the detailed studies by Woodward-Clyde Consultants at this site and based on our recent studies of similar faults within the Sierra Nevada foothills fault system (PG&E, 1992; 1994a, b). Perhaps the long-term separation rate on the fault is only 0.006 mm/yr, assuming that most of the vertical deformation across the one-kilometer-wide zone (about 83 meters) is associated with emplacement of a dacite intrusion, rather than actual displacement on the fault. Then a recurrence interval of about 25,500 years is suggested, which seems more reasonable for this tectonic setting.

Based on the continuity and geomorphic expression of the lineaments that delineate the fault between the Mokelumne River and San Andreas, the Poorman Gulch fault is at least 15 to 22 kilometers long. Dames and Moore (1993) assumed a maximum rupture length of 22 kilometers, based on air-photo interpretation, geomorphic analysis, and field reconnaissance. Apparently in that study, the south end of the Poorman Gulch fault was considered to extend several kilometers south of San Andreas. In this analysis we consider the Poorman Gulch fault to be 15 to 22 kilometers long, in order to incorporate this uncertainty in fault length.

**Rawhide Flat Faults**

The subparallel Rawhide Flat East and West faults cross Table Mountain 2 kilometers west of Jamestown. The northwest- striking faults are from 0.3 to 1.6 kilometers apart and each follows different traces of the basement Melones fault zone. In the Table Mountain area, the Melones fault zone is a 0.5- to 2-kilometers-wide band of strongly deformed rock that separates Jurassic low-grade metasedimentary, metavolcanic, and ultramafic rock of the Mother Lode belt on the southwest from more intensely metamorphosed greenschist-facies rock also of the Mother Lode

belt on the northeast (Wagner and others, 1981). Elongate serpentinite and ultramafic bodies are concentrated along the Rawhide Flat faults. Displacement on both faults is down-to-the-northeast normal with a possible right lateral component. Late Cenozoic displacement was recognized on the fault zone by Eric and others (1955) and Bateman and Wahrhaftig (1966). Woodward-Clyde Consultants (1978) and Biggar and others (1978) demonstrated late Quaternary activity on the fault zone, which was the basis for Jennings (1994) to show the central part of the zone as late Quaternary faults on the Fault Activity Map of California. We assume that these faults merge at depth and thus form a single potential seismic source, based on the close spacing and same sense of vertical slip.

At Table Mountain the Rawhide Flat East fault follows the western boundary of a 70-meter-wide zone of sheared and hydrothermally altered sericite-mariposite schist with interfingering quartz veins that is the principal trace of the Melones fault zone in the area (Eric and others, 1955; Biggar and others, 1978; Woodward-Clyde Consultants, 1978). Woodward-Clyde Consultants (1978) mapped the Rawhide Flat East fault as extending from Quartz Mountain on the southeast across Table Mountain at Rawhide Flat, along a linear tributary of Mormon Creek, to State Route 49 on the northwest, a distance of about 9 kilometers. Rogers (1966) mapped the associated bedrock fault trace to the northwest for a minimum distance of 16 kilometers (in Biggar and others, 1978). However there are no late Cenozoic deposits to evaluate the activity of this part of the fault.

Evidence for late Cenozoic displacement on the Rawhide Flat East fault includes a topographic survey across the Rawhide Flat East fault that shows a 17 meter-high, east-facing scarp on the surface of the Table Mountain Latite west of Rawhide Flat (Biggar and others, 1978; Woodward-Clyde Consultants, 1978). This scarp also has been shown on a geomorphic profile constructed on the latite by PG&E (data in PG&E Geosciences files).

Several features indicative of late Quaternary faulting were observed in the trenches excavated by Woodward-Clyde Consultants (1978) and Biggar and others (1978) across the Rawhide Flat East fault at the western border of Rawhide Flat. Four trenches at the site exposed a sharply defined shear zone within a 2.4- to 3.7-meter wide zone of clay gouge and sheared metasedimentary and metavolcanic rock. The shear zone strikes N22°E to N25°E and dips 65° to 85° northeast. A paleosol, the "paleo-B horizon", was truncated at the shear zone in three of the trenches. The contact between the paleo-B horizon and underlying bedrock was displaced 6 to 37 centimeters, down on the east across the shear zone. The paleo-B horizon was found to be patchy on the west side of the shear zone and continuous on the east in all four trenches. This is consistent with erosion on the relatively upthrown side of the fault. Two colluvial units overlie the paleo-B horizon on the west side of the shear zone and overlie the bedrock on the east side in all the trenches. In three of the trenches shears with the same attitude as the primary bedrock shear zone were observed to extend upward through the paleo-B horizon and into the lower of the two overlying colluvia. The paleo-B soil was juxtaposed with this colluvial unit across the shear zone in the three trenches.

The paleo-B soil was estimated to be at least 100,000 years old or older and the overlying colluvium was thought to be approximately 35,000 years old (Biggar and others, 1978). The

uppermost colluvial unit was interpreted by PG&E (data in PG&E Geosciences files) to be equivalent to the Sonora colluvium that began to accumulate about 14,000 years ago (Harden and Marchand, 1980; PG&E, 1992, 1994a, 1994b). Thus, the latest episode of displacement on the Rawhide Flat East fault is estimated to have occurred between about 35,000 and 14,000 years ago, during the latest Pleistocene.

North of Table Mountain, the Rawhide Flat West fault follows a shear zone along a gabbro-serpentinite contact for 0.4 kilometers before it passes into a serpentinite body and becomes indistinct (Woodward-Clyde Consultants, 1978; Biggar and others, 1978). As mapped by Eric and others (1955) the shear zone continues northwest for 6 kilometers through the serpentinite body to join the main trace of the Melones fault at the Stanislaus River. South of Table Mountain the fault is delineated by sheared serpentinite along or closely following the western contact of the serpentinite body, eventually forming a contact between serpentinite on the west and an interbedded tuff-slate sequence on the east. Mapping by Woodward-Clyde Consultants (1978) confirmed the interpretation of Eric and others (1955) that the shear zone joins the principal strand of the Melones fault zone 7 kilometers southeast of Table Mountain. Thus the Rawhide Flat West fault zone extends for a minimum distance of about 13 kilometers.

Late Cenozoic displacement on the Rawhide Flat West fault is indicated by the presence of an east-facing scarp on the Table Mountain Latite and late Quaternary displacement is suggested by trench exposures (Biggar and others, 1978; Woodward-Clyde Consultants, 1978). A topographic survey on the latite across the fault shows a 23-meter-high scarp (Biggar and others, 1978), which also is shown on a regional geomorphic profile constructed by PG&E (data in PG&E Geosciences files). On the north side of Table Mountain, the fault was trenched to assess evidence for Quaternary activity (Woodward-Clyde Consultants, 1978; Biggar and others, 1978). The trench exposed a sheared contact with highly weathered gabbro on the west and serpentinite on the east. Several faults with associated clay gouge were present within the serpentinite but faults within the gabbro were not associated with gouge. The well-developed paleo-B horizon extended the entire length of the trench as an unfaulted layer (Woodward-Clyde Consultants, 1978). However, the trench was subsequently extended to the east where the paleo-B horizon was found to be possibly vertically separated 0.23 meters down to the east. The possible vertical separation coincided with a polished east-dipping fault plane in clay gouge (Biggar and others, 1978).

The Rawhide Flat East fault extends from Quartz Mountain on the southeast to State Route 49 on the northwest, a distance of about 9 kilometers. The associated bedrock fault trace extends to the northwest (Rogers, 1966) suggesting that the minimum length of the fault may be 15 kilometers. The Rawhide Flat West fault extends from the Stanislaus River southeastward and joins the principal strand of the Melones fault zone 7 kilometers southeast of Table Mountain. Thus we assume that the length of the late Cenozoic Rawhide Flat faults is 15 kilometers.

**Sunnybrook East Fault**

The Sunnybrook East fault crosses State Highway 88/104 one kilometer east of Sunnybrook, California. Over much of its length the fault appears to coincide with the eastern contact of a

Mesozoic to Paleozoic ultramafic belt, that extends along a strand in the Bear Mountains fault zone of Clark (1960). The fault was identified by PG&E (1989) based upon fractures observed in the Mehrten Formation during aerial reconnaissance. From a field reconnaissance Dames and Moore (1993) noted the fractures, and identified an anomaly on geomorphic surfaces on the formation that indicated down-to-the-east vertical displacement across this suspected late Cenozoic fault.

A geomorphic profile across the fault indicates that the Sunnybrook East fault is associated with a 21 m/km gradient change, located between two Mehrten Formation remnants separated by a one-kilometer-wide gap north of State Highway 88/104 (data in PG&E Geosciences files). The remnant to the east slopes westward at a gradient of 29 m/km, whereas the remnant to the west slopes westward at a gradient of 8 m/km. Vertical separation is constrained to be less than about 10 meters. Mapping of the base of the Mehrten remnants by Taliaferro and others (1950) supports the gradient change but permits only minor, if any, vertical separation.

The Sunnybrook East fault appears to be delineated by a strong topographic lineament that extends from Sutter Creek southward to south of the Mokelumne River at Pardee Reservoir. The lineament is marked by aligned linear stream reaches, ridge-crest saddles, and a discontinuous east-facing escarpment. The geomorphic expression of the lineament diminishes near Sutter Creek suggesting that the fault dies out to the north. Between Sutter Creek and Rock Creek, in the vicinity of State Highway 88/104, the north-trending lineament borders (truncates?) the west end of the eastern Mehrten remnant. The lineament extends south-southeast from Rock Creek to south of the Mokelumne River. The Youngs Creek fault and the Spring Valley East fault of Woodward-Clyde Consultants (1978), located south of the river, were postulated by PG&E (1989) to be the southern continuation of the Sunnybrook East fault.

The suspected Sunnybrook East fault appears to have experienced late Cenozoic fault displacements from Sutter Creek to at least the Mokelumne River at Pardee Reservoir, a distance of 11 kilometers. Quaternary activity on the Sunnybrook East fault is inconclusive based on the available information. Late Cenozoic activity has not been shown on the Spring Valley East fault, but has been inferred on the Youngs Creek fault approximately 4 kilometers south of the river. In this evaluation, we consider the Sunnybrook East fault to be a seismic source distinct from the Youngs Creek fault, because the two faults are separated by a 4-kilometer-long gap where the geomorphic expression is weak and the Youngs Creek fault has little cumulative late Cenozoic displacement.

**Youngs Creek Fault**

The Youngs Creek fault crosses State Highway 12 about 7 kilometers west of San Andreas, California. The fault approximately coincides with the western contact of the Melange belt of Duffield and Sharp (1975), which is part of the Bear Mountains fault zone of Clark (1960). The fault is characterized by down-to-the-east normal displacement (Alt and others, 1977), with possibly a right-lateral component (Bryant, 1983b). Based on imagery analysis and field reconnaissance, Dames and Moore (1993) identified a moderately strong lineament that delineates the fault in the Valley Springs area. South of the Mokelumne River, the fault appears

to coincide with a linear drainage along the eastern flank of Buena Vista Mountain. As discussed above, to the north the fault does not appear to merge with the Sunnybrook East fault. Dames and Moore (1993) suggested that the fault may be the northern continuation of the Peoria Pass fault, located approximately 33 kilometers to the south. However, Dames and Moore considered less than half of this distance to represent an earthquake rupture segment.

Evidence for late Cenozoic normal displacements on the Youngs Creek fault includes displacement found during field mapping, leveling surveys on marker beds in the Mehrten and Spring Valley formations, and exploratory trench studies. The fault was identified as a late-Cenozoic fault by Woodward-Clyde Consultants (Alt and others, 1977; Woodward-Clyde Consultants, 1978) based on a 5.5 meter down-to-the-east vertical separation of a marker bed in the Mehrten Formation and of the top of the Chili Hill Tuff member of the Valley Springs Formation. In the vicinity of Spring Valley the fault was mapped as cutting several remnants of these late Cenozoic formations (Biggar and others, 1978; Woodward-Clyde Consultants, 1978).

Three exploratory trenches were excavated across the Youngs Creek fault in the Mehrten Formation to the north of Spring Valley by Woodward-Clyde Consultants (1978). All three trenches exposed east-dipping faults and shears within the rocks of the Mehrten Formation. In Valley Springs trench 1, a buried paleosol ("paleo B horizon") overlying the fault was not displaced or affected by the fault. However, the paleo B horizon had apparently been involved in soil creep (Biggar and others, 1978), which may have distorted the original geometric relationships (Bryant, 1983b). In Valley Springs trenches 2 and 3, colluvial units extended unbroken across the fault. These units were estimated to range in age from 10,000 to 100,000 years. The paleo B horizon was present in trench 3 to the west of the fault, but not to the east. Thus, this unit does not provide any definite conclusions regarding the recency of displacement on the fault. Woodward-Clyde Consultants (1978) concluded that late Quaternary activity of the Youngs Creek fault could not be adequately evaluated at the Valley Springs trench site. Bryant (1983) concluded that Quaternary faulting had occurred on segments of the Youngs Creek fault and, therefore, is considered by the California Division of Mines and Geology to be a Quaternary fault (Jennings, 1994).

A trench investigation of the Youngs Creek fault was conducted by the U.S. Army Corps of Engineers (1994) for the New Hogan Dam. A field review of trench T-1 at the Youngs Creek trench site by Dr. William D. Page, PG&E Geosciences Department (in U.S. Army Corp of Engineers, 1994) indicates that deposits equivalent to the Modesto Formation had not been displaced by the fault. These deposits range in age from about 14,000 to 60,000 years.

The Youngs Creek fault extends from the Mokelumne River at Pardee Reservoir to the Calaveras River at New Hogan Reservoir. Dames and Moore assumed a maximum rupture length along the Youngs Creek Fault of 16 kilometers, which we adopted in this evaluation. However, in addition we consider a 22-kilometer long rupture of the entire Youngs Creek fault.

## SAN ANDREAS FAULT SYSTEM

**1857 Rupture Segment**—The San Andreas fault system extends from the California-Mexico border northwest to Punta Gorda in coastal northwestern California. This major crustal structure accommodates about 75% of the Pacific-North American plate motion. This major continental transform fault is characterized by large-magnitude right-lateral displacements of 10's to 100's of kilometers.

The first of two great earthquakes on the San Andreas fault system during the past 200 years occurred in 1857. The 1857 Fort Tejon earthquake (M~8) rupture began near the southern end of the creeping section of the San Andreas fault at Parkfield and propagated southeastward through the Carrizo Plain and the Big Bend near Cajon Pass (Hill and others, 1990). Right lateral offset along this 305- to 380-kilometer-long segment of the San Andreas fault (Jennings, 1994; Peterson and others, 1996) decreased southeastward from 9.5 meters on the Carrizo Plain at Wallace Creek (Sieh and Jahns, 1984), to 6 meters at Fort Tejon, to 3 to 4 meters along the southern part of the break (Seih, 1978). Late Holocene paleo-earthquakes at Wallace Creek have produced similar amounts of offset (approximately 9.5 to 12.3 meters)(Sieh and Jahns, 1984), suggesting repeated 1857-type events have ruptured the Carrizo Plain section of the fault system.

Although the creeping and Parkfield sections of the San Andreas fault are closer to the Merced Hydroelectric system, we consider the 1857 segment to be a more significant ground-motion source. This is because the creeping and Parkfield sections appear to be releasing shear strain aseismically and in moderate-magnitude earthquakes (respectively) and, thus, lacks the known seismic potential of the 1857 segment to generate great earthquakes.

The ephemeral channel of Wallace Creek has been repeatedly offset during the Holocene by movement along the San Andreas fault (Sieh and Jahns, 1984). The present channel is offset 128 meters and it was cut about 3,700 years ago, yielding a lateral slip rate of about 34 mm/yr. Latest Pleistocene (~13,250 years old) alluvial fan deposits of Wallace Creek are offset 475 meters, suggesting that the latest Pleistocene rate is slightly higher than the late Holocene rate (c.f., 36 mm/yr and 34 mm/yr).

Recurrence intervals differ significantly along the 1857 segment of the San Andreas fault, between the Carrizo Plain and the Mojave Desert sections, which, if correct, shows that this section of the fault does not always rupture in a 'characteristic' earthquake. At Wallace Creek the recurrence interval of 1857-type earthquakes is 240 to 450 years for the latest three intervals (Sieh and Jahns, 1984). However, on the Mojave Desert section at Pallet Creek the average recurrence interval for the latest 10 earthquake cycles is 132 years, but ranges from as little as 44 years to as long as 332 years (Sieh and others, 1989). Thus, it appears that several of the paleo-earthquakes recorded at Pallet Creek did not rupture as far northwest as Wallace Creek and, therefore, may have been comparatively small events.

Based on our analysis of the above information, we conclude that the San Andreas fault system is the most active fault in California and, therefore, we consider the fault to be a distant seismic source for dams in the Mokelumne-Stanislaus Hydroelectric Systems.

## SIERRA NEVADA-COAST RANGE BOUNDARY ZONE

**San Joaquin Fault**—The San Joaquin fault zone is about 24 kilometers southwest of Modesto, along the western margin of the San Joaquin Valley. Pliocene fanglomerate and Quaternary Los Banos alluvium to the west have been uplifted and monoclinally folded along most of the fault zone. Quaternary alluvial fan and San Luis Ranch Alluvium have accumulated on the relative downthrown side of the fault (Wagner and others, 1991). The San Joaquin fault zone is a blind thrust or reverse fault within the Sierra Nevada-Coast Range boundary zone. To the north the fault zone merges with the Black Butte fault and to the south it is separated from the O'Neil fault by an approximately 5-kilometer-wide right step (Wagner and others, 1991).

Herd (1979) noted that the late Pliocene and Pleistocene Tulare Formation and Pleistocene stream terraces abruptly end at an alignment of east-facing scarps along the east flank of the Diablo Range from near O'Neil Forebay northwestward to Vernalis. Herd named this zone of deformation the San Joaquin fault zone an inferred it to be a normal fault zone. South of Orestimba Creek, the Tulare Formation, which contains the Corcoran Clay Member (ash form the Bishop tuff; approximately 600,000 to 700,000 years old), has been offset and tilted eastward along an intervening zone of east-dipping reverse faults. West of Gustine the fault zone is about 8 kilometers wide. Herd (1979) concluded that the Tulare Formation was shed eastward from the Diablo Range before inception of movement on the San Joaquin fault zone. Thus, Herd concluded that movement along the San Joaquin fault zone began in the past 600,000 years.

Information gained by recent earthquakes (e.g., 1983 Coalinga M=6.5 earthquake) and from seismological (e.g., Wong and others, 1988) and geological studies (e.g., Unruh and Moores, 1992; Sowers and others, 1998a) indicates that crustal shortening and reverse faulting characterize the Sierra Nevada-Coast Range boundary zone. Current researchers interpret the San Joaquin fault zone to be a blind thrust or reverse fault (Sowers and others, 1998a), rather than a normal fault.

Recently Sowers and others (1998a) excavated trenches across a scarp preserved on two late Pleistocene stream terraces of Lone Tree Creek, near the north end of the fault. On the older terrace the scarp is 5.5 meters high and slopes 6 degrees eastward. On the younger terrace the scarp is 2.5 meters high and slopes 3 degrees; the original terrace gradient is 1 to 2 degrees. The trench exposures showed that the alluvial deposits and surficial soils are continuous across the scarp, providing positive evidence that the fault did not reach the surface, but remains blind based on soil-profile development the older terrace is estimated to be 200,000 to 50,000 years old and the younger terrace is estimated to be 50,000 to 10,000 years old. The next younger terrace, which is not measurably deformed, is estimated to be 15,000 to 5,000 years old (Sowers and others, 1998b, in progress).

Based on the field relationships, Sowers and others (1998a; 1988b, in progress) concluded that the scarp is the surface expression of a monoclinal fold above an underlying blind thrust or reverse fault. The difference in scarp height (and slope) indicates at least two late Pleistocene folding (i.e., faulting) events, with the most recent faulting event occurring prior to about 5,000 years ago.

If we assume that the San Joaquin fault zone dips 45 ± 15 degrees and apply the relationships between scarp height and ground-surface slope of Caskey (1995, his Figure 2b) to determine dip-slip offset, deformation of the Lone Creek terraces yields a late Quaternary slip rate of 0.13 ± 0.1 mm/yr and a late Pleistocene rate of 0.3 ± 0.24 mm/yr

The Working Group on Northern California Earthquake Potential (1996) subdivided the San Joaquin fault zone (their definition of the fault zone includes both the San Joaquin fault zone of Herd (1979) and the O'Neil fault of Wagner and others (1991)) into two separate rupture segments (GV8 and GV9), each about 40 to 45 kilometers long. They assumed that the slip rate on these segments is similar to the Coalinga segment of the Sierra Nevada-Coast Range boundary zone, which is about 1.5 ± 1 mm/yr, considerably higher than the rates suggested from the data provided by Sowers and others (1998b, in progress).

Based on our analysis of the above information, we conclude that the San Joaquin fault zone has had late Pleistocene displacement and, therefore, we consider it to be a distant potential seismic source for dams in the Mokelumne-Stanislaus Hydroelectric System.

## REFERENCES FOR APPENDIX A


Alt, J.N., Schwartz, D.P., and McCrumb, D.R., 1977, Earthquake evaluation studies of the Auburn Dam Area, regional geology and tectonics: (unpublished) report by Woodward-Clyde Consultants for the U.S. Bureau of Reclamation, v. 3., 118 p., 4 appendices.

Bartow, J.A., Marchand, D.E., and Shipley, S., 1981, Preliminary geologic map of Cenozoic deposits of the Copperopolis Quadrangle, California: U.S. Geological Survey Open-File Report 81-1048, scale 1:62,500.

Bateman, P.C. and Wahrhaftig, C., 1966, Geology of the Sierra Nevada, California: *in* Bailey, E.H., ed., Geology of northern California, California Division of Mines and Geology Bulletin 190, p. 107-172.

Bell, J.W., 1984, Quaternary fault map of Nevada, Reno Sheet: Nevada Bureau of Mines and Geology Map 79, 1:250,000 scale.

Biggar, N, Cluff, L.S., and Ewoldsen, H., 1978, Geologic and seismologic investigations, New Melones Dam project, California: report by Woodward-Clyde Consultants to U.S. Army Corps of Engineers, Sacramento, 246 p., Appendix A.

Bryant, W.A., 1983a, Faults in Antelope Valley, Slinkard Valley, and along the West Walker River, Mono County: California Division of Mines and Geology Fault Evaluation Report FER-154, 14 p., map scale 1:62,500.

Bryant, W.A., 1983b, Southern Foothills fault system, Amador, Calaveras, El Dorado, and Tuolumne Counties: California Division of Mines and Geology Fault Evaluation Report FER-148, 12 p. plus figures.

Bryant, W.A., 1984, Evidence of recent faulting along the Antelope Valley fault zone, Mono County, California: California Division of Mines and Geology, Open-File Report 84-56, scale 1:48,000.

Caskey, 1995, Geometric relationships of dip slip to a faulted ground surface: new nongrams for estimating components of fault displacement: Journal of Structural Geology, v. 17, p. 1197-1202.

Clark, L.D., 1960, Foothills fault system, western Sierra Nevada, California: Geological Society of America Bulletin, v. 71, p.483-496.

Clark, M.M., 1967, Pleistocene glaciations of the drainage of the West Walker River, Sierra Nevada, California: Unpublished Ph.D. thesis, Stanford University, 130 p.

Clark, M.M, 1972, Deposits and extent of Pleistocene glaciers of the upper West Walker drainage, Sierra Nevada, California: Unpublished map in California Divisions of Mines and Geology files, scale 1:62,500.

Clark, M.M, 1975, Faulted deformation in the upper drainage of the West Walker River near Sonora Junction, California, in Cenozoic deformation along the Sierra Nevada province and Basin and Range province boundary: California Geology, v. 28, no. 5, p. 103-104.

Clark, M.M., Harms, K.H., Lienkaemper, J.J., Harwood, D.S., Lajoie, K.R., Matti, J.C., Perkins, J.A., Rymer, M.J., Sarna-Wojciki, A.M., Sharp, R.V., Sims, J.D., Tinsley, J.C. III, and Ziony, J.I., 1984, Preliminary slip rate table and map of late Quaternary faults of California: U.S., Geological Survey Open-file Report 84-106.

Curtis, G.H., 1951, The geology of Topaz Lake quadrangle and the eastern half of the Ebbetts Pass quadrangle: Berkeley, University of California, unpublished Ph.D. dissertation, 310 p.

Dames and Moore, 1993, Photogeologic and imagery analysis for the geologic and seismologic investigation, New Hogan Dam, Calaveras County, California: unpublished consulting report submitted to U.S. Army Corp. of Engineers, Sacramento, p. 51, 14 figures, 1 plate, 1 appendix.

dePolo, C.M., and Anderson, J.G., 2000, Estimating the slip rates of normal faults in the Great Basin, USA: Basin Research, v. 12, p. 227-240.

Dohrenwend, J.C., 1982, Surficial geologic map of the Walker Lake 1° by 2° Quadrangle, Nevada-California: U.S. Geological Survey Miscellaneous Field Studies Map MF-1382-C, scale 1:250:000.

Duffield, W.A. and Sharp, R.V., 1975, Geology of the Sierra Nevada foothills melange and adjacent areas, Amador County, California: U.S. Geological Survey Professional Paper 827, 30 p.

Eric, J.H., Stromquist, A.A., and Seinney, C.M., 1955, Geology and mineral deposits of the Angles Camp and Sonora qauadrangles, Calaveras and Tuolumne counties, California: California Division of Mines and

Geology, Special Report 41, 55 p.

Gardner, J.V., Dartnell, P., Mayer, L.A., and Hughes-Clark, J., 1999, Bathymetry and selected perspective views of Lake Tahoe, California and Nevada: U.S. Geological Survey Water Resources Investigation Report 99-4043, ~1:62,500 and 1:100,000 scale.

Goldman, H.B., 1964, Sand and gravel in California, and inventory of deposits-Pt.B, Central California: California Division of Mines and Geology Bulletin 180-B, 58 p.

Halsey, J.H., 1953, Geology of parts of the Bridgeport, Calif. and Wellington, Nevada, quadrangles: Unpublished Ph.D. thesis, University of California, Berkeley, 301 p., map scale 1:125,000.

Hamilton, D. H., Harlan, R.D., and Castle, J.A., 2005, Phase II, Seismic Fault Investigation for North Fork Stanislaus River Hydro Electric Development Project, FERC Project No. 2409-CA, and Donnells Project, FERC Project No. 2005-CA: unpub. Consulting report submitted to Northern California Power Agency and Tri-Dam Project, Murphys, California, 70 p., 3 tables, 18 figures, 11 plates.

Harden, J.W., and Marchand, D.E., 1980, Quaternary stratigraphy and interpretation of soil data from the Auburn, Oroville, and Sonora areas along the Foothills fault system, western Sierra Nevada, California: U.S. Geological Survey, Open File Report 80-305, 56 p.

Hawkins, F.F., LaForge, R., and Hansen, R.A., 1986, Seismotectonic study of the Stampede, Prosser Creek, Boca, and Lake Tahoe dams, Truckee/Lake Tahoe area, northeastern Sierra Nevada, California: Seismotectonic Report No. 85-4, 210 p.

Herd, D.G., 1979, The San Joaquin fault zone – Evidence for late Quaternary faulting along the west side of the northern San Joaquin Valley, California: Geological Society of America Abstracts with Programs, v. 11, no. 3, p. 83.

Hill, D.P., Eaton, J.P., and Jones, L.M., 1990, Seismicity, 1980-86: in The San Andreas fault system, California, U.S. Geological Survey Professional Paper 1515, p. 123-151.

Huber, N.K., 1981, Amount and timing of late Cenozoic uplift and tilt of the central Sierra Nevada, California—Evidence from the upper San Joaquin River basin: U.S. Geological Survey Professional Paper 1197, 28 p.

Hyne, N.J., Chelminski, P., Court, J.E., Gorsline, D.S., and Goldman, C.R., 1972, Quaternary history of Lake Tahoe, California-Nevada: Geological Society of America Bulletin, v. 83, no. 5, p. 1435-1448.

Ichinose, G.A., Satake, K., Anderson, J.G., Schweickert, R., and Lahren, M., 2000, The potential hazard from tsunami and seiche waves generated by future large earthquakes within lake Tahoe, California-Nevada: Geophys. Res. Lett. 27, p. 1203-1206.

Jennings, C. W., 1994, Fault activity map of California with locations and ages of recent volcanic eruptions: California Division of Mines and Geology, Geologic Data Map No 6, 1:750,000 scale.

Knuepfer, P.L.K., 1989, Implications of the characteristics of end-points of historical surface fault ruptures for the nature of fault segmentation: in Schwartz, D. P., and Sibson, R. H., eds., Conference on Fault Segmentation and Controls of Rupture Initiation and Termination, U.S. Geological Survey Open-File Report 89-315, pp. 193-228.

Lahren, M.M. and Schweickert, R.A., 1991, Tertiary brittle deformation in the central Sierra Nevada, California: Evidence for late Miocene and possibly younger faulting: Geological Society of America Bulletin, v. 103, p. 898-904.

Lahren, M.M., Schweickert, R.A., Smith, K., Karlin, R., and Howles, J., 1999, Active faults of the Lake Tahoe basin, California and Nevada: Implications: Geological Society of America Abstracts with Programs, vol. 31, No. 6, P. A-72.

Lindgren, W., 1897, Description of the Truckee quadrangle, California: U.S. Geological Survey Geologic Atlas, Folio 39, scale 1:125,000.

Loomis, A.A., 1983, Geology of the Fallen Leaf Lake 15' quadrangle, El Dorado County, California: California Division of Mines and Geology Map Sheet 32, scale 1:62,500.

Malone, M.D., Borchardt, G., Hart, E.W., and Korbay, S.R., 1992, "Pseudo-mole tracks" from clay beds east of Healdsburg: *in* Borchardt, G. and others, eds., Proceedings of the Second Conference on Earthquake Hazards in the Eastern San Francisco Bay Area: California Division of Mines and Geology Special Publication 113, p. 419-425.

Martinelli, Diane M., 1989, Geophysical investigations of the northern Sierra Nevada-Basin and Range boundary, west-central Nevada and east-central California, unpublished masters thesis, University of Nevada Reno, 172 pp.

Olig, S., Sawyer, T., Wright, D., Wong, I., Terra, F., and Anderson, L., 2005, Preliminary seismic source characterization of faults near Stampede and Prosser Creek Dams—Washoe Project and Boca Dam—Truckee Storage Project: unpublished report by the URS project team for the U.S. Bureau of Reclamation, Denver, Colorado, 22 p., plus tables, figures, and plates (1:100,000).

Page, W.D., McLaren, M. K., Tsai, Y.-B., and Sawyer, T. S., 1994, Reconnaisance report on the September 12, 1994, Double Spring Flat earthquake, M 6.3, Douglas County, Nevada: report by PG&E to Division of Safety of Dams, 14 p. plus figures.

Peterson, M.D., Bryant, W.A., Cramer, C.H., Cao, C. Reichle, M.S., Frankle, A., Lienkaemper, J., McCrory, P., and Schwartz, D.P., 1996, Probabilistic seismic hazard assessment for the State of California, EOS Transactions, AGU (abstract).

PG&E, 1989, Static and dynamic stability assessment, Ione Canal Dam: Report by PG&E Engineering Department, San Francisco, California.

PG&E, 1991a, Characterization of potential earthquake sources for Echo Lake Dam, El Dorado County, California, State Dam No. 97-052,: Internal report, 16p. plus figures.

PG&E, 1991b, Characterization of potential earthquake sources for Lake Francis Dam, State Dam No. 1034-009: report to the Yuba County Water Agency, Marysville, for the California Division of Safety of Dams, 36 p. plus figures and plates.

PG&E, 1994a, Characterization of potential earthquake sources for Rock Creek (Drum) Dam: report to Division of Safety of Dams, Sacramento, 93 p., plus figures and plates.

PG&E, 1994b, Characterization of potential earthquake sources for, Ralston Afterbay Dam, State Dam No. 1030-4, FERC Project No. 2079: report to Placer County Water Agency, Foresthill, for the Federal Energy Regulatory Commission, 93 p.

PG&E, 1992, Supplement to characterization of potential earthquake sources, Lake Francis Dam: report to the California Division of Safety of Dams, v.1 and 2.

Ramelli, A.R., dePolo, C.M., and Bell, J.W., 1994, Synthesis of data and exploratory trenching along the northern Sierra Nevada fault zone: U.S. Geological Survey, National Earthquake Hazards Reduction Program Final Technical Report, 65 p, 1:100,000 scale plate.

Ramelli, A.R., Bell, J.W., dePolo, C.M., and Yount, J.C., 1999, large-magnitude, late Holocene earthquakes on the Genoa fault, west-central Nevada and eastern California: Bulletin of the Seismological society of America, v. 89, no. 6, p. 1458-1472.

Rodgers, T.H., 1966, Geologic map of the California, San Jose sheet: California Division of Mines and Geology, scale 1:250,000.

Rood, D.H., Busby, C., and Wagner, D., 2004, New, Preliminary, and ongoing geologic work in the Sonora Pass Region: Volcanological Society of Sacramento, Field Trip in Honor of Garniss Curtis and Burt Slemmons, July 22-25, 2004, Guidebook, Paper III, 14 p., 25 figures.

Schweickert, R.A., Lahren, M.M., Karlin, R.E., Smith, K.D., and Howle, J.F., 2000, Preliminary Map of Pleistocene to Holocene faults in the Tahoe Basin, California and Nevada: Nevada Bureau of Mines and Geology Open-File Report 2000-4, 1:100,000.

Sieh, K.E., 1978, Pre-historic large earthquakes produced by slip on the San Andreas fault at Pallett Creek, California: Journal of Geophysical Research, v. 83, p. 3907-3939.

Sieh, K.E. and Jahns, R.H., 1984, Holocene activity of the San Andreas fault at Wallace Creek, California: Geological Society of America Bulletin, v. 95, p. 883-896.

Sieh, K.E., Stuiver, M., and Brillinger, D., 1989, A more precise chronology of earthquakes produced by the San Andreas fault in southern California: Journal of Geophysical Research, vol. 94, no. B1, p. 603-623.

Slemmons, D.B., 1953, Fault map of the Walker Lake 1°X2° sheet: unpublished map compiled for Figures 3, 4, 5, 6 and 8 in Slemmons (1967), 1:250,000 scale map.

Slemmons, D.B., 1966, Cenozoic volcanism of the central Sierra Nevada, California: California Division of Mines and Geology Bulletin 190, p. 199-214.

Sommerville, M.R., Peppin, W.A., and VanWorner, J.D., 1980, An earthquake sequence in the Sierra Nevada-Great Basin boundary zone, Diamond Valley: Seismological Society of America Bulletin, c. 70, no. 5, p. 1547-1555.

Smith, T.C., 1984, Genoa fault, Alpine County, California: Department of Conservation, Division of Mines and Geology Fault Evaluation Report 156.

Sowers, J.M., Simpson, G.D., Lettis, W.R., and Randolph, C.E., 1998a, Late Pleistocene monoclinal folding on the San Joaquin fault near Tracy, California: Geological Society of America Abstracts with Programs, v. 30, no. 5, p. 65.

Sowers, J.M., Simpson, G.D., Lettis, W.R., and Randolph, C.E., 1998b (in progress), Monoclinal folding of fluvial terraces along the San Joaquin fault near Tracy, California: unpublished Final Technical Report to the U.S. Geological Survey National Earthquake Hazards Reduction Program.

Stewart, J.H., Carlson, J.E., and Johannesen, D.C., 1982, Geologic map of the Walker Lake 1° by 2° Quadrangle, California and Nevada: U.S. Geological Survey Miscellaneous Field Studies Map MF-1382-A, scale 1:250:000.

Taliaferro, N.L. and summer field class, 1950, Geologic map of the Sutter Creek 15' quadrangle: University of California Berkeley, unpublished map, scale 1:62,500.

Unruh, J.R., 1991, The uplift of the Sierra Nevada and implications for late Cenozoic epeiorogeny in the western cordillera: Geological Society of America Bulletin, v. 103, p. 1395-1404.

Unruh, J.R. and Moores, E.M., 1992, Quaternary blind thrusting on the southwestern margin of the Sacramento Valley, California,: Tectonics, v. 11, no. 2, p. 192-203.

U.S. Army Corps of Engineers, 1994, Geologic and seismologic investigation (fault study), New Hogan Dam and Reservoir (New Hogan Lake), Calaveras River, California: report by Sacramento District, 44 p. plus figures, sheets, tables, and appendices.

Wagner, D.L., Jennings, C.W., Bedrossian, T.L., and Bortugno, E.J., 1981, Geologic map of the Sacramento Quadrangle, California: California Division of Mines and Geology, Sacramento, scale 1:250,000.

Wagner, D.L., Bortugno, E.J., and McJundin, R.D., 1991, Geologic Map of the San Francisco-San Jose Quadrangle: California Division of Mines and Geology, Map No. 5a.

Wagner, D.L., Saucedo, G.J., and Grose, T.L.T., 1989, The Honey Lake fault zone, northeastern California, its nature, age and displacement (abstract): EOS, v. 70, no. 43, p. 1358.

Wong, I.G., Ely, R.W., and Killmann, A.C., 1988, Contemporary seismicity and tectonics of the northern and central Coast Ranges – Sierran block boundary zone, California: Journal of Geophysical Research, v. 93, no., B-7, p. 7813-7833.: report to Pacific Gas and Electric Company, San Francisco, 166 p.

Woodward-Clyde Consultants, 1978, Foothills fault system study: Stanislaus Nuclear Project, Site Suitability/Site Safety Report, Appendix C.4, v. 6, report for Pacific Gas and Electric Company, San Francisco, 166 p. plus tables and figures.

Working Group on Northern California Earthquake Probabilities, 1996, Database of potential sources for earthquakes large than magnitude 6 in northern California: U.S. Geological Survey Open-File Report 96-705.